Dissertation

submitted to the

Combined Faculties for the Natural Sciences and for Mathematics

of the Ruperto-Carola University of Heidelberg, Germany

for the degree of

Doctor of Natural Sciences

Deciphering the interplay between exo-erythrocytic *Plasmodium berghei* parasites and the host hepatic miRNA expression

presented by

Christiane Elisabeth Hammerschmidt-Kamper

Diploma-Biologist

Born in Hilden

Dissertation

submitted to the

Combined Faculties for the Natural Sciences and for Mathematics

of the Ruperto-Carola University of Heidelberg, Germany

for the degree of

Doctor of Natural Sciences

presented by

Christiane Elisabeth Hammerschmidt-Kamper

Diploma-Biologist

Born in Hilden

Oral examination: …….

Deciphering the interplay between exo-erythrocytic *Plasmodium berghei* parasites and the host hepatic miRNA expression

Referees: Prof. Dr. Michael Lanzer

Dr. Ann-Kristin Müller

Hiermit erkläre ich, dass ich die hier vorliegende Arbeit im Zeitraum von Januar 2009 bis Juli 2012 unter der Anleitung von Dr. Ann-Kristin Müller selbst durchgeführt und verfasst habe und mich keiner anderen als der von mir ausdrücklich bezeichneten Quellen und Hilfen bedient habe.

…….. ……..

Datum Christiane Elisabeth Hammerschmidt-Kamper

Parts of this work are in preparation for publication:

Hammerschmidt-Kamper C., Börner K., Knapp B., Kaderali L., Mueller A.-K., Grimm D.

The agent within: Exo-erythrocytic *Plasmodium* parasites manipulate host cell miRNAs from the inside

Meinen Eltern, Netti und Daniel

“Alles Wissen und alles Vermehren unseres Wissens endet nicht mit einem Schlußpunkt, sondern mit einem Fragezeichen.”

Hermann Hesse

Summary

The different life cycle stages of the malaria parasite *Plasmodium* depend on tight interactions between the parasite and the respective host tissue. During the clinically silent liver-phase, the parasite undergoes enormous multiplication and thus requires host hepatic proteins for its growth and development. Several studies using genetically modified parasites lacking defined liver-stage specific genes, proved the tight interaction between parasite proteins and host hepatic factors and the dependency of the parasite on these host factors for completion of its liver-stage development. These parasites were furthermore able to induce specific host immune responses.

MicroRNAs (miRNAs) and the RNAi machinery are more and more recognized to be important in the interplay between pathogens and hosts. Initially discovered as defense mechanisms of the host against pathogens, growing evidence proves the abuse of the host RNAi machinery by the pathogen for its own benefit. Additionally, miRNAs gain increasing importance as fine-tuning molecular triggers in causing but also in defense against a very diverse set of diseases. Thus, interest arose in investigating the influence persisting infections with *Plasmodium* and *Toxoplasma* might have on the miRNA expression pattern of the respective affected host tissue.

The aim of this study was to understand the interplay between the malaria liver-stage and the host hepatic RNAi machinery and miRNA expression in general and to shed some light onto the mechanisms underlying host immunity induced by immunization with genetically attenuated (GAP) as well as radiation-attenuated (RAS) parasites. For this purpose I used a two-fold approach. On the one hand I analyzed by quantitative real-time PCR (qPCR) *Xpo-5*, *Ago-2*, *Dicer*, *TRBP* and *Drosha* transcription levels in murine hepatic tissue 24h and 40h after infection with *Pb*NK65 WT, GAP and RAS salivary gland sporozoites and compared them to respective transcription levels in naïve mice. On the other hand I investigated the host hepatic miRNA expression using the same sample pool to detect host hepatic miRNAs that are differentially expressed upon *Plasmodium* liver-stage infection. I could demonstrate a transcriptional down-regulation of all five host RNAi machinery components investigated, which was more pronounced in livers 40h post infection with both attenuated parasites. Additional Western blot analyses were performed and proved the results from the qPCR analysis for Xpo-5 and Drosha on protein level. Furthermore, a total number of 31 dys-regulated host miRNAs was observed with distinct expression patterns for each of the sample groups, reflecting the unique features of the different parasite strains applied as well as the results of the preceding analyses of host hepatic RNAi machinery components. Two interesting candidate miRNAs, miR-21 and miR-155, were chosen for further functional analysis. After confirming over-expression of these two candidate miRNAs in infected murine hepatic tissue by ex *vivo* imaging, their impact on induction of protection upon GAP and RAS immunization was analyzed by down-regulation of these two miRNAs *in vivo*. These experiments indicated that the observed expressional up-regulation of both miRNAs might play a supportive role in GAP-induced immunity.

Zusammenfassung

Die verschiedenen Schritte während des Lebenszyklus des Malaria Parasiten bedürfen einer sehr engen Interaktion zwischen dem Parasit und dem betroffenen Gewebe des Wirts. Um das enorme Wachstum und die anschließende Differenzierung in invasive Stadien während der klinisch unauffälligen Leberstadienentwicklung gewährleisten zu können, rekrutiert der Parasit Proteine der Wirtszelle. In mehreren Studien wurden genetisch veränderte Parasiten verwendet, denen genau definierte Lebergene fehlten, um diese enge Interaktion zwischen Parasit und Wirtsleberzelle zu untersuchen. So konnte man die Abhängigkeit des Parasiten von Wirtszellfaktoren für eine erfolgreiche Leberstadienentwicklung zeigen. Außerdem waren diese genetisch veränderten Parasiten in der Lage, Immunität in dem entsprechenden Wirt zu induzieren.

Es wird zunehmend klar, wie wichtig MicroRNAs (miRNAs) und die RNAi Maschinerie für das Zusammenspiel von Pathogen und Wirt sind. Ursprünglich als Verteidigungsmechanismus des Wirts gegen Pathogene entdeckt, wurde nach und nach gezeigt, dass Pathogene in der Lage sind, die RNAi Maschinerie des Wirts für ihre eigenen Zwecke zu missbrauchen. Darüber hinaus zeigt sich immer deutlicher, wie wichtig miRNAs für die Feinabstimmung sowohl bei der Auslösung von verschiedenen Erkrankungen, als auch bei ihrer Bekämpfung sind. Basierend auf diesen Erkenntnissen konzentrieren sich aktuelle Forschungen auf die Untersuchung des Einflusses, den eine bestehende Infektion mit *Plasmodium* oder *Toxoplasma* auf die RNAi Maschinerie und die miRNA Expression des betroffenen Wirtsgewebes hat.

Das Ziel der vorliegenden Studie war das Zusammenspiel zwischen Malaria Leberstadien und der RNAi Maschinerie und miRNA Expression in der Wirtsleber im Allgemeinen zu untersuchen. Außerdem sollten die Mechanismen der durch die Immunisierung mit genetisch attenuierten (GAP) und bestrahlungsattenuierten (RAS) Parasiten hervorgerufenen Immunität analysiert werden. Dazu wurden auf der einen Seite mittels quantitativer real-time PCR (qPCR) die Transkriptionslevel von *Xpo-5*, *Ago-2*, *Dicer*, *TRBP* and *Drosha* in murinem Lebergewebe 24 und 40 Stunden nach Infektion mit *Pb*NK65 WT, GAP und RAS Speicheldrüsen Sprozoiten bestimmt und mit den Transkriptionsleveln aus naiven Mäusen verglichen. Auf der anderen Seite wurde mit denselben Proben die Expression von hepatischen miRNAs untersucht. Dadurch sollten miRNAs der Wirtsleber identifizieren werden, die in ihrer Expression durch das Vorhandensein von Leberstadien der unterschiedlichen angewandten Stämme beeinflusst werden. Ich konnte eine Herunterregulierung der Transkription aller fünf untersuchten Komponenten feststellen, welche 40 Stunden nach Infektion mit den attenuierten Parasiten besonders stark ausgeprägt war. Zusätzliche Western Blot Analysen wurden durchgeführt und bestätigten die Ergebnisse der qPCR Analyse für Xpo-5 und Drosha auch auf Proteinebene. Weiter wurden insgesamt 31 unterschiedlich regulierte hepatische Wirts miRNAs entdeckt, die für jede der verwendeten Probengruppen ein spezielles Expressionsprofil aufwiesen, welches nicht nur die einzigartigen Eigenschaften der verschiedenen eingesetzten Stämme widerspiegelte, sondern auch die zuvor beobachteten Veränderungen in den Transkriptionsraten der RNAi Maschinerie

Komponenten. Zwei interessante miRNAs, miR-21 und miR-155, wurden hinsichtlich einer möglichen biologischen Funktion genauer untersucht. Nachdem durch *ex vivo* Bildgebung gezeigt werden konnte, dass beide miRNAs tatsächlich in infiziertem Lebergewebe überexpremiert werden, wurde ihre Beteiligung am Hervorrufen von Immunantworten durch Immunisierung mit GAP und RAS untersucht. Dazu wurden beide miRNAs unabhängig von einander *in vivo* in der Mausleber herunterreguliert und dann das Potenzial von GAP und RAS Immunisierungen beobachtet. Diese Experimente zeigten, dass miR-21 und miR-155 an der durch GAP Immunisierung hervorgerufenen Immunität beteiligt sind.

Table of contents

List of abbreviations

α	anti
aa	amino acids
AAV	Adeno-associated virus
ACT	artemisinin-base combination therapies
Ago-2 / *Ago-2*	Argonaute-2
AMA-1 / *ama-1*	apical membrane antigen-1
amp	ampicllin
An. stephensi	*Anopheles stephensi*
APS	ammonium persulphate
bp	base pair
BSA	bovine serum albumin
°C	degree Celsius
CDC	Center for Disease Control
cDNA	complementary DNA
C. elegans	*Caenorhabditis elegans*
CO_2	carbon dioxide
CQ	chloroquine
CSP / *csp*	circumsporozoite protein
C_T	threshold cycle
Da	dalton
ddH_2O	double distilled water
Δ	delta
DEPC	diethylpyrocarbonate
DMEM	Dulbecco's MEM Medium
DMSO	dimethylsulfoxid
DNA	desocyribonuleic acid
dNTP	desoxyribonucleosid-triphophate
ds-RBD	dsRNA-binding domain
dsRNA	double stranded RNA
DTT	dithiothreitol
E. coli	*Escherichia coli*
EDTA	ethylenediaminetetraacetic acid
E. papillata	*Eimeria papillata*
FCS	fetal calf serum
for	forward
g	gram

GAP	genetically attenuated parasite
gDNA	gemonic DNA
h	hour(s)
HBSS	Hank's Balanced Salt Solution
HBV	hepatitis B virus
HCV	hepatitis C virus
HCC	hepatocellular carcinoma
HRP	horseradish peroxidase
HSP70	heat shock protein 80
IFA	indirect immunofluorescence analysis
i.p.	intraperitoneal
i.v.	intravenous
k	kilo
kan	kanamycin
kb	kilobase pair
kDa	kilo dalton
K/X	Ketamin/Xylazin
l	liter
LB	Luria Broth
µ	micro
µg	microgram
µl	microliter
µm	micrometer
µM	micromolar
M	molar
mA	milliampere
MCS	multiple cloning site
mg	milligram
min	minute(s)
miRISC	miRNA-induced silencing complex
miRNA, miR	microRNA
ml	milliliter
mm	millimeter
mM	millimolar
MOPS	3-(N-morpholino)propanesulfonic acid
MSP-1 / *msp-1*	merozoite surface protein-1
n	nano
N_2	liquid nitrogen

nm	nanometer
O_2	oxygen
OD	optical density
oligo(dT)	tyrosine oligo
o/n	over night
ORF	open reading frame
P.	*Plasmodium*
pABA	4-aminobenzoeic acid
PAGE	polyacrylamide gel electrophoresis
PBS	phosphate buffered saline
Pb, *P. berghei*	*Plasmodium berghei*
PCR	polymerase chain reaction
PEG	polyethylene glycol
pH	potential hydrogenii
PQ	primaquine
pre-miRNA	precursor miRNA
pri-miRNA	primary miRNA
P/S	penicillin and streptomycin
PV	parasitophorous vacuole
PVM	parasitophorous vacuolar membrane
Py, *P. yoelii*	*Plasmodium yoelii*
rAAV	recombinant Adeno-associated virus
RAS	radiation attenuated sporozoite
rev	reverse
RIN	RNA integrity number
RLU	relative light units
RNA	ribonucleic acid
RNAi	RNA interference
rpm	rounds per minute
rRNA	ribosomal RNA
RT	room temperature or reverse transcriptase
+RT	with reverse transcriptase
-RT	without reverse transcriptase
RT-PCR	reverse transcriptase PCR
SDS	sodium dodecylsulphate
sec	second(s)
sg	salivary glands
spz	sporozoite

TAE	Tris-acetic acid EDTA
Taq	*Thermus aquaticus*
TBS	tris-buffered saline
TBST	tris-buffered saline/tween
TE	Tris/EDTA
TEMED	triethylmethylethyldiamine
TFB	transformation buffer
Tg, *T. gondii*	*Toxoplasma gondii*
TRBP / *TRBP*	human immunodeficiency virus transactivating response RNA-binding protein
TRIS	tris (hydroxymethyl)-aminomethane
U	units
UIS / *uis*	upregulated in infective sporozoites
UTR	untranslated region
UV	ultra violet
qPCR	quantitative real-time PCR
V	volt
v/v	volume to volume
vol	volume
w/v	weight to volume
WHO	World Health Organization
WT	wildtype
Xpo-5 / *Xpo-5*	Exportin-5

List of figures

List of tables

1 Introduction

1.1 Malaria

Female mosquitoes of the genus *Anopheles* transmit single-cell eukaryotic *Plasmodium* parasites, which are the causative agent of the infectious disease malaria. According to the World Health Organization (WHO), malaria is still one of the major causes of mortality and morbidity, especially in the developing countries. In 2010, an estimated 3.3 billion people were at risk of malaria and an estimated 1,238,000 deaths were reported that year (Murray et al., 2012). Although the disease is present in several regions of the world like Africa, South-East-Asia, Middle- and South-America (figure 1.1.1), people living in sub-Saharan Africa have the highest risk of getting infected. It is estimated that 81% of reported cases and 91% of deaths due to malaria in 2010 occurred in the African regions. From all people concerned, children under the age of five years and pregnant women especially in their first pregnancies are the most severely affected ones (Murray et al., 2012).

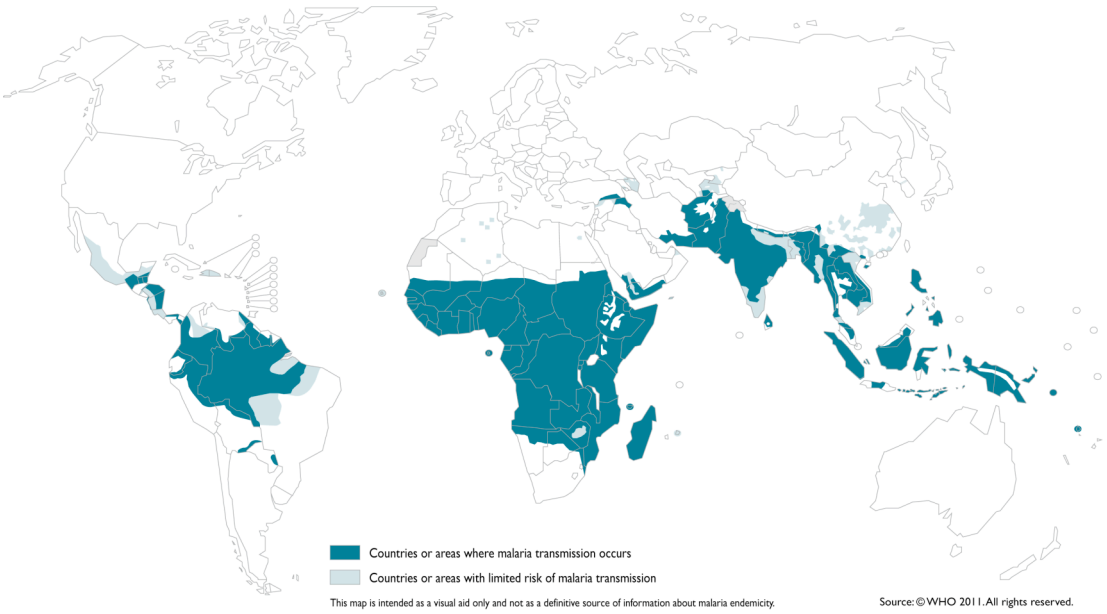

Figure 1.1.1: Global distribution of countries and areas at risk of malaria transmission in 2010. Malaria transmission mainly takes place in countries and areas of the tropical and sub-tropical region. Indicated in petrol are countries and areas where malaria transmission occurs and in light petrol are countries or areas with limited risk of malaria transmission (WHO 2011).

It is most probably that the term malaria originates from the Italian word “mal’aria”, which means “spoiled air”, as people assumed for hundreds of years that the feverish disease was caused by miasmas rising from swamps. As Antoni van Leeuwenhoek discovered bacteria in 1676, followed by the development of the germ theory of infection, postulated by Louis Pasteur and Robert Koch in 1878-1879, people concentrated on the search for the cause of malaria (Cox, 2010; Guillemin, 2001). In 1880, Charles Louis Alphonse Laveran discovered the parasites in the blood of malaria patients. 17

years later, in 1897, Ronald Ross identified culicine mosquitoes as the responsible vector for avian malaria caused by *Plasmodium relictum* (Ross, 1897a, b). This was also confirmed for human malaria, which is transmitted by *Anopheles* mosquitoes, between 1898 and 1900 by the Italian scientists Giovanni Battista Grassi, Amico Bignami, Giuseppe Bastianelli, Angelo Celli, Camillo Golgi and Ettore Marchiafava (Cox, 2010; Tuteja, 2007).

Malaria is a disease, known for more than 4000 years and yet it still remains one of the major public health problems, especially in developing countries. This leads to a subsequent great economic impact for the affected countries. Thus the average loss of the annual economic growth was estimated to be 1.3% in countries with high transmission rates and to cost Africa more than $12 billion annually (WHO, 2009).

Several attempts were made during the last years to eradicate malaria. Among these were the widespread distribution of insecticide-treated bed nets as well as extensive indoor spraying and providing of antimalarials. All these measures were demonstrated to reduce malaria mortality and morbidity in several countries but nevertheless they do not provide a general solution for the problems in sub-Saharan Africa and South-East Asia (Greenwood et al., 2005; Mendis et al., 2009). One of the main reasons for the failure to eradicate malaria is the consequent emergence of resistant *Plasmodium* parasite strains to the available drugs. Drugs like chloroquine, mefloquine, quinine, amodiaquine and sulfadoxine-pyrimethamine became more and more useless. This led to the application of artemisinin-based combination therapies (ACT). The class of artemisinins induces rapid clearance of asexual blood stages and in addition also reduces the number of sexual stages, which are responsible for transmission by the mosquito. A drawback of this class is its short half-life. But when combined with a longer lasting partner drug, the ACT is expected to allow fewer development of drug resistance (Lin et al., 2010). But not only the parasites themselves developed resistance. Also the *Anopheles* mosquito vector became first resistant to DDT, which was used intensively for indoor and outdoor spraying, as well as to the repellents used for treatment of bed nets (Enayati and Hemingway, 2010). Thus, new intervention strategies need to be developed, including transgenic mosquitoes, larviciding in urban areas as well as more effective drugs and ultimately anti-infective vaccines (Enayati and Hemingway, 2010; Mendis et al., 2009).

1.1.1 The causative agent of malaria: *Plasmodium*

The causative agent of malaria are eukaryotic single-celled organisms of the genus *Plasmodium*, belonging to the phylum Apicomplexa (class: *Sporozoa*; order: *Coccidia*; suborder: *Haemosporidiae*; family: *Plasmodiidae*), which comprises more than 5000 protozoan parasites. Among these, important human and animal pathogens like *Toxoplasma gondii*, *Eimeria spp.* and *Theileria spp.* can be found. The phylum is characterized by the presence of unique specialized organelles in addition to the 'usual' cellular components comprising mitochondrium, Golgi apparatus and nucleus. During evolution apicomplexans additionally obtained a red algae-derived apicoplast, dense granules, the apical polar

ring, serving as a microtubule-organizing center, the conoid as well as micronemes and rhoptries, the latter two being an unique set of secretory vesicles. All these structures except the apicoplast define the apical complex (Kappe et al., 2004). Micronemes and rhoptries, both located at the apical tip of the invasive stages of *Plasmodium* (ookinete, sporozoite and merozoite), and the proteins they contain are important for apicomplexan motility, host cell invasion and generation of the non-phagosomal parasitophorous vacuole (PV) (Baum et al., 2008; Hakansson et al., 2001; Kappe et al., 2004; Lingelbach and Joiner, 1998). The apicoplast is homologous to the chloroplasts found in plants and was acquired by secondary endosymbiosis of a red algae, which in turn had taken up a free-living cyanobacterium (Kalanon and McFadden, 2010). Similar to plant chloroplasts, it is semi-autonomous with its own genome and expression machinery (Vaishnava and Striepen, 2006; Waller and McFadden, 2005). Genomic analyses demonstrated that the apicoplast harbors pathways for the biosynthesis of fatty acids, isoprenoids and haem (Gardner et al., 2002; Ralph et al., 2004).

Almost 120 different *Plasmodium* species have been identified until today. They all share the characteristic of host-specificity. Until recently, four species were described to be pathogenic to man: *Plasmodium falciparum*, *Plasmodium vivax*, *Plasmodium malariae* and *Plasmodium ovale* (Carter and Mendis, 2002). But the recent finding that increasing numbers of humans were infected with *Plasmodium knowlesi* in Sabah and Sarawak, Malaysia, and later on also in other parts of southeastern Asia led to the inclusion of *P. knowlesi* as the fifth human malaria parasite (White, 2008). Each of these species elicits a different kind of malaria in the human host. Infection with *P. falciparum* leads to the most severe and potentially fatal Malaria tropica, found in sub-Saharan Africa and also infection with *P. knowlesi*, if untreated, can rapidly reach potentially lethal parasite densities in the blood. Malaria tertiana is elicited in the sub-tropics and tropics worldwide by the most widespread malaria parasite *P. vivax*, while *P. ovale* also induces this form of malaria, but is restricted to West Africa. Also distributed worldwide, but with a much lower frequency is Malaria quartana, caused by *P. malariae*. The human *Plasmodium* parasites do have in common the induction of fevers to their affected host, but according to the different length of asexual reproduction within the red blood cells, the periodicity differs. *Plasmodium ovale* and *P. vivax* induce fevers every 48h, while infection with *P. malaria* is accompanied with fevers every 72h. For infection with *P. falciparum* no such periodic fevers can be observed (Tuteja, 2007; White, 2008). Many other *Plasmodium* species developed host specificities to animals comprising primates and rodents as well as birds and reptiles. Rodents can be infected with *P. berghei*, *P. yoelii*, *P. chabaudi* and *P. vinckei* while the causative agent for malaria in birds are *P. gallinacum* and *P. relictum*. All *Plasmodium* species are transmitted to their vertebrate host by an arthropod-vector. The human and rodent species are transmitted by mosquitoes of the genus *Anopheles* (phylum: Arthropoda; class: *Insecta*; order: *Diptera*; suborder: *Nematocera*; family: *Culcidae*; subfamily: *Anophelinae*), of which 400 species are known and distributed worldwide. 60 of these species are able to transmit the human *Plasmodium* parasites under natural conditions. Among these, the most important ones are *A. gambiae*, *A. funestus*, *A. latens* and *A. cracens* (Collins, 2012; Tuteja, 2007).

As working with human subjects or samples encounters many limitations due to lack of clinical history of infections and legal authorization procedures, rodent *Plasmodium* species came more and more into the focus of research. In addition, establishment of the whole malaria life cycle under laboratory conditions provide many advantages. For this purpose, the parasite is transmitted from appropriate laboratory mouse strains to *Anopheles stephensi* mosquitoes kept under defined conditions (Killick-Kendrick, 1978; Scheller et al., 1994; Sinden, 1996; Yoeli et al., 1965). In this work the rodent parasite strain *P. berghei* was used, which is naturally transmitted by *Anopheles dureni millecampsi* to its natural mammalian hosts *Grammomys surdaster*, *Praomys surdaster* and *Leggada bella*, all of them mainly found in Zaire (Killick-Kendrick, 1978; Landau and Chabaud, 1994).

1.1.2 The *Plasmodium* life cycle

The *Plasmodium* life cycle is highly complex as it alternates between the insect primary host, which serves as vector and is place of the sexual reproduction (gamogony) and therefore also defined as definitive host, and the vertebrate secondary host, where the asexual replication (schizogony) takes place. The life cycle involves several different host tissues in which the parasite undergoes different morphological transitions. Thus, the parasite has to adapt to the different environmental conditions reigning within the two hosts and exploit them for its benefit. But at the same time the parasite has to circumvent immune responses of the host elicited by its presence. Therefore the parasite has developed specialized protein expression, which is required for its survival (Tuteja, 2007).

Infection with *Plasmodium* in the vertebrate host is initiated by the bite of a female Anopheline mosquito taking a blood meal. During this blood meal, a few dozen infectious salivary gland sporozoites are injected into the host's dermis. The sporozoites move through the dermis and access the blood stream by entering a blood vessel or they enter the lymphatic circulation (Amino et al., 2006; Frischknecht et al., 2004; Vanderberg and Frevert, 2004).

Once in the circulatory system, the sporozoites rapidly reach the liver sinusoids. Due to specific interactions between *Plasmodium* surface proteins like the circumsporozoite protein (CSP) and host molecules, such as highly sulfated heparan sulfate proteoglycans (HSPGs) on the liver cells, the sporozoites arrest in the liver sinusoids (Coppi et al., 2007; Sinnis and Coppi, 2007). After sequestration of the sporozoites, they cross the sinusoidal layer primarily through Kupffer cells, the resident macrophages of the liver (Baer et al., 2007b; Frevert et al., 2006), followed by traversal of several hepatocytes before they productively invade a final host hepatocyte and form a parasitophorous vacuole (PV), surrounding the parasite and forming a physical barrier between host and parasite (Lingelbach and Joiner, 1998). During their migration through cells, the sporozoites breach the hepatocyte plasmamembrane, which is then rapidly repaired (Mota et al., 2001). Within their PV, the invasive sporozoite dedifferentiates and develops into a liver trophozoite, followed by further growth and multiple rounds of DNA replication and nuclear divisions without immediate mitosis, called schizogony, resulting in a multinuclear syncytium (Vaughan et al., 2008), which

requires nutrients from the host cell and inhibition of host cell apoptosis (van de Sand et al., 2005). Repeated invaginations of the parasite membrane lead to formation of individual first-generation merozoites. When merozoite growth is completed, host cell death is induced and merozoite-filled vesicles, called merosomes, bud off the dying hepatocyte and into the sinusoidal lumen (Baer et al., 2007a; Sturm et al., 2006; Tarun et al., 2006). Via the blood stream the merosomes reach the lungs, where they accumulate and rupture to release the individual merozoites (Vaughan et al., 2008).

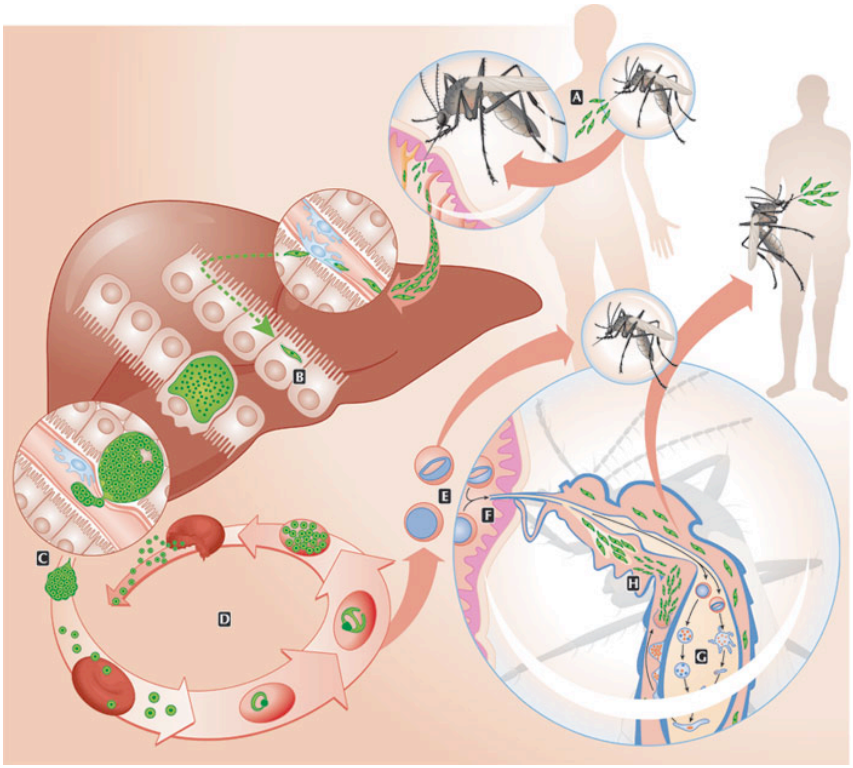

Figure 1.1.2: The *Plasmodium* life cycle (Portugal et al., 2011). *Plasmodium* sporozoites are injected into the mammalian host's dermis during the blood meal of a female Anopheline mosquito (A). After reaching a blood vessel within the dermis, the sporozoites are eventually transported to the liver, where they first traverse several liver cells before they invade a final one (B). Inside the hepatocyte they form a parasitophorous vacuole (PV) and inside this PV they replicate asexually and develop to first-generation merozoites, which are released into the blood stream in form of merosomes (C). During cycles of asexual replication, merozoites infect red blood cells (D). If replication cycles originate female and male gametocytes (E), they are ingested into the midgut by a female mosquito during another blood meal (F). Within the mosquito midgut, fertilization of gametes occurs, leading to formation of ookinetes, followed by generation of oocysts (G). From the oocysts released sporozoites migrate to the salivary glands of the mosquito and are released during the next blood meal (H).

Merozoites recognize and attach to red blood cells via interaction of the major merozoite surface protein 1 (MSP1) (Goel et al., 2003; Holder, 1994), followed by reorientation of the apical end of the merozoite towards the erythrocyte surface, supported by the apical membrane antigen 1 (AMA1) (Mitchell et al., 2004). Penetration of the red blood cell by the merozoite is associated with simultaneous formation of a PV (Lingelbach and Joiner, 1998). After completion of invasion, the merozoite transforms into a ring stage, followed by a growth phase leading to the formation of a trophozoite. The trophozoite undergoes asexual replication, the schizogony, generating 8-24

merozoites, depending on the parasite strain, which bud off the central syncytium. This is followed by secretion of exonemes initiating exit from the PV and subsequently from the host erythrocyte into the blood. By invasion of neighboring red blood cells a new cycle of schizogony is started. The rodent infecting *P. berghei* parasites prefer invasion of young, immature red blood cells, the so-called reticulocytes, but they are able to infect mature red blood stages as well during high parasitemia (Deharo et al., 1996). In contrast to this, human malaria parasites normally invade only mature red blood cells. Only the erythrocytic phase of malaria is symptomatic to the host. It is associated with fever, diarrhea and headaches in the case of mild or uncomplicated malaria, but can also induce anemia, respiratory insufficiency, organ failure and coma when suffering from severe or complicated malaria. Only if replication cycles produce male and female gametocytes, the malaria life cycle can be continued. These stages are taken up by a mosquito during another blood meal. According to changes in temperature (Sinden and Croll, 1975), pH value (Billker et al., 2000) and the presence of xanthurenic acid (Arai et al., 2001) within the mosquito midgut, the nucleus of a male gametocyte divides into four to eight nuclei, giving rise to microgametes, which are able to fuse with mature female gametocytes (macrogametes) to form a zygote. This zygote further develops to form an infective, motile ookinete, which crosses the mosquito midgut wall. Upon egress at the basal site of the midgut cell, the ookinete encounters the basal lamina. Here it arrests and transforms into an oocyst (Sinden and Billingsley, 2001). This oocyst gives rise to sporozoites by several mitotic divisions within a sporoblast. After active egress from the sporoblast, the elongated haploid sporozoites enter the haemolymph. When passing the salivary glands, the sporozoites adhere to the basal lamina and invade the glands from the basal side. Finally, the sporozoites accumulate in the salivary duct and can be deposited into the host dermis during a subsequent blood meal of the mosquito (Matuschewski, 2006; Mueller et al., 2010), initiating a new round in the parasite's life cycle.

1.1.3 *Plasmodium* liver-stage development

In contrast to the erythrocytic replication cycle, which induces the symptoms typical for malaria, the liver phase of the parasite is clinically silent. After deposition of *Plasmodium* sporozoites into the host's dermis (figure 1.1.2), they enter blood vessels and reach the liver sinusoid via the blood stream. One typical feature of the liver sinusoid (figure 1.1.3) is a layer of fenestrated endothelium cells, which allows flow-through of the oxygen-rich blood from the hepatic artery as well as nutrient-rich blood from the portal vein. The space of Disse separates the endothelial cells from the hepatocytes. It is hypothesized that highly sulfated heparan sulfate proteoglycans (HSPGs) protrude from this space of Disse, as well as from hepatocytes and stellate cells, through the fenestration into the sinusoid (Frevert, 2004). Due to the high sulfation level of the HSPGs within the liver, sporozoites are triggered to switch to invasion mode (figure 1.1.3, figure 1.1.4A). In contrast to this, the sulfation level of HSPGs within endothelial cells in the dermis is rather low, which induces migration of sporozoites (Coppi et al., 2007). After the sporozoite recognizes the HSPGs in the liver sinusoid, the circumsporozoite

surface protein (CSP) is processed to expose the C-terminal cell-adhesive thrombospondin repeat (TSR) domain, which allows attachment of the sporozoite to the endothelium (Coppi et al., 2011). But also other host molecules are important for recognition and invasion of hepatocytes. Among these are the serum glycoprotein fetuin A, the tetraspanin CD81 and scavenger receptor B1 (SRB1) (Graewe et al., 2012; Jethwaney et al., 2005; Prudencio et al., 2006).

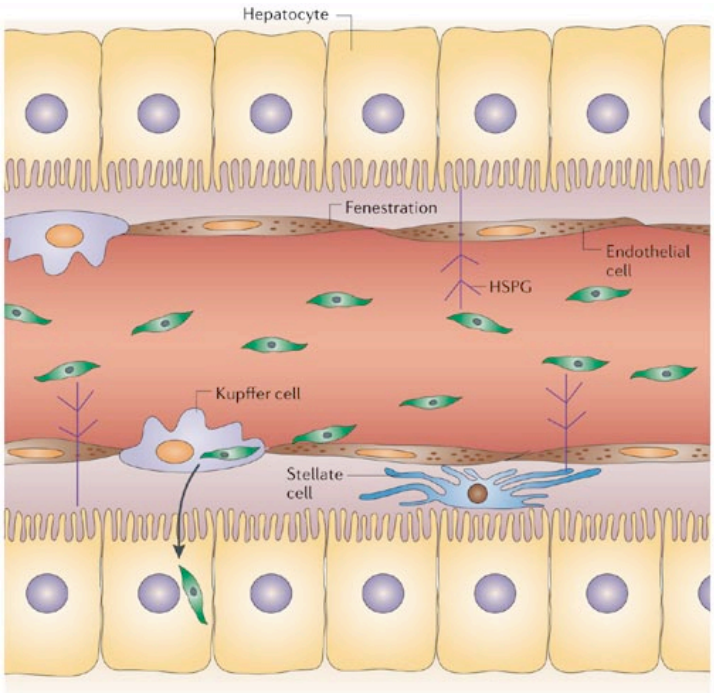

Figure 1.1.3: The liver sinusoid (Prudencio et al., 2006). The liver sinusoid comprises different cell types. After interaction with heparan sulfate proteoglycans (HSPGs) from hepatocytes and stellate cells, sporozoites sequester and cross the sinusoid via Kupffer cells.

In a next step the sporozoite traverses through Kupffer cells to enter the space of Disse (Baer et al., 2007b; Frevert et al., 2006). After crossing the space of Disse, the sporozoite traverses through several hepatocytes before it invades a final one and forms a parasitophorous vacuole (PV) (Mota et al., 2001) (figure 1.1.4B). This traversal is associated with breaching of the respective cells, followed by rapid repair (Mota et al., 2001). This cell wounding may release hepatocyte growth factor (HGF), which in turn promotes survival of hepatocytes (Leiriao et al., 2005a). Parasitic proteins have been shown to be important for this cell traversal. Sporozoite microneme protein essential for cell traversal (SPECT), SPECT2, cell traversal protein for ookinete and sporozoite (CelTOS) and the phospholipase *Pb*PL were reported to be associated with this process. SPECT2 and *Pb*PL seem to be involved in pore formation, while CelTOS may be required for the movement through the host cell cytosol (Bhanot et al., 2005; Ishino et al., 2005a; Ishino et al., 2004; Kariu et al., 2006). A different set of proteins is reported to be involved in the final invasion step. CSP seems to have an active role in sporozoite attachment to the hepatocyte, while thrombospondin related anonymous protein (TRAP) is required for internalization. Also apical membrane antigen 1 (AMA1) as well as *Pb*36p and *Pb*36 were reported

to be important either for invasion or recognition of hepatocytes and thus to commit infection (Ishino et al., 2005b; Matuschewski et al., 2002a; Pinzon-Ortiz et al., 2001; Silvie et al., 2004).

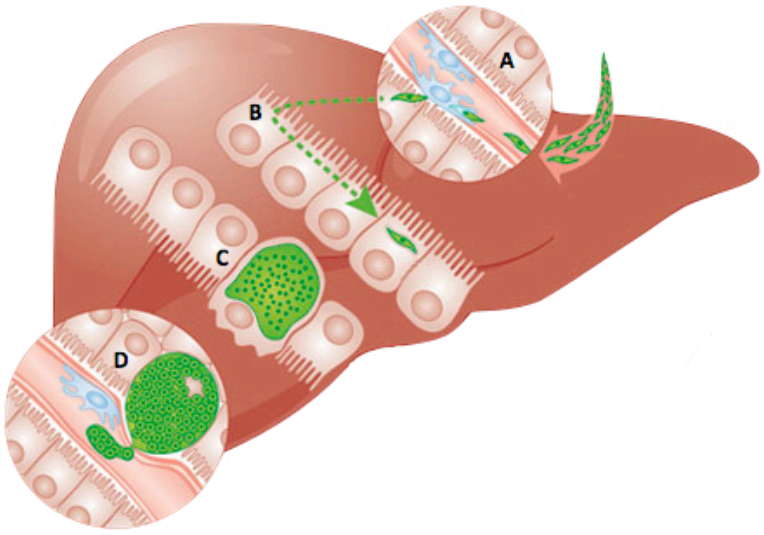

Figure 1.1.4: The *Plasmodium* liver phase (Portugal et al., 2011). *Plasmodium* sporozoites reach the liver sinusoid via blood vessels and after crossing the sinusoid layer through Kupffer cells (A), they traverse several hepatocytes (B) before invading a final one, where they form a parasitophorous vacuole (PV). Inside this PV they replicate asexually, forming merozoites (C). These merozoite-filled vesicles, merosomes, bud off the dying hepatocyte and enter the blood stream (D) via which they reach the lungs.

Once the parasite established itself within a hepatocyte, it quite successfully blocks its host cell to undergo programmed cell death (Leiriao et al., 2005a; Rennenberg et al., 2010; van de Sand et al., 2005). But in spite of this observed inhibition of programmed cell death, also uptake of apoptotic, infected hepatocytes by macrophages and dendritic cells in the liver was reported and is discussed to be associated with presentation of parasitic antigens (Leiriao et al., 2005b; Renia et al., 2006). During the first 24h within the invaded hepatocyte, the parasite remodels its parasitophorous vacuolar membrane (PVM). Furthermore it changes its shape by rounding up to a trophozoite, which was observed to be located in close proximity to the host cells nucleus (Graewe et al., 2012). Knockout of several parasite genes proved their importance for this early stage of development. Among these are up-regulated in infective sporozoites 3 and 4 (*uis3*, *uis4*) and *Pb36p* (Matuschewski et al., 2002b; Mueller et al., 2005a; Mueller et al., 2005b; van Dijk et al., 2005). After generation of a trophozoite, the parasite's nucleus divides repeatedly and generates within 35h up to 30,000 new nuclei, the PV is following this growth by expanding its size (Graewe et al., 2012) (figure 1.1.4C). Due to this rapid growth and the associated synthesis of large amounts of additional membrane, the parasite needs supply with huge amounts of e.g. lipids. As the parasite is not able to provide all these lipids by itself, it is most likely that it takes up the required lipids from the host hepatocyte, as demonstrated by direct interaction between parasitic UIS3 and host liver fatty acid binding protein (L-FABP) (Mikolajczak et al., 2007), as well as other host molecules, like Apolipoprotein A1 (ApoA1), which localizes to the PV 24h post infection and seems to interact with UIS4 (A.-K. Mueller, personal

communication, Schulz et al., unpublished data). Furthermore it was shown, that *Plasmodium* liver stages continuously divert cholesterol from the host hepatocytes until the release of merozoites (Labaied et al., 2007). The rapid division of the parasite leads to formation of a multinucleated schizont, the so-called syncytium, postponing cytokinesis until the nuclear division process is finished. When the division is complete, cytokinesis takes place and daughter cells, the merozoites, are formed by repeated invaginations of the parasite membrane (Graewe et al., 2012).

After formation of merozoites, parasite proteins are activated by proteases and released to first permeabilize and subsequently disrupt the PVM (Sturm et al., 2009), releasing the merozoites into the host hepatocyte, which then detaches from its surroundings (Graewe et al., 2012). In parallel host cell death is induced (Heussler et al., 2010; Sturm et al., 2006) and vesicles, so-called merosomes, containing up to several thousand merozoites enveloped into host-cell membrane, bud off the dying hepatocyte and are released into adjacent blood vessels (Baer et al., 2007a; Sturm et al., 2006), thus circumventing the host's immune system (figure 1.1.4D). Finally the merosomes accumulate within the pulmonary capillaries of the lung, where they release their content for infection of red blood cells (Baer et al., 2007a).

An exception from this continuously progressing liver stage development is provided by *P. vivax* and *P. ovale*, because they are able to generate dormant liver stages, hypnozoites, which remain in the liver for weeks to many years before they progress with the onset of pre-erythrocytic schizogony, and thus resulting in relapses of the malaria infection (Tuteja, 2007).

1.1.4 Attenuation of *Plasmodium* liver-stage development

As the liver stage of the *Plasmodium* parasite is the only clinically silent stage of the entire pathogenic cycle, it provides an ideal target for drug intervention as well as vaccine development. Within the last decades, several reports demonstrated the success of attenuated whole-organism vaccines, aiming at this specific step of the parasites' life cycle. A report from 1941 demonstrates how old this idea already is (Mulligan et al., 1941). Mulligan et al. inactivated *Plasmodium gallinaceum* sporozoites by ultra-violet irradiation and injected them into chicken. Upon injection of large doses of these irradiated sporozoites, they were able to induce partial active immunization against mosquito-borne infection with the homologous *Plasmodium* strain. A study forming the basis for subsequent attenuation strategies was performed in 1967 (Nussenzweig et al., 1967). Random point-mutations in the parasites' genome were induced by γ-irradiation. This did not affect the sporozoite survival or its capacity to invade hepatocytes. But it resulted in an arrest of the parasite during different stages of liver-stage development. If applied in repeated doses, these radiation-attenuated sporozoites (RAS) are able to induce sterile protection in animals and humans to subsequent challenge with homologous *Plasmodium* parasites (Hoffman et al., 2002; Nussenzweig et al., 1967). As γ-irradiation induces random DNA breaks within the genome, the result is a highly heterogenous population of

sporozoites and hence the induced immune mechanisms in the mammalian host are likely to be different.

Thus a new strategy was developed, using defined gene deletions and generating homogenous populations of genetically attenuated parasites (GAP). Genetic deletion of two genes, up-regulated in infectious sporozoites (*uis3* and *uis4*), gave rise to *Plasmodium berghei* parasites that were able to complete the life cycle normally except for the liver-stage development, where they growth-arrested 24h after hepatocyte invasion (Mueller et al., 2005a; Mueller et al., 2005b). Immunization with these attenuated parasites completely protected mice against subsequent infectious WT sporozoites challenge (Mueller et al., 2005a; Mueller et al., 2005b). Another study demonstrated that targeted deletion of the early liver-stage specific gene *p36p*, a member of the 6-cysteine family of *Plasmodium* surface proteins, elicited lasting and complete immunity against re-infection (van Dijk et al., 2005). As the protein p36p is assumed to be involved in hepatocyte invasion, knock-out of *p36p* as well as its neighboring paralogous gene, *p36*, led to failure of productive hepatocyte invasion, while traversal of these cells was not affected (Ishino et al., 2005b). It was further demonstrated that deletion of *p36* together with *p52* in *Plasmodium yoelii* resulted in complete attenuation of the liver-stage development and conferred sterile immunity against natural infection (Labaied et al., 2007). Protection induced by the *uis3*$^{-}$ and *uis4*$^{-}$ parasites was associated with induction of strong, interferon-γ-dependent CD8^{+} T-cell responses (Jobe et al., 2007; Mueller et al., 2007; Tarun et al., 2007).

Another still experimental approach for whole-organism vaccines is the exposure of wildtype sporozoites under drug cover. So far three different drugs have been reported for this approach and have been shown to induce pre-erythrocytic immune responses (Matuschewski et al., 2011). Exposure to infective sporozoites during oral administration of Chloroquine (CQ) was able to induce protection, mainly by CD8^{+} T-cells (Beaudoin et al., 1977; Belnoue et al., 2004), but brief and mild malaria episodes can occur (Matuschewski et al., 2011). Sporozoite exposure under Primaquine (PQ) cover induces long lasting protection by taking advantage of the mode of action of PQ, which kills intrahepatic parasites (Putrianti et al., 2009). However, a drawback of this approach is associated with severe side effects of PQ (Lell et al., 2000). The third approach might be the most promising one. In this case, individuals are exposed to infectious wildtype sporozoites under azithromycin (AZ) cover. This antibiotic is licensed for children and women during pregnancy due to its excellent safety record and furthermore accumulates within the hepatic tissue as a result of its slow elimination from the body (Girard et al., 1987). Administration of AZ induces a delayed death phenotype allowing the malarial parasite to complete the maturation of liver stages but ending in the development of nonviable liver-stage merozoites (sterile merozoites are formed) (Friesen et al., 2010). Again a robust CD8^{+} T-cell mediated immune response against subsequent challenges with mosquito-derived salivary gland sporozoites is induced and confers the observed protection (Matuschewski et al., 2011).

1.2 MicroRNAs

MicroRNAs (miRNAs) are small non-coding RNAs of typically ~21 nucleotides found in metazoa, plants and protozoa where they serve as regulators of gene expression. They were initially discovered in *Caenorhabditis elegans*. Lee et al. described small RNAs encoded by the gene *lin-4*, which were complementary to *lin-14* and thus negatively regulated the level of LIN-14 protein (Lee et al., 1993). In parallel, Wightman et al. observed the same: a temporal gradient in LIN-14 protein, generated post-transcriptionally by multiple elements located in the *lin-14* 3'UTR, which were regulated by the heterochronic gene *lin-4* (Wightman et al., 1993). Today this family of small RNAs is predicted to control the activity of 30-60% of all protein coding genes by binding to and thus typically silencing the corresponding mRNAs in mammals (Filipowicz et al., 2008; Friedman et al., 2009). But also enhancing functions in RNA synthesis are reported for miRNAs (Jopling et al., 2008; Jopling et al., 2005). Furthermore, it was shown that miRNAs have the capacity to control the epigenetic machinery by direct targeting of its enzymatic components (Iorio et al., 2010). Therefore they participate in the regulation of almost every cellular process investigated so far, such as differentiation, embryogenesis, inflammation, viral infection and carcinogenesis (Bartel, 2009; Bushati and Cohen, 2007).

1.2.1 Biogenesis and function of miRNAs – the RNAi machinery

MiRNAs are encoded in introns of coding genes and in introns and exons of non-coding transcripts (Rodriguez et al., 2004). Their biogenesis comprises several steps, which initiate in the nucleus and later continue in the cytoplasm (figure 1.2.1). They are transcribed by RNA polymerase II as precursor molecules (pri-miRNAs), which fold into hairpin structures. The hairpin structures characteristically contain imperfectly base-paired stems. These precursor molecules often contain sequences for several different miRNAs and are processed by the RNaseIII endonuclease Drosha (Lee et al., 2003), which typically functions in complexes with proteins containing dsRNA-binding domains (dsRBDs). In mammals the dsRBD protein binding to Drosha is the DiGeorge syndrome critical region gene 8 (DGCR8) (Landthaler et al., 2004). Together with Drosha, it forms a complex called microprocessor which cleaves the pri-miRNAs to precursor-miRNAs (pre-miRNAs), characterized by a ~70 nucleotide hairpin structure with a 2-nt 3' overhang (Bushati and Cohen, 2007; Filipowicz et al., 2008; Krol et al., 2010; Rana, 2007). In *C. elegans*, *D. melanogaster* and mammals spliced-out introns perfectly corresponding to pre-miRNAs (mirtrons) were observed, which circumvent processing by Drosha/DGCR8 (Filipowicz et al., 2008; Krol et al., 2010). After binding to the 2-nt 3' overhang, Exportin-5 (Xpo-5) (Brownawell and Macara, 2002; Yi et al., 2003) transports the pre-miRNA into the cytoplasm. For further cleavage of the pre-miRNA, the cytosolic RNaseIII endonuclease Dicer (Hutvagner et al., 2001) forms a complex with the dsRBD protein TAR RNA binding protein (TRBP) (Gatignol et al., 1991) to generate the miRNA:miRNA* duplex containing 2-nt 3' overhangs.

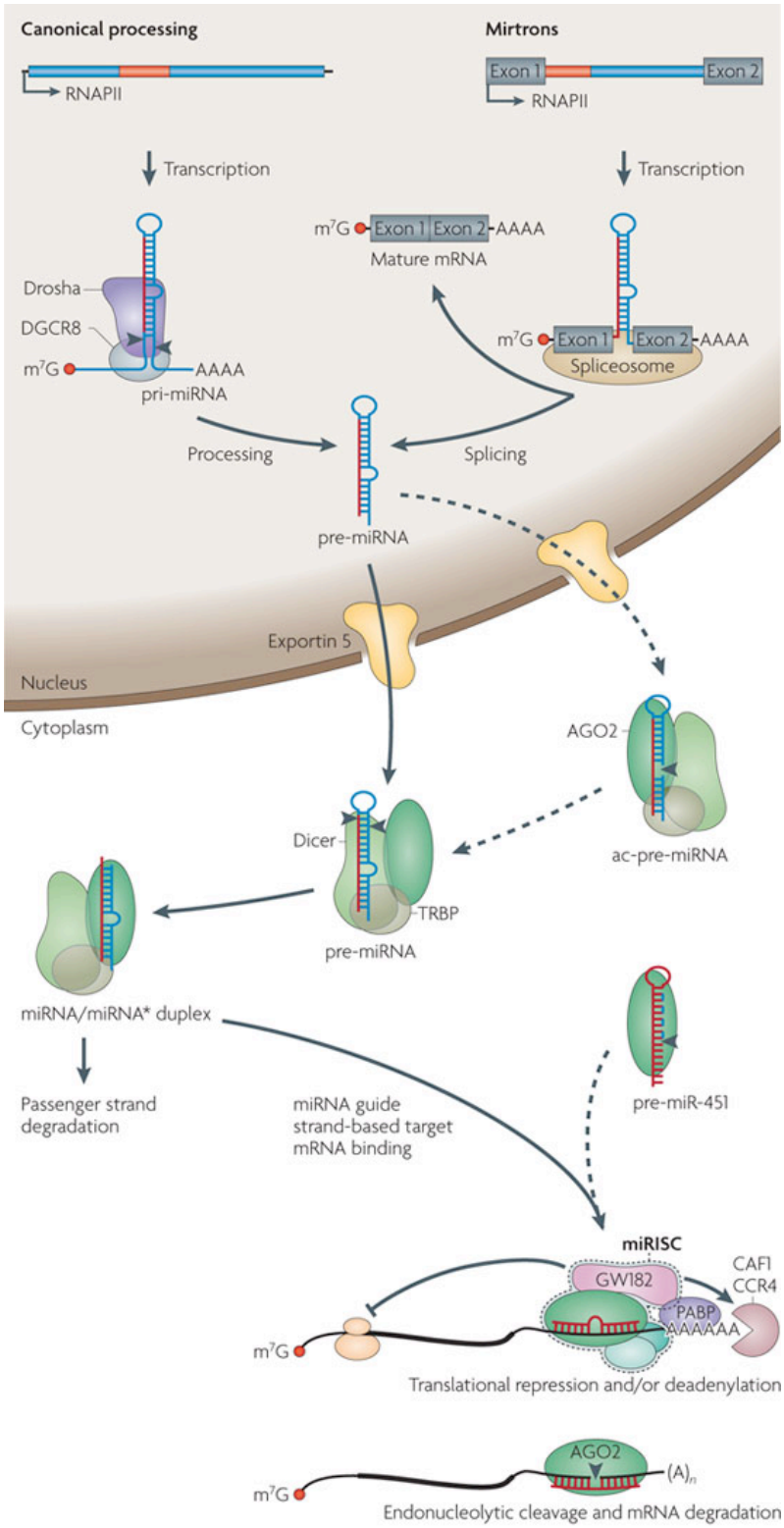

Figure 1.2.1: Biogenesis of miRNAs and their assembly in miRNA-induced silencing complexes (miRISC) (Krol et al., 2010). MicroRNAs are processed in several steps taking place both in the nucleus and in the cytoplasm from a primary miRNA (pri-miRNA) to a mature miRNA. A detailed description of this process can be found in section 1.2.1.

In mammals, Argonaute-2 (Ago-2) can support or even completely replace Dicer processing by cleaving the 3' arm of some pre-miRNAs, thus forming a processing intermediate called Ago-2-cleaved

precursor miRNA (ac-pre-miRNA). Processing of pre-miR-451 is independent of Dicer, but requires cleavage by Ago-2 (Cheloufi et al., 2010; Cifuentes et al., 2010; Krol et al., 2010; Yang et al., 2010).

Once incorporated into the miRNA-induced silencing complex (miRISC) containing a member of the Argonaute family, the miRNA guides this complex to the mRNA targets by base-pairing interactions (Bushati and Cohen, 2007; Filipowicz et al., 2008; Krol et al., 2010). Mammals contain four Ago proteins, Ago-1 to Ago-4. Ago-2 is the only family member possessing the capability to directly cleave a targeted mRNA in the context of the miRISC due to its RNase-H like P-element induced wimpy testis (PIWI) domain (Liu et al., 2004; Meister et al., 2004). The miRNA 5' nucleotides 2-8 ("seed region") typically base-pair perfect with the 3' UTR of the target mRNA. In the regions adjacent to the seed region the complementarity between miRNA and target mRNA varies. If base-pairing is perfect or nearly perfect, Ago-2 mediated cleavage of the target mRNA can be observed (Huntzinger and Izaurralde, 2011). If this base-pairing is imperfect, four distinct ways for translational repression in mammals have been proposed: inhibition of translation initiation, inhibition of translation elongation, co-translational protein degradation, and premature termination of translation (Carthew and Sontheimer, 2009; Eulalio et al., 2008; Fabian et al., 2010; Filipowicz et al., 2008; Huntzinger and Izaurralde, 2011; Wu and Belasco, 2008).

1.2.2 MiR-21, miR-155 and immunity

MiRNAs were found to be involved in regulation of immunity, including the development and differentiation of immune cells, antibody production, antigen presentation, T-cell receptor signaling as well as release of inflammatory mediators (Alam and O'Neill, 2011; Baltimore et al., 2008; Bi et al., 2009; Lu and Liston, 2009; Pedersen and David, 2008; Turner et al., 2011). While a large collection of miRNAs participate in the fine-tuning of many aspects of the immune system, the following two sections will focus on two miRNAs, miR-21 and miR-155, which proved to be particularly important for this study.

1.2.2.1 MiR-21 and immunity

MiR-21 was shown to be involved in the control of malignant cell proliferation, invasion and metastasis and is therefore referred to as "oncomiR" or "oncogene" (Connolly et al., 2008; Meng et al., 2007). Expression of miR-21 was found to be up-regulated in the context of several different types of cancer like hepatocellular carcinoma (Bihrer et al., 2011; Connolly et al., 2008; Jiang et al., 2008; Karakatsanis et al., 2011; Xu et al., 2011), breast cancer (Si et al., 2007), colorectal cancer (Shibuya et al., 2010) and glioblastoma (Chan et al., 2005) and is frequently associated with poor prognosis. It was observed that when up-regulated, miR-21 has anti-apoptotic effects (Chan et al., 2005; Li et al., 2009; Si et al., 2007). Several direct targets of miR-21 have been identified so far that may explain the anti-

apoptotic function of this miRNA as well as its influence on invasion and formation of metastasis. One of the first identified targets was the tumor suppressor gene tropomyosin 1 (TPM1) (Zhu et al., 2007). The fact that TPM1 was implicated in cell migration may partly explain the influence of miR-21 on invasion and formation of metastasis. Other targets identified and participating in invasion and metastasis formation were programmed cell death 4 (PDCD4) and maspin, which both reduce invasiveness of cells. Expression of both genes was inversely correlated with miR-21 expression in breast cancer (Zhu et al., 2008). Several studies also identified the phosphatase and tensin homolog (PTEN) tumor suppressor gene as a direct target of miR-21 and hence supported a role of this miRNA in tumor growth, invasion and formation of metastasis (Lou et al., 2010; Meng et al., 2007; Zhang et al., 2012a; Zhang et al., 2010). Other tumor-associated target genes are those encoding reversion-inducing-cysteine-rich protein with kazal motifs (RECK) (Ziyan et al., 2011) and tumor-associated protein 63 (TAp63) (Papagiannakopoulos et al., 2008). Notably miR-21 is also involved in controlling immune responses independent of malignancies. In the context of hypoxia, miR-21 is positively regulated via an AKT-dependent pathway and mediates its anti-apoptotic effects via suppression of Fas ligand (FasL) (Sayed et al., 2010). Furthermore, miR-21 is induced upon LPS stimulation in a NF-κB-dependent manner in macrophages via MyD88, resulting in promotion of IL-10 production by regulation of PDCD4 (Alam and O'Neill, 2011). Thus, miR-21 might be involved in re-establishing a homeostatic state of the immune system. Another study validated *WNT1* and *JAG1* as targets for miR-21 and showed that translational repression of these genes fostered differentiation of dendritic cells (DC) from monocytes (Hashimi et al., 2009). Finally miR-21 is important for Toll-like receptor signaling (Quinn and O'Neill, 2011) and is up-regulated in antigen-experienced $CD8^+$ T-cell subsets (Salaun et al., 2011).

1.2.2.2 MiR-155 and immunity

Similar to miR-21, miR-155 has also been labeled “oncomiR”. Encoded within a section of the non-coding RNA known as *bic* (B-cell integration cluster) (Tam, 2001; Tam et al., 1997), elevated expression of this miRNA was observed in B-cell lymphomas and Hodgkin’s lymphomas (Eis et al., 2005). Besides its oncogenic influence on cells of the myeloid and lymphoid lineage, miR-155 plays a significant role in immune responses (Baltimore et al., 2008; Bi et al., 2009; Lu and Liston, 2009; Pedersen and David, 2008). It was shown that miR-155 is involved in innate immunity, as it was up-regulated upon stimulation with LPS. In turn, it targeted and suppressed genes involved in LPS signaling, like Fas-associated death domain (FADD), IκB kinase ε (IKKε), and the receptor (TNFR superfamily)-interacting serine-threonine kinase 1 (Ripk1), while it enhanced TNF-α translation (Tili et al., 2007). DCs depend on miR-155 in two ways: on the one hand, for their maturation, and on the other hand, for their optimal function (Rodriguez et al., 2007). In macrophages the intracellular expression of miR-155 is induced during the inflammatory response to viral as well as bacterial triggers like tumor necrosis factor, interferons and other TLR ligands (O'Connell et al., 2007). A study

investigating the potential effect of miR-155 up-regulation on hepatitis B virus (HBV) infection in human hepatoma cells described miR-155 as a positive regulator of JAK/STAT signaling by its targeting of SOCS1 (suppressor of cytokine signaling 1). This led to an increase in IFN-inducible antiviral gene expression and enhanced innate antiviral immunity, in turn resulting in a mild anti-HBV effect (Su et al., 2011a). In B chronic lymphocytic leukemia (B-CLL) and in osteogenic differentiation a suppressive effect of miR-155 on SOCS1 expression is reported as well and SOCS1 is mentioned as direct target for miR-155 (di Iasio et al., 2012; Wu et al., 2012; Zhang et al., 2012b). In the context of breast cancer expression of miR-155 is inversely correlated with SOCS1 expression (Jiang et al., 2010). Another study demonstrated that miR-155 modulates a microglia-mediated immune response by down-regulating SOCS1. This leads to a promotion of cytokine and nitric oxide production (Cardoso et al., 2012). Furthermore, inducible miR-155 feedback promotes type I interferon signaling in antiviral innate immunity and again SOCS1 is described as respective target of miR-155 (Wang et al., 2010). Finally also allograft survival is affected by miR-155 which directly regulates SOCS1 expression (Zhang et al., 2011). However miR-155 is not only important for innate immunity. In the context of experimental autoimmune encephalomyelitis, miR-155 promoted T-cell-dependent tissue inflammation by inducing polarization of T_h17 cells (O'Connell et al., 2010). High levels of miR-155 expression are induced upon antigen receptor stimulation of B-cells, T-cells and macrophages (Baltimore et al., 2008; Turner et al., 2011). Furthermore, miR-155 is essential for the differentiation of switched plasmablasts into mature antibody-secreting plasma B-cells, the induction of T_h1 cells (Calame, 2007; Teng et al., 2008; Turner and Vigorito, 2008; Vigorito et al., 2007), and it is up-regulated in antigen-experienced $CD8^+$ T-cell subsets (Salaun et al., 2011). As dys-regulation of miR-155 has severe consequences, such as cancerous phenotypes and inflammatory diseases, stringent regulation of this miRNA is utmost essential. It was shown that endogenous IL-10 is able to feed-back on the immune system to regulate miR-155 expression in a STAT3-dependent manner (Quinn and O'Neill, 2011).

1.3 *Plasmodium* and microRNAs

Over the last decade, several groups have aimed to identify miRNAs generated by the Malaria parasite *Plasmodium spp*. and to demonstrate that RNAi is suitable to study gene function in *Plasmodium* parasites. A first study indeed reported a growth defect of *P. falciparum* parasites after application of dsRNA against dihydroorotate dehydrogenase (DHODH), an enzyme essential for the pyrimidine synthesis of the parasite (McRobert and McConkey, 2002). While the authors were able to show a reduction in DHODH mRNA levels by RT-PCR in dsRNA-treated parasites, they failed to confirm these findings by Northern blot analysis. In addition, they could not rule out unspecific effects of dsRNA introduction. A second approach to treat *P. falciparum* with dsRNA against falcipain resulted in an enlargement of parasitic food vacuoles shown to be responsible for digestion of host hemoglobin, consistent with inhibition of falcipain (Malhotra et al., 2002). However, albeit the authors reported an accumulation of 25-nt small RNA species, they could not demonstrate irrevocably that these were true siRNAs processed by the parasite and not by potentially contaminating white blood cells. In a third approach mice infected with *P. berghei* were injected with siRNA against berghepain (Mohmmed et al., 2003). The resulting down-regulation of berghepain mRNA induced an enlargement of food vacuoles similar to the aforementioned results of McRobert and McConkey. Nonetheless, the observed small RNAs specific to berghepain-2 RNA could again not clearly be linked to processing by the parasite.

The aforementioned studies applied exogenous dsRNAs or siRNAs to demonstrate proper processing by the parasite. In two separate but similar studies no such exogenous RNAs have been applied. The authors aimed at identifying endogenous miRNAs produced by *P. falciparum* blood-stages (Rathjen et al., 2006; Xue et al., 2008). However, in both studies only the presence of human miRNAs could be observed. A more recent study demonstrated that *Plasmodium* parasites lack the enzyme machinery that is required for RNAi-based ablation of gene expression (Baum et al., 2009). In addition, the authors did not obtain any experimental evidence for functional RNAi in *Plasmodium*. In contrast to these results, a new study provided evidence for a non-canonical RNAi-related pathway, which allowed transcriptional down-regulation of the hypusinated form of either eIF-5A or DHS upon transfection of *P. berghei* ANKA merozoites with EIF-5A-shRNA or DHS-shRNA (Schwentke et al., 2012).

While the abovementioned early studies all aimed at identifying miRNAs of *Plasmodial* origin and at demonstrating that RNAi can be used in *Plasmodium*, recent research mainly concentrates on the host in this parasite-host-interaction. Several studies were performed to investigate whether *Plasmodium* parasites may influence their host's miRNA expression profile. *Anopheles gambiae* miRNAs expressed upon *P. berghei* infection were isolated using a direct cloning procedure (Winter et al., 2007). They identified 18 miRNAs including three miRNAs that were unique to the mosquito. Only four of these miRNAs, including the three mosquito-specific candidates, were affected by the presence of the parasite. Three of them, aga-miR-34, aga-miR-1174 and aga-miR-1175 were down-

regulated while aga-miR-989 was up-regulated. Two other studies were performed to shed some light on the miRNA expression pattern of the mammalian host. The first used miRNA microarray screening technology to investigate changes in the mouse liver miRNA expression profile after infection with self-healing *P. chabaudi* blood-stage parasites (Delic et al., 2011). The authors found a set of three miRNAs that were up-regulated upon infection whereas 16 miRNAs were down-regulated. These changes were still observed after homologous re-infection. Curiously, the dys-regulated miRNAs were either of unknown function or associated with apoptosis and cancer, but not known to be involved in innate or adaptive immune responses. The second study investigated the host's miRNA expression in experimental cerebral versus non-cerebral murine malaria. Therefore, the authors used quantitative reverse transcription-PCR to analyze selected miRNAs (let-7i, miR-27a, miR-150, miR-210, miR-155, miR-126) that had previously been reported to be involved in the regulation of normal immune and inflammatory responses (El-Assaad et al., 2011). Let-7i, miR-27a and miR-150 were significantly up-regulated in experimental cerebral malaria whereas the remaining three miRNAs remained unchanged. They argued that miR-150 may regulate the accumulation of monocytes and $CD8^+$ T-cells post-infection and miR-27a expression coincides with an increased TNF expression during experimental cerebral malaria.

Many aspects of the interaction between *Plasmodium* and its host during the different parasitic life-cycle stages are still unclear. And research, investigating influences the persisting parasite might have on the host RNAi machinery and host miRNA expression is still in its infancy. Thus, this highly exciting and rapidly emerging research field might contribute to the generation of a full and comprehensive picture of these interactions at the molecular level. Furthermore, it might be important for the development of novel malaria vaccines and biotherapeutics.

1.4 Adeno-associated virus (AAV) as tool for cell- and tissue-specific gene expression

The Adeno-associated virus (AAV) is a member of the family *Parvoviridae* (parvovirus), genus *Dependovirus*. Parvoviruses are among the smallest animal DNA viruses. Their virion, composed entirely of DNA and proteins, has a diameter of approximately 25 nm. They belong to the genus *Dependovirus* because they require co-infection with helper viruses like the name-giving Adenovirus (Ad) or Herpes simplex virus (HSV) for productive infection in cell culture. AAV has a single-stranded DNA genome of about 4.7 kb, containing only three open reading frames (ORF). These ORFs are flanked by inverted terminal repeat elements (ITR), the minimal *cis*-acting elements necessary for viral genome integration, replication as well as packaging into the capsid shell. The first ORF (*rep*) encodes four Rep proteins, which are involved in replication of the viral genome by regulating transcription, viral DNA replication and DNA packaging into the preformed viral capsid within the cell nucleus. The second ORF (*cap*) encodes the three capsid proteins Vp1, Vp2 and Vp3 that make up the virion. They are translated from the same primary transcript via alternative splicing and initiation at different start codons. To form the viral capsid, 60 total copies of these proteins self-assemble prior to loading the viral DNA (Grieger and Samulski, 2005; Kwon and Schaffer, 2008). The third ORF encodes for a protein that is essential for targeting newly synthesized capsid proteins to the host cell nucleolus and is involved in the capsid assembly reaction (Sonntag et al., 2011; Sonntag et al., 2010).

AAVs offer the possibility to deliver genes with high efficiency and specificity to both dividing and non-dividing cells and in the absence of viral pathogenicity. Therefore they belong to the most promising viral vectors in gene therapy. Formation of stable episomal DNA forms allows long-term gene expression from recombinant AAV (rAAV) in the absence of chromosomal integration, which significantly adds to the high safety profile of AAV vectors (Berns and Linden, 1995; Grimm and Kleinschmidt, 1999).

Over 100 AAV serotypes have been isolated over the past decade from different animal species including humans and non-human primates or as contaminants in different Adenovirus stocks (Kwon and Schaffer, 2008). In numerous *in vitro* and *in vivo* studies, they have demonstrated different cell and tissue tropisms, which would allow cell- or tissue-specific gene expression. It has been shown that optimal serotypes for liver are AAV8 and AAV9, while a strong tropism for skeletal muscle has been noted for AAV1, AAV6, AAV7, AAV8 and AAV9. As another example, the central nervous system can be targeted by AAV1, AAV4 and AAV5. In addition to liver and skeletal muscle, AAV8 also targets heart and pancreas. As final examples, AAV9 is a potent serotype in the lung, and AAV2 can also mediate gene expression in the kidney (Wu et al., 2006).

AAV2 is the most broadly studied serotype and therefore is often used for pseudotyping. In general pseudotyping means the genome of one serotype is cross-packed into the capsid of another serotype to achieve a different cell or tissue tropism. It was demonstrated that the AAV tropism is determined

by the AAV capsid proteins but not by the Rep proteins (Grimm et al., 2006). Thus for generation of recombinant vectors, the *rep* and *cap* genes can be excised and replaced by a gene of interest that will become flanked by the ITRs. The three viral ORFs are then supplied as helper genes *in trans* to package the transgene into the capsid. The choice of a *cap* gene of a selected serotype permits to determine the tropism of the resulting particles (Grieger et al., 2006; Wu et al., 2006).

So far, vectors based on multiple serotypes, especially AAV1, 2 and 8, have been used in clinical trials for several diseases like cystic fibrosis, hemophilia B, prostate and melanoma cancers, Canavan disease, Alzheimer's, Parkison's, muscular dystrophy or rheumatoid arthritis, or for development of HIV vaccines (Carter, 2005). In the context of this work, their application for targeting the liver is important. Subsequent to the identification of the high liver tropism of AAV8 (Gao et al., 2004; Gao et al., 2002), several studies demonstrated that potent hepatic transduction can be achieved by applying AAV8 either by direct infuson into the portal vein or by intravenous injection (Grimm et al., 2006; Malato et al., 2011; Nakai et al., 2005; Thomas et al., 2004).

1.5 Aim of this study

All the different steps taking place during liver-stage development require a tight interaction between parasite and host. Some direct interactions between parasite proteins and hepatic host cell factors have already been demonstrated (section 1.1.3). Studies using attenuated parasites further showed aspects of this tight interaction as well as immune responses of the hepatic host cell, induced by the arresting parasites (section 1.1.4). In addition, miRNAs and the RNAi machinery are more and more recognized as important regulators in the interplay between pathogens and hosts. Thus, the question arises whether this machinery is also involved in Malaria infection and pathology. Several miRNA profiles investigating the influence of a persistent *Plasmodium* or *Toxoplasma* infection showed differentiated miRNA expression levels in the respective host tissue (section 1.3). Nevertheless, until now no study concentrated on the host hepatic RNAi machinery and miRNA expression during a liver-stage infection and investigated the influences developing and attenuated exo-erythrocytic parasites have, although these different parasites elicit very specific host cell responses, e.g. immune responses, and the underlying mechanisms are not fully understood so far.

The aim of this study was to achieve a more comprehensive picture of the interplay between the malaria liver-stage and the host hepatic tissue with a focus on the potential influences of the persisting liver-stage parasite on the host hepatic RNAi machinery as well as on the hepatic miRNA expression. Does the presence of a liver-stage parasite alter the expression pattern of key components comprising the RNAi machinery? If so, does this altered expression pattern remain static during the developmental process of the parasite or does it show a dynamic behavior according to the different phases of liver-stage development? And do parasites that arrest during their liver-stage development induce different gene expression patterns than wild-type (WT) parasites that obviously are able to successfully complete this part of the life cycle? Is this altered expression pattern of RNAi machinery components unique for a persisting malaria liver-infection or does it show indeed similarities to other hepatic disorders? Similar questions should be answered regarding the hepatic miRNA expression pattern. Are some miRNAs rather general regulators, activated due to the persisting liver-stage parasite? Do attenuating parasites induce different host hepatic miRNA expression patterns than WT parasites? Moreover, when comparing the obtained results to existing literature describing host hepatic miRNA expression patterns during an ongoing blood-stage infection with *P. chabaudi* (Delic et al., 2011), are there common miRNA signatures due to a general presence of malaria parasites? Or does the liver respond to the different parasitic life-cycle stages (exo-erythrocytic *versus* erythrocyctic) with specific miRNA expression patterns? To answer these questions gene, protein and miRNA expression analyses were performed comparing the expression levels of livers 24h and 40h after infection with WT, GAP and RAS to the expression levels of livers obtained from naïve mice. *In vivo* experiments were conducted to validate the biological relevance of selected candidate miRNA signatures.

2 Material and methods

2.1 Laboratory equipment

Laboratory equipment as used in both Parasitology unit of Department of Infectious Diseases, Heidelberg, and Bioquant, Heidelberg.

Agilent 2100 bioanalyzer	Agilent Technologies, EU
a-Hyb™ Hybridization Station	Miltenyi Biotec GmbH, Bergisch Gladbach
Analytical scales BL510	Sartorius GmbH, Göttingen
Autoclave	Systec GmbH, Wettenberg
Binocular SMZ 1500	Nikon, Japan
Gas burner, Soudagaz X2000 PZ	Campinggaz
Camera (Gel photography)	INTAS, Göttingen, Germany
Centrifuges:	
- Megafuge 1.0 R	Heraeus Instruments, Hanau
- Microcentrifuges 5415 R, 5415 D	Eppendorf, Hamburg
- Ultracentrifuge RC5B Plus	Sorvall, Thermo Fisher Scientific, USA
Digital timer	neoLab, Heidelberg
Electrophoresis System Horizon 11.14	Whatman Inc., USA
Electrophoresis Power Supply EPS 301	Amersham Pharmacia Biotech, Freiburg
Film developer Hyperprocessor	Amersham Pharmacia Biotech, Freiburg
Film developing cassettes	Dr Goos suprema GmbH, Heidelberg
Freezer -80 ºC	Sanyo
Freezers -20 ºC	Liebherr, Biberach
Fridges	Liebherr, Biberach
Glomax 96 microplate luminometer	Promega, USA
Heat block DB 1010	Alpha Laboratories, UK
Heat block thermomixer comfort	Eppendorf, Hamburg
Haemocytometer (Neubauer)	Labotec, Labor-Technik, Göttingen
Ice machine	ZIEGRA, Isenhagen
Incubators:	
- Hera Cell Incubator	Heraeus Instruments, Hanau
- Shaking Incubator Innova 4000/4300	New Brunswick Scientific Co. Inc.
- Multi-gas incubator (O_2, CO_2)	Mytron, Heiligenstadt
Liquid nitrogen tank	CBS, USA
Magnetic stirrer, Heidolph MR3001	NeoLab, Heidelberg
Microscopes	

- Light optical microscope, Axiostar plus	Zeiss, Jena
- Light optical microscope, Axioskop	Zeiss, Jena
- Light optical microscope, Axiovert 25	Zeiss, Jena
- Confocal microscope, Axiovert 100 M	Zeiss, Jena
Microwave oven	MDA
Mosquito cages	BioQuip Products Inc., USA
NanoDrop® ND-1000	Thermo Fisher Scientific, USA
PCR/qPCR-machines	
- GeneAmp PCR system 9700	Applied Biosystems, CA USA
- Mastercycler Gradient	Eppendorf, Hamburg
- RotorGene Q	Qiagen, Hilden
pH meter	Inolab, Heidelberg
Photometer	Eppendorf, Hamburg
Pipettes	
- Single channel pipettes 2 µl, 20 µl, 200 µl, 1000 µl	Abimed, Langenfeld
Pipetting aid pipetus®	Hirschmann Laborgeräte, Eberstadt
Precision balance	Mettler Toledo, Switzerland
QIAgility®	Qiagen, Hilden
Scan Array 4000XL	Packard Biochip Technologies, USA
SDS-PAGE system	Amersham Pharmacia Biotech, Freiburg
Sterile work bench Gelaire X	Flow Laboratories, Meckenheim
TissueRuptor®	Qiagen, Hilden
Vortex Genie 2	Scientific Industries Roth, Karlsruhe
Water bath Julabo U3	Julabo, Seelbach
Wet blot system	Amersham Pharmacia Biotech, Freiburg

2.2 Disposables

14 ml polystyrene round bottom tubes with lid	Greiner Bio-one, Frickenhausen
15 ml polypropylene tubes with lid	Sarstedt, Nümbrecht
50 ml polypropylene tubes with lid	Sarstedt, Nümbrecht
8-well chamber slides	Nunc, Langenselbold
96-well tissue culture plates	Greiner Bio-one, Frickenhausen
Aluminium foil	Roth, Karlsruhe
Amicon-Ultra-15 tubes	Millipore, Darmstadt
Cell culture flasks	
- Cellstar (Filter Cap, 75 cm^2)	Greiner Bio-one, Frickenhausen
- Nunc Flasks Nuclon (Filter Cap, 25 cm^2)	Nunc, Langenselbold
Cuvettes	Sarstedt, Nümbrecht
Cryovials	Greiner Bio-one, Frickenhausen
Dialysis cassettes Slyde-A-Lyzer G2 (20K MWCO)	Pierce, Thermo Fisher Scientific, USA
FACS tubes (5 ml)	Becton Dickinson, Heidelberg
Filter paper Whatman TM 3MM	Whatman, GE Healthcare, Dassel
Gloves, Peha-soft satin	Hartmann, Heidenheim
Immersion oil	Zeiss, Jena
Microscope cover slips	Marienfeld, Lauda-Königshofen
Needles, BD Microlance	Becton Dickinson, Heidelberg
Glass slides	Marienfeld, Lauda-Königshofen
Parafilm	Pechiney Plastic Packaging, USA
Pasteur capillary pipettes (190 mm)	Wu, Mainz
Petri dishes (94/16 mm)	Greiner Bio-one, Frickenhausen
Pipette filter tips, Biosphere	Sarstedt, Nümbrecht
Pipette tips	Sarstedt, Nümbrecht
PVDF membrane	Millipore, Darmstadt
Reaction tubes (0.5 ml, 1.5 ml, 2.0 ml)	Sarstedt, Nümbrecht
Rotor-Disc 100 (PCR tube rings)	Qiagen, Hilden
Safe-Lock Eppendorf tubes, nuclease-free (1.5 ml)	Eppendorf, Hamburg
Sterile pipettes (1 ml, 5 ml, 10 ml, 25 ml), Cellstar	Greiner Bio-one, Frickenhausen
Sterile syringe filter, Filtropur (0.22 µm pore size)	Sarstedt, Nümbrecht
Syringe, BD Microlance	Becton Dickinson, Heidelberg
Thermo well PCR tubes (0.2 ml)	Sarstedt, Nümbrecht
Tissue culture dishes (144 mm)	Nunc, Langenselbold
Biomax XAR Film	Kodak, USA

2.3 Strains

2.3.1 Bacteria strains

Escherichia coli XL1 blue	Stratagene, Agilent Technologies

2.3.2 Cell lines

HuH7	human hepatocarcinoma cell line (provided by Prof. Bartenschlager, Molecular Virology, Heidelberg)
Hek293T	human embryonic kidney cell line

2.3.3 Parasite strains

Plasmodium berghei NK65	(Yoeli and Most, 1965)
Plasmodium berghei NK65 *uis3(-)*	(Mueller et al., 2005b)

2.3.4 Mosquito strains

Anopheles stephensii NIJ	Nijmegen, Netherlands
Anopheles stephensii KAI	MPI für Infektionsbiologie, Berlin

2.3.5 Mouse strains

Naval Medical Research Institute (NMRI), outbred strain	Charles River Laboratory, Sulzfeld
Naval Medical Research Institute (NMRI), outbred strain	Janvier, France
C57BL/6, inbred strain	Charles River Laboratory, Sulzfeld
C57BL/6Rj, inbred strain	Janvier, France

2.4 Chemicals and reagents

Chemicals used for this study were typically purchased in p.a. quality either directly by the companies Roth, Merck, Sigma, Serva and AppliChem or provided by the Heidelberg Medical faculty chemical stock. Chemicals from other companies are listed below.

Agarose	Invitrogen, Frankfurt
BactoTM-Agar	Difco Laboratories, Augsburg
BactoTM-Trypton	Difco Laboratories, Augsburg
BactoTM-Pepton	Difco Laboratories, Augsburg
Butane/propane camping gas	Apragaz
Chemiluminescence substrate	Perkin Elmer, Rodgau-Jügesheim
Cellulose powder CF11 (fibrous)	Whatman, GE Healthcare, Dassel
Collagenase type IV	Sigma, Schweiz
Complete Solution for Protease Inhibition	Roche, Schweiz
Heparin	Braun, Melsungen
Lipofectamin	Invitrogen, Frankfurt
nuclease-free water	Ambion, Life Technologies GmbH, Darmstadt
Nycodenz powder	Axis-Shield PoC, Oslo
PBS-pellets	Gibco Invitrogen, Frankfurt
Percoll (1.124 g/ml)	Biochrom AG, Berlin
Polyethylenimine (PEI)	Polyscience Inc., USA
QIAzol® reagent	Qiagen, Hilden
Sea salt	Alnatura

2.5 Oligonucleotides

If not indicated otherwise, oligonucleotides were ordered as custom DNA oligonucleotides in desalted purity from Invitrogen, Frankfurt. Lyophilised oligonucleotides were briefly centrifuged and dissolved in ddH_2O in a concentration of 100 µM and stored at -20°C.

*m*GAPDH_For	5'-CAAGGTCATCCATGACAACTTTG-3'	(Fermentas)
*m*GAPDH_Rev	5'-GTCCACCACCCTGTTGCTGTAG-3'	(Fermentas)
*m*GAPDH_qPCR_For	5'-GGAGATTGGTTTTGACGTTTATGTG-3'	
*m*GAPDH_qPCR_Rev	5'-AAGCATTAAATAAAGCGAATACATCCTTAC-3'	
AldoA-For	5'-CAGGAAAGCAACTGCCACCGGCAC-3'	
AldoA-Rev	5'-GGATTCACACGGTCGTCTGCAGTC-3'	

Oligonucleotide sequences provided by AG Grimm:

miR155 rand2 for	5'-TCGA G ACCCCTATCACG*TCA*AGCATTAA TCTAGA GC-3'
miR155 rand2 rev	5'-GGCC GC TCTAGA TTAATGCT*TGA*CGTGATAGGGGT C-3'
#389 Psi-miR21-b3nt for	5'-TCGA G TCAACATCAG*GAC*ATAAGCTA TCTAGA GC-3'
#390 Psi-miR21-b3nt rev	5'-GGCC GC TCTAGA TAGCTTAT*GTC*CTGATGTTGA C-3'
#487 miR155 rand '2' for 1	5'-CGATGCCTAGG ACCCCTATCACGTCAAGCATTAA G-3'
#488 miR155 rand '2' for 2	5'-CTAGG ACCCCTATCACGTCAAGCATTAA GCTAGCG-3'
#489 miR155 rand '2' rev 1	5'-CTAGC TTAATGCTTGACGTGATAGGGGTCCTAGGCAT-3'
#490 miR155 rand '2' rev 2	5'-TCGACGCTAGC TTAATGCTTGACGTGATAGGGGTC-3'

#393 Sp-2x miR21 for

5'-CGATCCTAGGtcaacatcaggacataagctaccggtcaacatcaggacataagctaG-3'

#394 Sp-2x miR21 rev

5'-CTAGCtagcttatgtcctgatgttgaccggtagcttatgtcctgatgttgaCCTAGGAT-3'

#267 miR122-spGCCA for

5'-CCATCGATGCCTAGGACAAACACCATGCCAACACTCCAGCTAGCGTCGACGGCC-3'

#268 miR122-spGCCA rev

5'-GGCCGTCGACGCTAGCTGGAGTGTTGGCATGGTGTTTGTCCTAGGCATCGATGG-3'

2.6 Antibodies

2.6.1 Primary antibodies for immunofluorescence assays

mouse anti-*Pb*CSP	1:300 dilution	(Nussenzweig and Nussenzweig, 1989)
mouse anti-*Pb*HSP70	1:1 dilution	(Tsuji et al., 1994)

2.6.2 Secondary antibodies for immunofluorescence assays

goat anti-mouse Alexa Fluor 488	1:300 dilution	Invitrogen, Frankfurt
goat anti-mouse Alexa Fluor 546	1:300 dilution	Invitrogen, Frankfurt

2.6.3 Primary antibodies for Western blot analysis

polyclonal rabbit anti-mouse Drosha	1:1000 dilution	Abcam, UK
polyclonal rabbit anti-mouse Exportin-5	1:400 dilution	Abcam, UK
monoclonal mouse anti-mouse β-actin	1:1000 dilution	Santa Cruz Biotechnology, USA

2.6.4 Secondary antibodies for Western blot analysis

goat anti-rabbit IgG, HRP conjugated	1:10,000 dilution	Jackson ImmunoResearch Lab., UK
goat anti-mouse IgG, HRP conjugated	1:10,000 dilution	Jackson ImmunoResearch Lab., UK

2.7 Buffer, media and solutions

2.7.1 Molecular biology

3 M sodium acetate (NaAc) – solution	24.06 g NaAc
	add 100 ml ddH_20
	pH 5.2
50x TAE-buffer	2 M Tris
	1 M acetic acid
	50 mM EDTA
	pH 8.0

2.7.2 Biochemistry

NuPAGE SDS gels (4 – 12%)	Invitrogen, Frankfurt
NuPAGE 25x MOPS buffer	Invitrogen, Frankfurt
RIPA buffer	50 mM Tris-HCl, pH 7.5
	150 mM sodium chloride (NaCl)
	5 mM EDTA
	50 mM sodium fluoride (NaF)
	0.5% sodium deoxycholate (NaDOC)
	0.1% SDS
	1% Triton x-100
freshly added directly before use	1 mM DTT
	protease inhibitor
2x SDS-loading buffer	250 mM Tris, pH 6.8
	6.6% SDS
	24% glycerin
	10 mM EDTA
	6% β-mercaptoethanol
	bromophenol blue
1x transfer buffer	12 mM TrisBase
	96 mM glycine
	20% methanol

10x TBS	20 ml 1 M Tris, pH 7.6 80 g sodium chloride (NaCl) add 1 l ddH_20
1x TBST	100 ml 10x TBS 900 ml ddH_20 1 ml Tween 20

2.7.3 Antibiotics

Ampicillin stock, 1000x	100 mg/ml ampicillin in 50% EtOH
Chloramphenicol stock, 1000x	30 mg/ml chloramphenicol in 100% EtOH
Kanamycin stock, 1000x	50 mg/ml kanamycin in ddH_20
Tetracycline stock, 1000x	5 mg/ml tetracycline in 70% EtOH

Stock solutions were sterile filtered and diluted 1:1000 for final concentration.

2.7.4 Culture and transformation of *E. coli*

Luria Broth (LB)-medium	10 g/l Bacto-Trypton 5 g/l yeast extract 10 g/l sodium chloride (NaCl) pH 7.5
LB-Agar	LB-medium (as described above) 15 g/l agar

Preparation of competent cells:

TBF I	30 mM potassium acetate (CH_3CO_3K) 50 mM manganese(II) chloride ($MnCl_2$) 100 mM potassium chloride (KCl) 15% glycerine adjust pH 5.8 with 0.2 M acetic acid sterile filtered, store at 4°C in the dark
TBF II	10 mM MOPS 75 mM calcium chloride ($CaCl_2$) 10 mM potassium chloride (KCl)

	15% glycerine adjust pH 7.0 with NaOH sterile filtered, stored at 4°C in the dark

2.7.5 *Anopheles* mosquito breeding

Breeding water	1‰ sea salt in ddH_20
10% sucrose nutrient solution	10 g sucrose 20 µg para-aminobenzoic acid add 100 ml ddH_20

2.7.6 Cell culture

Cell culture media and supplements were purchased from Gibco, Karlsruhe.

Cell culture medium for HuH7 (DMEM complete)	1 x Dulbecco's Modified Eagle Medium, 10% FCS, 1% penicillin/streptomycin sterile, stored at 4°C
Cell culture medium for Hek293T (DMEM complete)	1 x Dulbecco's Modified Eagle Medium, 10% FCS, 1% penicillin/streptomycin, 1% glutamine sterile, stored at 4°C
Mammalian cell freezing solution	80% FCS, 20% DMSO or 90% FCS, 10% DMSO mixed 1:1 with complete culture medium
Anti-contamination cocktail, 100x	60 mg penicillin 100 mg kanamycin 50 mg 5-fluorocytosine 10 mg chloramphenicol sterile filtered
Na-HEPES resuspension buffer	50 mM HEPES 0.15 M sodium chloride (NaCl) 25 mM EDTA

Cesium chloride ($CsCl_2$) topping solution	$CsCl_2$ (RI = 1.3710 at room temperature) in Na-HEPES resuspension buffer
Benzonase buffer	50 mM Tris-HCl 2 mM magnesium chloride ($MgCl_2$) pH 8.5
40% PEG8000/2.5 M NaCl	40% PEG8000 2.5 M sodium chloride (NaCl)

2.7.7 Parasitological methods

Parasite freezing solution	10% glycerine in Alsever's Solution (Sigma)

2.7.8 Preparation of primary mouse hepatocytes

10x EGTA buffer	12.5 g glucose 14.9 g HEPES 2.35 g EGTA 25 ml 200 mM glutamine ad 250 ml ddH_2O
1x EGTA buffer contains	1:10 dilution of 10x EGTA buffer in 1x PBS 2 mM glutamine 0.5% glucose 25 mM HEPES 2 mM EGTA pH 7.4
10x Collagenase buffer	12.5 g glucose 14.9 g HEPES 1.10 g calcium chloride ($CaCl_2$) 25 ml 200 mM glutamine ad 250 ml ddH_2O
1x Collagenase buffer	1:10 dilution of 10x collagenase buffer in 1x Williams E medium (Gibco)

contains	2 mM glutamine
	0.5% glucose
	25 mM HEPES
	3 mM calcium chloride ($CaCl_2$)
	pH 7.4
	add 15 mg collagenase type IV per 50 ml
	sterile filtered
Percoll	9,748 ml Percoll (1.124 g/ml)
	10.252 ml 1x HBSS

2.8 Plasmids

All vectors for *in vitro*, *in vivo* and *ex vivo* application were provided by AG Grimm, Bioquant, Heidelberg.

2.8.1 Commercially available plasmids

psiCheck™-2 plasmid (Promega)

Oligonucleotide sequences for miRNA binding sites:

rand2 miR-155 imperfect for 5'-TCGA Gacccctatcacg*tca*agcattaaTCTAGA GC-3'

#134 miR-122 imperfect for 5'-TCGA G ACAAACACCAT_ACGA_ACACTCCA TCTAGA GC-3'

#238 miR-21 imperfect for 5'-TCGA G TCAACATCAG*GAC*ATAAGCTA TCTAGA GC-3'

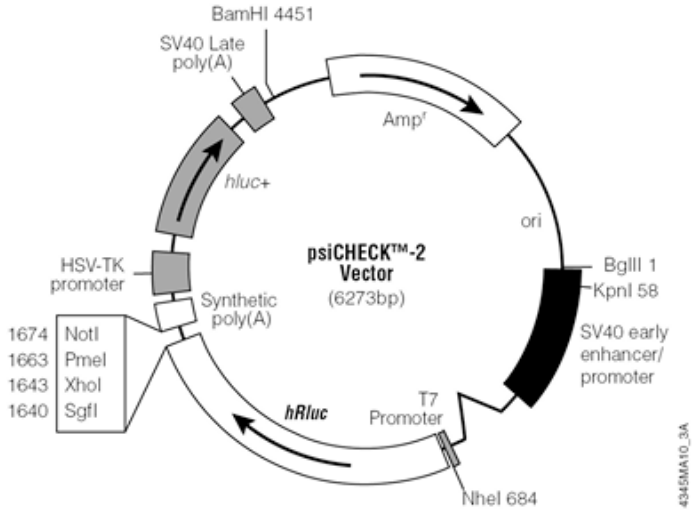

Figure 2.8.1: psiCheck™-2 plasmid for Dual Luciferase assay. The psiCheck™-2 plasmid co-encodes both firefly (*Photinus pyralis)* and *Renilla* (*Renilla reniformis*) luciferase.

2.8.2 Firefly luciferase expression plasmids

Oligonucleotide sequences for miRNA binding sites:

miR-155 rand2 for 5'-TCGA G ACCCCTATCACG*TCA*AGCATTAA TCTAGA GC-3'

miR-155 rand2 rev 5'-GGCC GC TCTAGA TTAATGCT*TGA*CGTGATAGGGGT C-3'

#389 Psi-mir21-b3nt for 5'-TCGA G TCAACATCAG*GAC*ATAAGCTA TCTAGA GC-3'

#390 Psi-mir21-b3nt rev 5'-GGCC GC TCTAGA TAGCTTAT*GTC*CTGATGTTGA C-3'

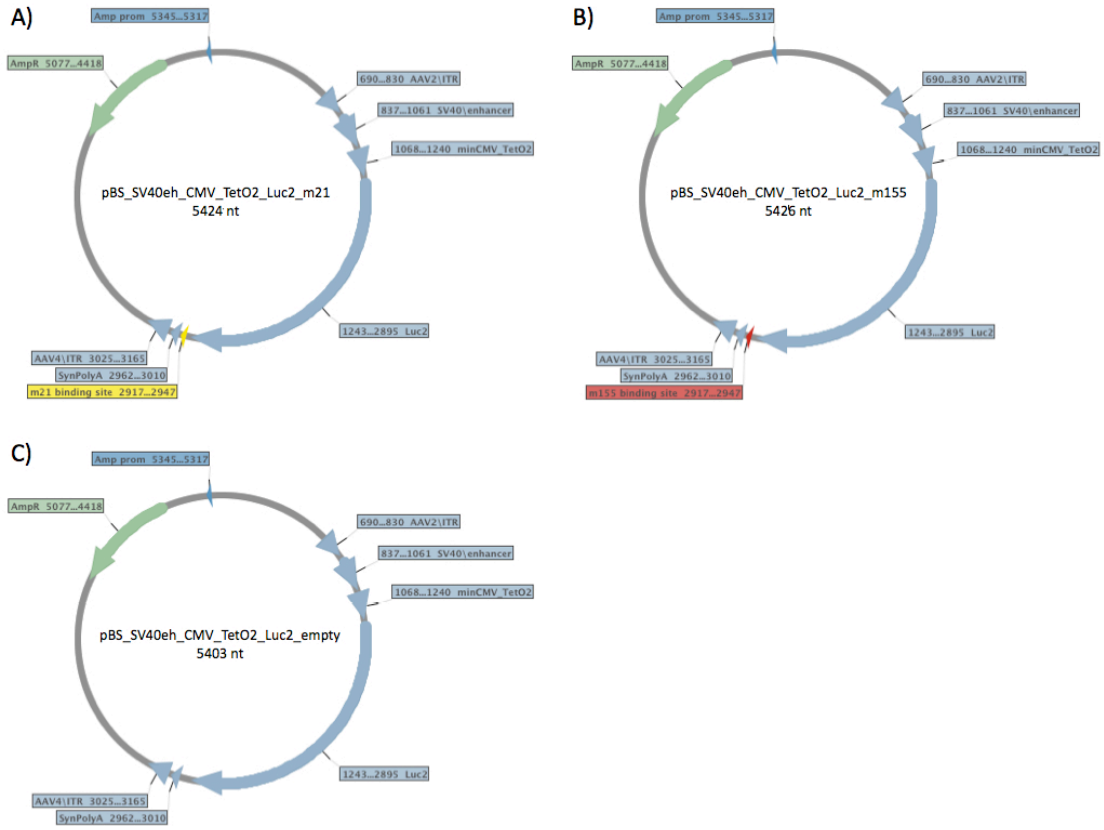

Figure 2.8.2: Luciferase plasmids for *ex vivo* imaging. A pBS_SV40eh_CMV_TetO2_Luc2 plasmid served as backbone and was supplemented with binding sites for miR-21 with a 3-nt-bulge (A) or miR-155 with a 4-nt-bulge (B). The empty plasmid (C) was used for reference measurements.

2.8.3 Sponge expression plasmids

Oligonucleotide sequences for miRNA binding sites. In all cases oligonucleotides were concatemerised using the integrated restriction sites before being cloned into the plasmid backbone.

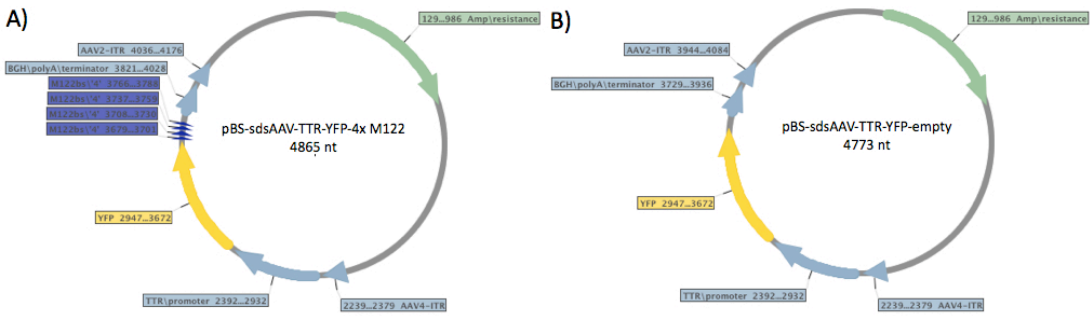

Figure 2.8.3: Sponge plasmids for *in vitro* down-regulation of miR-122. A pBS-sdsAAV-TTR-YFP plasmid served as backbone and was supplemented with binding sites for miR-122 (A). The empty plasmid (B) was used as a control.

#267 miR122-spGCCA for

5’-CCATCGATGCCTAGGACAAACACCATGCCAACACTCCAGCTAGCGTCGACGGCC-3’

#268 miR122-spGCCA rev

5’-GGCCGTCGACGCTAGCTGGAGTGTTGGCATGGTGTTTGTCCTAGGCATCGATGG-3’

#393 Sp-2x miR21 for

5’-CGATCCTAGGtcaacatcaggacataagctaccggtcaacatcaggacataagctaG-3’

#394 Sp-2x miR21 rev

5’-CTAGCtagcttatgtcctgatgttgaccggtagcttatgtcctgatgttgaCCTAGGAT-3’

#487 miR155 rand ‘2’ for 1 5’-CGATGCCTAGG ACCCCTATCACGTCAAGCATTAA G-3’

#488 miR155 rand ‘2’ for 2 5’-CTAGG ACCCCTATCACGTCAAGCATTAA GCTAGCG-3’

#489 miR155 rand ‘2’ rev 1 5’-CTAGC TTAATGCTTGACGTGATAGGGGTCCTAGGCAT-3’

#490 miR155 rand ‘2’ rev 2 5’-TCGACGCTAGC TTAATGCTTGACGTGATAGGGGTC-3’

For miR155 oligonucleotides #487 miR155 rand ‘2’ for 1 and #488 miR155 rand ‘2’ for 2 as well as #489 miR155 rand ‘2’ rev 1 and #490 miR155 rand ‘2’ rev 2 were primarily annealed, than concatemerised and finally cloned into the plasmid backbone.

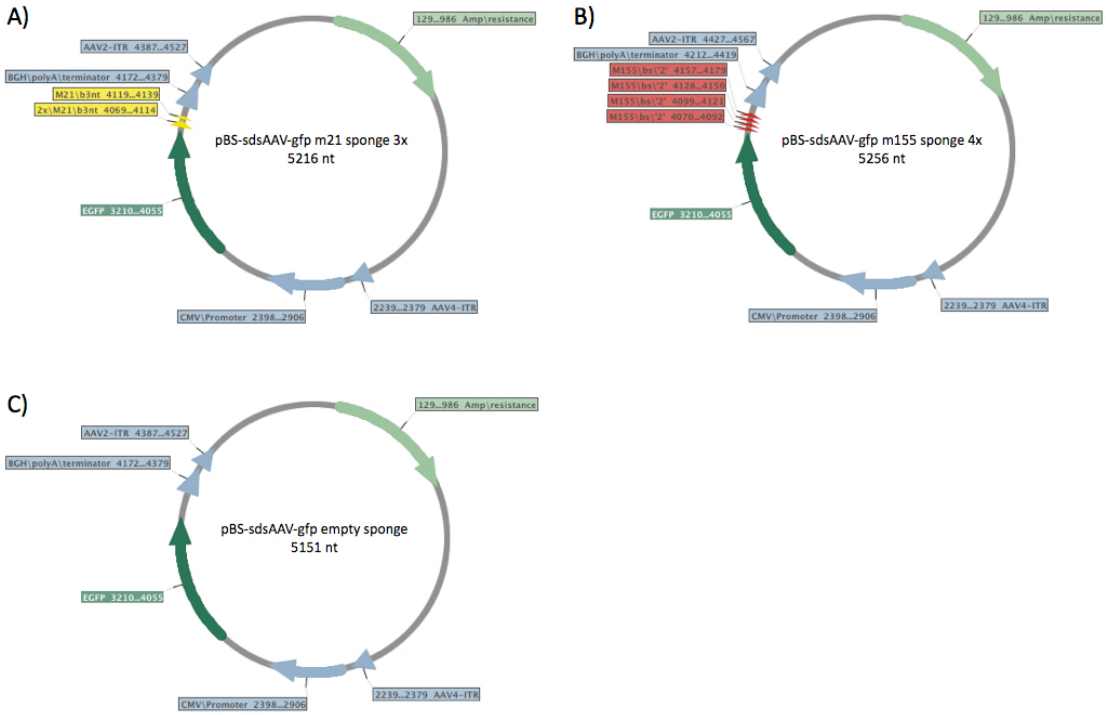

Figure 2.8.4: Sponge plasmids for *in vitro* and *in vivo* down-regulation of miR-21 and miR-155. A pBS-sdsAAV-gfp plasmid served as backbone and was supplemented with binding sites for miR-21 (A) or miR-155 (B). The empty plasmid (C) was used as a control.

2.8.4 *Tough decoy* RNA (TuD) expression plasmids

Oligonucleotide sequences for miRNA binding sites:

miR21 TuD for 5'-TCCca tcaacatcagaaaataagcta CAAGTATTCTGGTCACAGAATACAAC tcaacatcagaaaataagcta a-3'

miR21 TuD rev 5'-TCGGT TAGCTTATTTTCTGATGTTGA GTTGTATTCTGTGACCAGAATACTTG TAGCTTATTTTCTGATGTTGA-3'

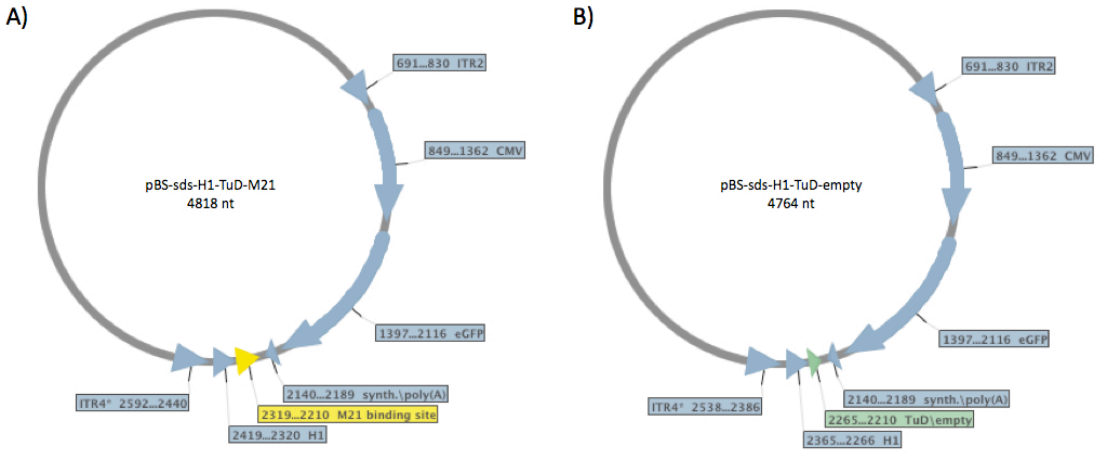

Figure 2.8.5: TuD plasmids for *in vitro* down-regulation of miR-21. A pBS-sds-H1-TuD plasmid served as backbone and was supplemented with binding sites for miR-21 (A). The empty plasmid (B) was used as a control.

2.9 Molecular biological methods

2.9.1 RNA isolation from mouse hepatic tissue and cDNA synthesis for RT and qPCR

RNA was isolated either from freshly isolated mouse livers (section 2.14.3) or after separation and purification of primary murine hepatocytes and remaining murine liver cells (section 2.14.4).

2.9.1.1 QIAzol total RNA isolation from whole tissue preparations

Mice were perfused with 10-20 ml 1x PBS, livers were removed and cut into small pieces using clean scissors as quick as possible. Liver pieces were immediately shock-frozen in liquid nitrogen and transferred in pre-cooled 2 ml Eppendorf tubes. Liver pieces were stored at -80°C (section 2.14.3).
2 ml cooled QIAzol reagent (Qiagen) (4°C) was provided in 5 ml FACS tubes. One frozen liver piece was transferred into the QIAzol reagent and immediately disrupted and simultaneously homogenized for 30-40 seconds using a TissueRuptor (Qiagen) and plastic disposables. As soon as the tissue lysate was uniformly homogenous it was transferred into two nuclease-free 1.5 ml Eppendorf tubes (1 ml per tube) and incubated for 5 minutes at room temperature for dissociation of nucleoprotein complexes. After adding 200 µl chloroform, tubes were vigorously shaken for 15 seconds and incubated for 3 minutes at room temperature. Subsequent centrifugation for 15 minutes at 4°C and 12,000 x g separated the lysate into three phases. The upper, colorless, aqueous phase contained the RNA and was transferred to a new nuclease-free 1.5 ml Eppendorf tube. After addition of 500 µl isopropanol (2-propanol) the solution was mixed thoroughly, incubated for 10 minutes at room temperature and spun for 10 minutes at 12,000 x g at 4°C. The supernatant was carefully aspirated and the RNA pellet was washed with 75% ethanol. After centrifugation for 5 minutes at 7,500 x g and 4°C the ethanol was removed and the tube briefly centrifuged at 4°C to collect remaining ethanol. The remaining ethanol was aspirated and the RNA pellet was air dried no longer than 10 minutes at room temperature. According to its size, the RNA pellet was resuspended in 50-150 µl nuclease-free H_2O (Ambion) and incubated for 10 minutes at 60°C. Isolated RNA was stored at -80°C.

2.9.1.2 QIAzol total RNA isolation from separated and purified murine hepatocytes and remaining murine liver cells

Hepatocytes and remaining liver cells were separated and purified as described in section 2.14.4. Pelleted hepatocytes were resuspended in 2 ml QIAzol reagent and transferred to two 1.5 ml nuclease-free Eppendorf tubes (1 ml per tube) while remaining liver cells were resuspended in 1 ml QIAzol reagent due to lower amount of recovered cells and transferred to one 1.5 ml nuclease-free

Eppendorf tube. Cells were thoroughly homogenized by pipetting and vortexing. Further procedures were followed exactly as described in 2.9.1.1.

2.9.1.3 Determination of RNA integrity

After QIAzol isolation, concentration and possible contamination of RNA was measured using a NanoDrop spectrophotometer. RNA samples with 260/280 ratios between 1.8 and 2.0 were used for further analysis. For analysis of RNA integrity an Agilent 2100 bioanalyzer and 2100 expert Eukaryote Total RNA nano chips (RNA 6000 Nano Assay) were used. The gel-dye mix was prepared and loaded onto the RNA 6000 Nano chip. RNA 6000 Nano marker was added to all sample wells and ladder well followed by applying the respective samples and ladder. Samples were previously prepared to a concentration of 400 ng in 5 µl nuclease-free H_2O. The chip was horizontally vortexed for 1 minute at 2400 rpm and run in the Agilent 2100 bioanalyzer.

2.9.1.4 DNase treatment of total RNA

After RNA isolation, remaining DNA contaminations were removed by digestion with DNase using Turbo DNA Free Kit (Ambion). In each reaction 10 µg total RNA was digested in a final volume of 50 µl. Therefore, the RNA was mixed with 1/10 volume of 10 x TURBO DNase buffer (Ambion) and 1 µl TURBO DNase (Ambion) and incubated for 30 minutes at 37°C. 1/10 volume of the resuspended DNase Inactivation Reagent (Ambion) was added, mixed thoroughly and incubated for 2 minutes at room temperature under repeated inverting. The reaction was centrifuged for 1 minute at 10,000 x g and room temperature and the supernatant containing the RNA was transferred to a fresh nuclease-free Eppendorf tube. DNase treated RNA was stored at -80°C.

2.9.1.5 First strand cDNA synthesis

The messenger RNA (mRNA) contained in 1 µg of DNase treated total RNA was transcribed into complementary DNA (cDNA) using the First Strand cDNA Synthesis Kit (Fermentas) according to the manufacturer's manual using random hexamer oligonucleotides. For each RNA sample one additional reaction without reverse transcriptase (-RT) was set up to exclude genomic DNA (gDNA) contaminations. The initial optional denaturation step of the total RNA for 5 minutes at 65°C was performed. Reverse transcription was carried out in a PCR cycler by incubating the reaction for 5 minutes at 25°C followed by 60 minutes at 37°C and terminating the reaction by heating at 70°C for 5 minutes. The transcribed product was directly used for reverse transcriptase PCR (2.9.1.6) or quantitative Real-time PCR (2.9.1.8) or stored at -20°C.

2.9.1.6 Control reverse transcription PCR (RT-PCR)

After transcription of mRNA into cDNA, control reverse transcription PCR (RT-PCR) was performed to check for gDNA contaminations. Specific DNA fragments were amplified by Polymerase chain reaction (PCR) (Saiki et al., 1985) using specific oligonucleotides. For this control RT-PCR, primers amplifying a 496 bp fragment of the *Mus musculus* glyceraldehyde-3-phosphate dehydrogenase (GAPDH) coding sequence were used: *m*GAPDH_For, 5'-CAAGGTCATCCATGACAACTTTG-3' and *m*GAPDH_Rev, 5'-GTCCACCACCCTGTTGCTGTAG-3', provided by Fermentas First Strand cDNA Synthesis Kit. 0.5 µl cDNA was used in a reaction volume of 10 µl. Furthermore the reaction contained 50 pmol of the specific *m*GAPDH oligonucleotides (Fermentas, see above), 0.2 mM dNTPs, 1.5 mM $MgCl_2$, 1 x Taq reaction buffer (+ KCl) and 2.5 U Taq polymerase (all Fermentas) filled up to 10 µl with ddH_2O. Reaction tubes were placed into a thermal cycler running the program with an initial denaturation of the cDNA for 5 minutes at 94°C, followed by 35 cycles with a denaturation at 94°C for 30 seconds, annealing of the specific oligonucleotides at 55°C for 30 seconds and extension of the newly synthesized DNA strand at 72°C for 90 seconds. A final extension for 10 minutes at 72°C was carried out. For each sample one tube containing cDNA synthesized with reverse transcriptase (+RT) and one tube without (-RT) control was prepared. Amplified DNA was stored at 4° C for short-term and at -20° C for long-term storage.

2.9.1.7 Analysis of DNA fragments by agarose gel electrophoresis

Amplified DNA fragments were separated according to their size by agarose gel electrophoresis. Typically, 1% agarose gels were used and prepared by dissolving an appropriate amount of agarose in 1x TAE buffer under heating in the microwave. Ethidium bromide was added to a final concentration of 50 ng/ml. Prior to loading, samples were mixed with 1/5 volume of 6x Orange Loading Dye (Fermentas). For size discrimination 1 µg GeneRuler 1 kb DNA ladder (Fermentas) was loaded as well. The gel was run for 1 hour at 100 V in 1x TAE buffer in a Whatman Horizon 11.14 electrophoresis chamber. Thereby, the negatively charged DNA migrates towards the anode. Separated DNA fragments were visualized by exposure of the DNA-intercalating ethidium bromide to UV-light and fluorescence was recorded with an electrophoresis documentation and analysis system (INTAS).

2.9.1.8 Quantitative real-time PCR (qPCR) of cDNA conducted from mRNA

Quantitative real-time PCR (qPCR) was performed to determine relative abundance of *Xpo-5*, *Ago-2*, *Dicer*, *TRBP*, *Drosha* and *Aldolase 1*, *A* isoform transcripts. For amplification of these genes of interest, except *Aldolase 1*, *A* isoform, pre-designed QuantiTect Primer Assays (Qiagen) were used. QuantiTect Primer Assays were reconstituted to a 10x concentration by adding 1.1 ml nuclease-free H_2O (Ambion). Primers for *Aldolase 1*, *A* isoform were adapted from (Su et al., 2011b) with the following sequences: AldoA-For, 5'-CAGGAAAGCAACTGCCACCGGCAC-3'; AldoA-Rev, 5'-GGATTCACACGGTCGTCTGCAGTC-3'. Primers for the housekeeping gene *mGAPDH* were self designed:

*m*GAPDH_qPCR_For, 5'-GGAGATTGGTTTTGACGTTTATGTG-3'; *m*GAPDH_qPCR_Rev, 5'-AAGCATTAAATAAAGCGAATACATCCTTAC-3'. QPCR was performed using the 2x QuantiTect SYBR Green PCR Master Mix (Qiagen). For each reaction 13 µl master mix were prepared containing as final concentration 1x QuantiTect SYBR Green PCR Master Mix and 1x QuantiTect Primer Assay. If self designed primers (AldoA, *m*GAPDH) were used, 25 pmol of each forward and reverse primer were added to the master mix instead of the QuantiTect Primer Assay. Master mix was pipetted into Rotor-Disc 100 PCR tube rings (Qiagen) by a pipetting robot (QIAgility, Qiagen). 20 ng cDNA was added to a final volume of 15 µl per reaction. Each sample was pipetted in duplicates. The qPCR was performed in a Rotor-Gene Q cycler (Qiagen) starting with an initial activation step at 95°C for 15 minutes, followed by 40 cycles of 15 seconds denaturation at 94°C, 30 seconds annealing at 55°C and 30 seconds extension at 72°C. During the extension phase fluorescence data collection was performed. The amplification was followed by generation of a melting curve comprising a ramp from 55°C to 95°C rising by 1°C each step to check for the formation of primer dimers and thus false-positive signals.

2.9.2 Sample preparation, microarray analysis and miRNA validation

For the microarray analysis RNA samples from whole liver preparations (2.9.1.1) were used. They were checked for RNA integrity (2.9.1.3) and DNase digested (2.9.1.4). Absence of contaminating gDNA was tested as described in sections 2.9.1.5-2.9.1.7. RNA samples regarded as suitable were used for the further experiments.

2.9.2.1 Febit miRNA screening

Total RNA samples treated and tested as mentioned in 2.9.2 were given to Febit for miRNA screening. Febit conducted a one-color microarray. Raw data processing was also performed by Febit. I received compressed background substracted raw data. These intensities for the single miRNAs were then further processed by Bettina Knapp, PhD (AG Kaderali, Bioquant, Heidelberg) for comparison of groups by applying ANOVA.

2.9.2.2 MiRNA labeling

3 µg of total RNA per sample was labeled using Exiqon mercury LNA microRNA Array Power Labeling Kit (Exiqon). This kit labels all small RNAs by removing 5'-phosphates from the terminal of the respective small RNAs using a Calf Intestinal Alkaline Phosphatase (CIP) followed by enzymatical attachment of a fluorescent label to the 3'-end of the small RNAs. According to the manufacturer's advice 3 µg total RNA was pipetted in 0.2 ml nuclease-free reaction tubes with 0.5 µl spike-in control RNA 1 and 0.5 µl spike-in control RNA 2 (both provided with miRXplore Microarray Kit (Miltenyi)),

0.5 µl CIP buffer and 0.5 µl CIP enzyme (both provided with Exiqon kit) to a final volume of 4 µl, mixed and briefly centrifuged. Reaction was incubated for 30 minutes at 37°C in a PCR cycler with heated lid. Subsequently, enzyme reaction was terminated and RNA denatured by incubation at 95°C for 5 minutes followed by snap cooling on ice. Afterwards 3 µl labeling buffer, 1.5 µl fluorescent dye, 2 µl DMSO and 2 µl labeling enzyme (all provided with Exiqon kit) were added, mixed by gentle vortexing and briefly centrifuged, followed by 1 hour incubation at 16°C in a PCR cycler with heated lid and protected from light. Labeling procedure was stopped by 15 minutes incubation at 65°C and labeled sample could be shortly stored on ice, protected from light until further processing. Naïve liver samples were labeled with Hy3 while non-naïve liver samples were conjugated to Hy5.

2.9.2.3 Hybridization of labeled RNA to microarrays

Hybridization of labeled small RNAs to microarrays was performed within one hour after finishing the RNA labeling procedure. RNA was hybridized to miRXplore microarrays 5.0 (Miltenyi) using the miRXplore Microarray Kit (Miltenyi) and an a-Hyb Hybridization Station (Miltenyi).

Table 2.9.1: Protocol for over night hybridization of miRNAs to microarray.

Experimental step	Buffer	Step	Medium	Temperature (°C)	Time (min)	Pump speed (ml/min)	Cycles
Prehybridization	Prehybridization solution, 1x conc	incub	3,3,3,3	42,42,42,42	5	1.0	-
Hybridization	Hybridization solution with labeled sample	incub	M,M,M,M	42,42,42,42	1020	1.0	-
High salt wash	Wash Buffer 1 (diluted)	wash	1,1,1,1	10,10,10,10	1	1.0	2
Low salt wash	Wash Buffer 2 (diluted)	wash	2,2,2,2	10,10,10,10	1	1.0	2
		end					

After preparation of buffers according to the manufacturer's protocol 12.5 µl of Hy3 labeled naïve samples, 12.5 µl of Hy5 labeled non-naïve samples, 75 µl nuclease-free water and 100 µl 2x Hybridization solution were mixed and incubated at 65°C for 5 minutes. Until further processing the samples were protected from light and kept at room temperature. Microarrays were loaded onto the pre-selected slide positions of the a-Hyb Hybridization Station and miRNA protocol was selected (table 2.9.1). Instructions of a-Hyb Hybridization Station for sample loading were followed and hybridization was performed over night. After termination of over night hybridization microarrays were directly removed from the station and not allowed to dry, followed by gentle horizontal rotation in 1x Wash Buffer 2 for 2-5 minutes, protected from light. Afterwards microarrays were shortly

dipped into autoclaved ddH_2O and dried by using compressed air. Microarrays were transferred into 15 ml polypropylene tubes with lid and protected from light until subsequent scanning.

2.9.2.4 Scanning of hybridized microarrays

After hybridization of labeled miRNAs to microarrays the microarrays were read with a Scanarray 4000 XL (Packard Biochip Technologies; provided by AG Hoheisel, DKFZ, Heidelberg). Relative intensities of each fluorophore represent relative abundance of the distinctive miRNAs. Sequences of 717 mouse miRNAs and additional human, rat and virus miRNAs were located in distinct spots on the microarray. All miRNAs sequences were spotted in quadruplicates to the array to provide technical replicates. Microarrays were scanned with 100% laser power but with different photomultiplier settings (100/100; 80/80; 75/75; 70/70; 65/65) for both lasers, one exiting at 550 nm and being detected at 570 nm (Hy3) and the other exiting at 650 nm and being detected at 670 nm (Hy5). Varying photomultiplier settings were chosen to obtain optimal images of both channels.

2.9.2.5 Analysis of microarray images

Image analysis was performed using the software GenePix Pro 6 (Axon instruments/Molecular Devices Corp.). Images of the Hy3 and Hy5 channel generated under optimal reading conditions were merged and loaded. GenePix Pro 6 software automatically recognized fluorescent spots and encircled them. Every circle set by the software was re-checked manually to exclude false-positive spots that represented unspecific blurs. Furthermore, the diameter of the drawn circles was adjusted to the actual diameter of the respective spots to reduce background signals.

2.9.2.6 Reverse Transcription for quantitative real-time PCR (qPCR) of miRNAs

Reverse Transcription was performed from total liver RNA samples after DNase treatment as introduced in section 2.9.2 using the miScript Reverse Transcription Kit (Qiagen). For the reverse transcription reaction 1 µg total RNA was mixed with 4 µl 5x miScript RT Buffer and 1 µl miScript Reverse Transcriptase Mix. Nuclease-free water was added to a final volume of 20 µl. The reaction was incubated for 60 minutes at 37°C and inactivated for 5 minutes at 95°C. During the reverse transcription reaction a universal tag sequence was added to the RNA, subsequently serving as complementary sequence for binding of the universal primer in the qPCR reaction. Amplified cDNA was stored at 4°C for short-term and at -20°C for long-term storage.

2.9.2.7 Validation of miRNAs by quantitative real-time PCR (qPCR)

For validation of miRNAs, quantitative real-time PCR (qPCR) was performed using pre-designed miScript Primer Assays (Qiagen) and the corresponding miScript SYBR Green PCR Kit (Qiagen). As housekeeping gene the miScript Primer Assay Hs_RNU1A_1 was used. miScript Primer Assays were reconstituted to a 10x concentration by adding 550 µl nuclease-free water (Ambion). For each reaction 13 µl master mix were prepared containing as final concentration 1x miScript SYBR Green PCR Master Mix, 1x miScript Primer Assay and 1x miScript Universal Primer (provided with miScript SYBR Green PCR Kit). Master mix was pipetted into Rotor-Disc 100 PCR tube rings (Qiagen) by a pipetting robot (QIAgility, Qiagen). 3 ng cDNA was added to a final volume of 15 µl per reaction. Each sample was pipetted in duplicates. The qPCR was performed in a Rotor-Gene Q cycler (Qiagen) starting with an initial activation step at 95°C for 15 minutes, followed by 45 cycles of 15 seconds denaturation at 94°C, 35 seconds annealing at 55°C and 30 seconds extension at 68°C. During the extension phase fluorescence data collection was performed. The amplification was followed by generation of a melting curve comprising a ramp from 55°C to 95°C rising by 1°C each step to check for the formation of primer dimers and thus false-positive signals.

2.9.3 Plasmid replication for *in vitro*, *in vivo* and *ex vivo* application

The plasmids used for *in vitro*, *in vivo* and *ex vivo* application, which are listed in section 2.7 were replicated in *Escherichia coli* XL1 blue cells. As generation of the different constructs was performed by AG Grimm, Bioquant, Heidelberg, the respective cloning steps are not described in this thesis. Sequences for miRNA binding sites are also stated in section 2.7. Plasmids were provided as small aliquots of maxi preparations done by AG Grimm for re-transformation by myself.

2.9.3.1 Preparation of transformation competent *Escherichia coli* XL1 blue cells

Escherichia coli (*E. coli*) XL1 blue cells were cultured over night in LB medium with tetracycline (5 µg/ml). After diluting the over night culture 1:100 in LB medium with tetracycline (5 µg/ml) it was cultivated at 37°C under constant shaking at 190-220 rpm until it reached an OD_{600} of 0.5. The culture was cooled down on ice followed by 5 minutes centrifugation at 1500 x g and 4°C. The cell pellet of 100 ml culture was resuspended in 30 ml cold TfBI, incubated for 15 minutes on ice and centrifuged again for 5 minutes at 1500 x g and 4°C. The cell pellet was resuspended in 8 ml TfBII and incubated another 15 minutes on ice. 200 µl aliquots of the suspension were prepared and instantly frozen at -80°C.

2.9.3.2 Transformation of competent *Escherichia coli* XL1 blue cells

For transformation, 200 µl competent *Escherichia coli* (*E. coli*) XL1 blue cells (section 2.9.3.1) were thawed on ice. After adding 10 µl of a 1:10 dilution of the provided plasmid, cells were incubated for 30 minutes on ice followed by 45 seconds heat shock at 42°C. Subsequently, cells were incubated for another 2 minutes on ice. Afterwards, 1 ml pre-warmed LB medium was added to the cells and they were incubated for 1 hour at 37°C under constant shaking at 190-220 rpm. Cells were briefly centrifuged and the majority of supernatant was removed by pipetting. The cells were resuspended in the remaining supernatant, spread on LB agar plates supplemented with ampicillin (100 µg/ml) and incubated over night at 37°C.

2.9.3.3 Plasmid isolation with NucleoBond® Xtra Maxi Kit (Macherey Nagel)

After transformation (2.9.3.2) single colonies were used to inoculate 5 ml LB medium with ampicillin (100 µg/ml) each. After incubating these cultures over night at 37°C under constant shaking at 190-220 rpm they were transferred into 400 ml LB medium with ampicillin (100 µl/ml) each and incubated again over night at 37°C under constant shaking. Afterwards cultures were centrifuged due to the big volume in several steps at 4000 rpm and 4°C for 10 minutes each. Cell pellets were resuspended in resuspension buffer. After adding lysis buffer, mixture was incubated for 5 minutes at room temperature. In the meantime the NucleoBond Xtra Column and the column filter were equilibrated using the equilibration buffer. Before loading the suspension to the column filter, neutralization buffer was added and mixed by inverting the tube. After washing, the column filter was discarded. The column was washed once more before the plasmid DNA was eluted by adding elution buffer. Plasmid DNA was precipitated by adding isopropanol and 30 minutes centrifugation at 4000 rpm and 4°C. Plasmid DNA pellet was washed with 70% ethanol and centrifuged for 45 minutes at 4000 rpm and room temperature followed by aspiration of ethanol and 20 minutes air drying of the pellet. Finally the pellet was resuspended in 1 ml sterile filtered ddH_2O.

2.9.3.4 Determination of DNA concentration by photometric measurement

In order to determine the DNA concentration of the plasmid preparations (2.9.3.3) the DNA was diluted 1:100 in ddH_2O. The absorption of the dsDNA at 260 nm was measured in a photometer (Eppendorf) and DNA concentration was calculated according to the following equation:

$$\Delta OD_{260} \times 50\ \mu g/ml \times \text{dilution factor} = \text{concentration dsDNA } [\mu g/ml]$$

The purity of the DNA preparation was shown by the ratio of OD_{260}/OD_{280}. Plasmid DNA preparations with OD_{260}/OD_{280} ratios between 1.8 and 2.0 were used for further experiments.

2.9.4 Titration of recombinant Adeno-associated viral (rAAV) particles

After isolation of recombinant Adeno-associated viral (rAAV) particles (section 2.10.5), 10 µl of each rAAV preparation was mixed with 10 µl TE buffer (1 mM Tris-HCl, 0.01 mM EDTA pH 8.0) and 20 µl 2 M NaOH for alkaline lysis of the viral capsids, incubated at 56°C for 30 minutes. After neutralization with 38 µl 1 M HCl, volumes were adjusted to 1 ml with ddH_2O generating a 1:100 dilution of the rAAV preparations. For determination of genomic titers samples were measured in triplex by quantitative real-time PCR and number of rAAV genomes was defined by a plasmid standard curve, run in parallel. For each triplex 17.5 µl 2x Sensimix II Probe Mix (Bioline) was mixed with 1 µl forward primer (10 µM), 1 µl reverse primer (10 µM), 0.35 µl probe (10 µM) and 5 µl sample or standard. The volume was adjusted to 35 µl with nuclease-free water (Ambion). After an initial denaturation step for 10 minutes at 95°C, 40 cycles were run with 10 seconds of denaturation at 95°C followed by 20 seconds annealing and extension at 60°C. Data collection was performed during annealing and extension. Primers and probes used for these analyses are listed below.

Target	Probe (5'→3')	5' primer (5'→3')	3' primer (5'→3')
eGFP	FAM-ACGACGGCAACTACA-BHQ1	GAGCGCGCACCATCTTCTTCAAG	TGTCGCCCTCGAACTTCAC
CMV	FAM-AGTCATCGCTATTACCATGG-BHQ1	TGCCCAGTACATGACCTTATGG	GAAATCCCCGTGAGTCAAACC

2.10 Cell culture

2.10.1 Thawing, culture and freezing of human hepatocarcinoma cells (HuH7) and human embryonic kidney cells (Hek293T)

Cells of the human hepatoma cell line HuH7 and human embryonic kidney cell line Hek293T were kept as frozen stocks in 80% FCS, 20% DMSO in liquid nitrogen. Cells were nearly completely thawed as quick as possible in 37°C water bath until only a small piece of ice was left. They were immediately transferred into 10 ml pre-warmed DMEM culture medium. In the case of HuH7 cells this medium was supplemented with 10% FCS and 1% penicillin/streptomycin (DMEM complete HuH7) and in the case of Hek293T cells this medium was additionally supplemented with 1% glutamine (DMEM complete Hek293T). Cells were centrifuged for 5 minutes at 200 x g. Afterwards cell pellet was resuspended in the respective fresh pre-warmed DMEM complete and transferred into a cell culture flask (25 cm^2 or 75 cm^2). Cells were incubated at 37°C and 5% CO_2 until a confluent monolayer was grown. For maintaining cells in culture, medium was removed, cells were washed carefully with HBSS, detached by adding 0.25% Trypsin/EDTA (Gibco) and incubated for 3-5 minutes at 37°C. After addition of 10 ml respective DMEM complete medium, cells were transferred to a 15 ml polypropylene tube and centrifuged for 5 minutes at 200 x g. The cell pellet was washed once with HBSS and finally resuspended in 10 ml respective DMEM complete. Depending on the further purpose an aliquot of 200 µl up to 2 ml of the cell suspension was transferred to a new culture flask and filled up to 5 ml or 15 ml with respective DMEM complete, according to the size of the cell culture flask, 25 cm^2 or 75 cm^2, respectively. For freezing, trypsinized and washed cells were centrifuged for 5 minutes at 200 x g, resuspended in freezing solution (80% FCS, 20% DMSO) and instantly frozen at -80°C. For storage they were transferred to liquid nitrogen.

2.10.2 Determination of cell number

For seeding a defined amount of cells, the cell number was determined using a hemocytometer (Neubauer). Trypsinized cells were diluted in trypan blue for discrimination between vital and dead cells. Vital cells within the four outer large fields of the hemocytometer were counted. According to the equation below, the number of cells within the initial suspension was determined with 10^4 representing the chamber factor of the hemocytometer:

$$(\text{number of cells in four outer large fields} / 4) \times 10^4 \times \text{dilution factor} = \text{number of cells / ml}$$

2.10.3 Seeding of cells

In order to get a confluent monolayer of HuH7 cells in a 8-well-chamber-slide (LabTek slides), 20,000 HuH7 cells were seeded per well. For this purpose, the cell suspension with defined number of HuH7 cells (2.10.2) was diluted to final concentration of 20,000 cells in 400 µl. These 400 µl were added to each well. For growing confluent monolayers of Hek293T cells in 144 mm tissue culture dishes (Nunc) 5 x 10^6 cells in 22 ml DMEM complete were added per dish. 8-well-chamber-slides and tissue culture dishes were cultivated at 37°C and 5% CO_2. 8-well-chamber-slides could be used for further experiments the next day and tissue culture dishes two days after seeding.

2.10.4 Infection of HuH7 cells with salivary gland sporozoites

For infection of HuH7 cells in 8-well-chamber slides, medium was removed from the wells and 100 µl salivary gland sporozoite solution containing 20,000 sporozoites in RPMI/3% BSA was applied to each well. Hepatocytes were incubated with sporozoites for 90 minutes at 37°C and 5% CO_2. Afterwards medium was removed, cells were carefully washed once with pre-warmed DMEM complete and each well was filled with 400 µl DMEM complete supplemented with 1x anti-contamination cocktail to prevent contamination with bacteria derived from the mosquitoes' salivary glands. Hepatocytes were incubated at 37°C and 5% CO_2 for 10h, 24h, 40h and 60h as indicated in the respective experiments. During the incubation period medium was changed once a day to fresh DMEM complete supplemented with 1x anti-contamination cocktail.

2.10.5 Production of recombinant Adeno-associated viral (rAAV) particles

Two days prior to polyethylenimine (PEI) transfection, Hek293T cells were seeded into 144 mm tissue culture dishes. For each dish 5 x 10^6 cells in 22 ml DMEM complete were added and allowed to grow for two days. For subsequent *in vivo* application of rAAV particles 40 plates per plasmid were seeded and purified by centrifugation on a density gradient of cesium chloride. Cells were then transfected with a total of 44.1 ng DNA, containing each 14.7 ng generated plasmid (sections 2.8.2 and 2.8.3), adenoviral helper plasmid pVAE2AE4-5 (Matsushita et al., 1998), and AAV8 capsi expression plasmid p5E18-VD2/8 (Gao et al., 2002). According to the PEI transfection method DNA was mixed with water up to 790 µl, then 790 µl NaCl (300 mM) were added and mixed by inverting. 352 µl PEI (linear, MW 25000, PolyScience Inc.) was mixed with 438 µl water, then 790 µl NaCl (300 mM) were added and mixed by inverting. PEI solution was added into DNA solution, mixed and incubated at room temperature for 10 min. The entire solution was applied drop wise directly onto the cells. Cells were further incubated for three days. Cells were then scraped into the medium and collected in a conical tube and centrifuged for 15 minutes at 400 x g. Supernatant was carefully discarded, pellet was resuspended in 50 ml 1x PBS and transferred into a 50 ml polypropylene tube and centrifuged for

10 minutes at 400 x g. Supernatant was again carefully discarded and pellet was resuspended in 5 ml benzonase buffer. The resuspended pellet was conducted to three freeze and thaw cycles using liquid nitrogen for freezing and 37°C water bath for thawing. 0.8 µg/ml benzonase was added, inverted, incubated for 1 hour at 37°C with repeated inversion every 10 minutes and centrifuged for 15 minutes at 2500 x g. Supernatant was transferred to a fresh 50 ml polypropylene tube. For precipitation of proteins 1/39 volume 1 M cesium chloride (final concentration of 25 mM $CaCl_2$) was added, incubated on ice for 1 hour and centrifuged for 15 minutes at 10,000 x g and 4°C. Supernatant was transferred to a fresh 50 ml polypropylene tube. In a next step the rAAVs were precipitated using PEG8000. For this purpose ¼ volume PEG8000/2.5 M NaCl was added to the transferred supernatant, thoroughly mixed and incubated over night on ice. Next rAAVs were precipitated by centrifugation at 2500 x g for 30 min and 4°C, supernatant was discarded. Pellet was resuspended in 10 ml Na-HEPES resuspension buffer and volume was adjusted to 24 ml with this resuspension buffer. 13.2 g cesium chloride were added, inverted and allowed to warm up to room temperature. Refractory index (RI) was adjusted to 1.3710 using a refractometer. In case RI was too high, Na-HEPES resuspension buffer was carefully added and if RI was too low, grains of $CaCl_2$ were added. Solution was pipetted into centrifugation tubes (Optiseal, 29.9 ml) without inclusion of air bubbles and filled up to the top with topping solution. Centrifugation tubes were sealed and solution was centrifuged for 23 hours at 45,000 rpm and 21°C, without break. The next day the lower 17 ml of the gradient were collected as ten different fractions in 15 ml polypropylene tubes. RI of these fractions was determined and fractions with RI from 1.3711 to 1.3766 were pooled for further processing. Remaining fractions were discarded. The pooled fractions were dialyzed in 700 ml 1x PBS using Slyde-A-Lyzer G2 Dialysis cassettes (20K MWCO, 15 ml, Pierce). For this purpose each rAAV sample was adjusted to 9 ml. 1x PBS was changed after 30 minutes, 1 hour, 2 hours, over night, 2 hours, 2 hours. Except for the first dialysis step PBS was constantly stirred. Finally rAAV samples were concentrated using Amicon-Ultra-15 tubes (Millipore). For this purpose rAAV samples were applied on filter and with several centrifugation steps for 2 minutes at 500 x g the final volumes were reduced to 1-1.5 ml. 100 µl aliquots of rAAV samples were directly stored at -80°C.

2.11 Cell biological methods

2.11.1 Immunofluorescence assays

2.11.1.1 Two-color host cell invasion assay

For the two-color host cell invasion assay HuH7 cells were seeded in 8-well-chamber slides as described in section 2.10.2 at a density of 20,000 cells per well and incubated for one day. In a next step 20,000 salivary gland sporozoites per well were added onto the cells in a volume of 100 µl and allowed to invade for 90 minutes at 37°C and 5% CO_2. Afterwards medium was removed and cells were fixed with 400 µl pre-cooled (4°C) 4% PFA/PBS per well for 10-20 minutes at room temperature or over night at 4°C in a humid chamber, followed by two washing steps with 200 µl 1% FCS/PBS per well. Unspecific binding sites for subsequently applied antibodies were blocked by incubation with 400 µl 10% FCS/PBS for 60 minutes at 37°C or over night at 4°C in a humid chamber. Blocking solution was removed and 100 µl primary antibody, mouse anti-*Pb*CSP hybridoma supernatant 1:300 diluted with 10% FCS/PBS, was applied and incubated for 45 minutes at 37°C in a humid chamber for staining of extracellular sporozoites. After careful aspiration of primary antibody, cells were washed three times with 1% FCS/PBS, followed by addition of secondary antibody, goat anti-mouse Alexa Fluor 488 (Invitrogen) diluted 1:300 with 10% FCS/PBS and incubation at 37°C for 45 minutes in a humid chamber. Then cells were washed three times with 1% FCS/PBS and permeabilized by adding 100 µl ice-cold (-20°C) 100% methanol for 15 minutes at room temperature. After two more washing steps with 1% FCS/PBS cells were blocked again with 10% FCS/PBS for 30 minutes at 37°C in a humid chamber, followed by application of 100 µl primary antibody, mouse anti-*Pb*CSP hybridoma supernatant 1:300 diluted with 10% FCS/PBS and incubation at 37°C for 45 minutes in a humid chamber for staining of intracellular sporozoites. Cells were washed three times with 1% FCS/PBS and secondary antibody goat anti-mouse Alexa Fluor 546 (Invitrogen), diluted 1:300 with 10% FCS/PBS was applied at 37°C for 45 minutes in a humid chamber. For at least 5 minutes before final washing steps, Hoechst diluted 1:10,000 with 10% FCS/PBS was added for staining of nuclei. Finally, after the last three washing steps with 1% FCS/PBS a cover slip was mounted onto the slide with 50% glycerol and sealed with nail polish.

2.11.1.2 Liver-stage development assay

For the liver-stage development assay HuH7 cells were seeded in 8-well-chamber slides as described in section 2.10.2 at a density of 20,000 cells per well and incubated for one day. In a next step 20,000 salivary gland sporozoites per well were added onto the cells in a volume of 100 µl and allowed to invade for 90 minutes at 37°C and 5% CO_2. Afterwards cells were washed once and medium was replaced by fresh DMEM complete supplemented with 1x anti-contamination cocktail and cells were

incubated at 37°C and 5% CO_2. Medium was changed once a day during incubation. Liver-stage development was stopped at 10h, 24h, 40h and 60h post invasion. The cells were fixed and simultaneously permeabilized by applying 100 µl of ice-cold (-20°C) 100% methanol to each well for 15 minutes at room temperature. Cells were then washed twice with 1% FCS/PBS and subsequently blocked with 400 µl 10% FCS/PBS per well for 30 minutes at 37°C or over night at 4°C. After removal of blocking solution 100 µl primary antibody, mouse anti-*Pb*HSP70 hybridoma supernatant diluted 1:1 with 10% FCS/PBS, was added for 30 minutes at 37°C. Afterwards cells were washed three times with 1% FCS/PBS and secondary antibody, goat anti-mouse Alexa Fluor 546 (Invitrogen) diluted 1:300 in 10% FCS/PBS, was applied for 30 minutes at 37°C. For at least 5 minutes before the next washing step, Hoechst diluted 1:10,000 with 10% FCS/PBS was added. After three final washing steps with 1% FCS/PBS a cover slip was mounted onto the slide with 50% glycerol and sealed with nail polish.

2.11.2 Microscopy

2.11.2.1 Immunofluorescence microscopy

The immunofluorescence microscopy allows localization of proteins and thus also of parasites expressing these proteins. For this purpose a specific primary antibody is used that recognizes the protein of interest and binds to it. The Fc portion of this primary antibody in turn is recognized by a secondary antibody, which is conjugated to a fluorophore. This fluorophore is excited with light of a defined wavelength and hence emits light of a defined longer wavelength. This emitted light is then detected through a filter and visualized.

2.11.2.2 Principle of confocal laser scanning microscopy

The confocal laser scanning microscopy allows generation of high-resolution optical images. A laser scanning microscope is in general a light microscope supplemented with a laser and scanning module (LSM). This module enables scanning of single horizontal planes of the specimen. Laser light of a defined wavelength is used to excite the fluorophores typically used for confocal laser scanning microscopy. Laser light that is scattered and reflected by the specimen is re-collected by the objective lens. On its way back, the light is deflected by a beam splitter, which allows passing of emitted fluorescent light while blocking light of the exciting wavelength, to the photodetection device, usually a photomultiplier tube (PMT). This PMT transforms the light signal into an electrical signal that can then be visualized on a computer screen. Presence of a pinhole blocks out-of-focus light and thus allows higher resolution of the image in comparison to conventional fluorescence microscopy.

2.11.3 Dual Luciferase assay

This assay was performed using the Dual Luciferase assay kit provided by Promega. For the Dual Luciferase assay 2 x 10^6 (Hek293T) or 1.1 x 10^6 (HuH7) cells were grown in 96-well tissue culture plates (Greiner). In general 2.5-5 ng (Hek293T) or 50 ng (HuH7) psiCheck-2 vector (Promega) and additional 50-100 ng plasmid of interest (section 2.8) were used. Hek293T cells were transfected using PEI (Polyscience Inc.) while transfection of HuH7 cells was performed with Lipofectamin (Invitrogen). Two days post transfection medium was removed from the cells and cells were subsequently lysed using 25 µl lysis buffer (provided with the kit) and incubated for 15 minutes at room temperature. 5 µl of the lysate were transferred to a white luminometer plate (Promega). After consecutive injection of 25 µl reconstituted luciferase assay buffer and Stop & Glow solution supplemented with Rluc (*Renilla* luciferase) substrate (all provided with the kit), *Renilla* and firefly activities were measured using a Glomax 96 microplate luminometer (Promega). During data analysis for each well Rluc values were first normalized to the corresponding Fluc (firefly luciferase) values, followed by normalization of samples containing plasmid of interest to their respective non-silencing controls.

2.12 *Plasmodium berghei* experimental methods

2.12.1 Microscopical demonstration of *Plasmodium berghei* using Giemsa staining

For discrimination between the different blood stages of *Plasmodium berghei* and for determining the percentage of parasitized erythrocytes in the blood, called parasitemia, blood smears are a simple, fast and convincing tool. Blood smears were prepared by smearing a drop of blood, withdrawn from the tail tip of an infected mouse, onto a microscopic glass slide. After air-drying the blood, it was fixed in 100% methanol for 10 seconds at room temperature. After another 5-10 minutes air-drying the glass slide was placed in a staining cuvette filled with fresh Giemsa staining solution (1:10 dilution of the stock solution in de-ionized water), allowed to stain for at least 15 minutes and carefully rinsed with tap-water followed by final air-drying and examination of the smear under a light microscope at 100x magnification with oil immersion.

2.12.2 Determination of parasitemia

The parasitemia reflects the percentage of parasitized erythrocytes in the blood of an infected mouse (or human) and is used to characterize the parasite load in the respective organism, thereby indicating the intensity of an active, clinical parasitic infection. Parasitemia was typically determined in an area of the blood smear (section 2.12.1) where erythrocytes were arranged in a monolayer. Due to a grid in the eyepiece of the microscope an area was defined. In 25 sections of the blood smear the number of infected erythrocytes within the area defined by the grid was counted. In 2 out of these 25 sections the total number of erythrocytes, infected as well as uninfected, was determined and an average was calculated. According to the equation below the parasitemia was determined in %:

(total number of infected erythrocytes / (average number of all erythrocytes x 25)) x 100
=
parasitemia (%)

2.12.3 Examination of exflagellation of *Plasmodium berghei* gametocytes

Exflagellation of male gametocytes is a prerequisite for the successful transmission of the parasite to the *Anopheles* mosquito. Thus it is necessary to observe exflagellation prior to the mosquitoes' blood meal on an infected mouse. For this purpose a drop of blood was withdrawn from the tail tip of an infected mouse, placed onto a microscopic glass slide and covered with a small cover slip. Exflagellation can be triggered by several factors, i.e. temperature decrease of 2-5°C (Sinden and Croll, 1975), change in pH value (Billker et al., 2000) and presence of xanthurenic acid (Arai et al., 2001) in the mosquito midgut. Thus for induction of exflagellation, glass slides were incubated for

10 minutes at room temperature. Exflagellation of male gametocytes, the differentiation of microgametocytes into eight microgametes, was then examined by light microscopy with 40x magnification. To improve probability of a successful mosquito infection, mosquitoes were only feed on mice if at least 4-6 spots with exflagellating microgametes could be detected within one visual field.

2.12.4 Cryopreservation of *Plasmodium berghei*

Blood stage parasites can be stored for long-term as frozen parasite stocks. For this purpose, 100 µl of infected blood, freshly withdrawn from an infected mouse, were mixed with 200 µl freezing solution containing 10% glycerine in Alsever's solution (Sigma) and instantly frozen in liquid nitrogen. For large stocks, 300 µl fresh infected blood were mixed with 600 µl freezing solution.

2.13 *Anopheles stephensi* experimental methods

2.13.1 Breeding of *Anopheles stephensi* mosquitoes

For the production of eggs, female mosquitoes require a blood meal. Under laboratory conditions mosquitoes are feed on naïve NMRI mice to induce egg production. Mice were anesthetized by intraperitoneal injection of ketamine/xylazine and subsequently placed on top of a mosquito cage for 15 minutes. Mosquitoes, typically aged between 5 to 7 days, were starved at least 2 hours prior to blood meal by withdrawal of salt and sugar pads. Egging usually occurred 4 days after the bloodmeal and therefore a petri dish with 1 ‰ sea salt in ddH_20 containing a filter paper was placed in the mosquito cage. After egging, the eggs were rinsed with 70% ethanol to decrease the amount of bacteria, followed by rinsing twice with ddH_20 containing 1 ‰ sea salt. For hatching of larvae, eggs were transferred to trays filled with ddH_20 containing 1 ‰ sea salt. Hatched larvae were fed with small pieces of dry cat food and trays were washed on every third day. Larvae were split to maintain an optimal density. On day 9 after blood meal, larvae transformed into pupae and trays were covered with nets. Mosquitoes hatched from the pupae, were aspirated with a vacuum aspiration device and transferred into small experimental cages. Mosquitoes were fed with 10% sucrose solution supplemented with 20 µg/ml para-aminobenzoic acid (pABA) and 1 ‰ sea salt in ddH_20. For this purpose, cotton pads were saturated with the solutions and placed on top of the cages. Uninfected mosquitoes were kept in the breeding room at 28°C and 80% humidity, while mosquitoes infected with *Plasmodium berghei* were transferred into incubators within the insectary and kept there at 20°C and 80% humidity with a light/dark cycle of 12 hours.

2.13.2 Preparation of blood meal with infectious parasite stages

Mice used for blood meal were usually injected with thawed parasite stabilates of the required *Plasmodium berghei* strain one to two days prior to collection of the respective experimental cages. Exflagellation was determined as described in section 2.12.3 four to seven days after injection of stabilates. If microgametes exflagellated well, mice were anesthetized with ketamin/xylazine and fed to the mosquitoes for 15 minutes. Blood meal was repeated the next day to ensure a good infection rate.

2.13.3 Examination of midgut oocysts (prevalence)

Nine to eleven days after the blood meal, the micro- and macrogametes had fused to form ookinetes, which matured to oocysts in the mosquito midgut. The infection rate, or prevalence, of the female mosquitoes can be calculated by visualizing the oocyte formation and determining the number of oocysts. For this purpose five to ten female mosquitoes were removed from the cage, transferred into

a 15 ml polypropylene tube and anesthetized on ice for a few minutes. The stunned mosquitoes were put on a glass slide in RPMI/3% BSA, the midguts were removed under visual control through a binocular microscope, transferred into a drop of RPMI/3% BSA on a new glass slide and covered with a cover slip. The oocysts were visualized using a light microscopy at 40x magnification. The proportion of infected mosquitoes among all examined mosquitoes gives the prevalence of infection and the number of oocysts within infected midguts provides information about the infectivity of a single mosquito.

2.13.4 Isolation and purification of salivary gland sporozoites

Between day 17 and day 21 after blood meal infectious sporozoites were isolated from the salivary glands of female *Anopheles* mosquitoes infected with *Plasmodium berghei*. For this purpose mosquitoes were removed from the cages, anesthetized as described in section 2.13.3 and the salivary glands were carefully removed under microscopic control in RPMI without supplementation of 3% BSA. Salivary glands were collected in RPMI in a 1.5 ml microfuge tube on ice and then homogenized for 2-3 minutes with a pestle. The suspension was centrifuged for 3 minutes at 1000 rpm and 4°C. The supernatant containing the sporozoites was transferred to a fresh 1.5 ml microfuge tube, the pellet was resuspended in 50-100 µl RPMI, homogenized once more for 2-3 minutes and centrifuged for 3 minutes at 800 rpm and 4°C. The supernatants were combined and the number of salivary gland sporozoites was determined as described in the following section.

2.13.5 Determination of the number of salivary gland sporozoites

The number of purified salivary gland sporozoites was assessed using a hemocytometer (Neubauer). For this purpose, 2-10 µl of combined supernatants containing the sporozoites (section 2.13.4) were diluted 1:10 with RPMI and sporozoites within the four outer large fields of the hemocytometer were counted. According to the equation below the number of sporozoites within the combined supernatants was determined with 10^4 representing the chamber factor of the hemocytometer:

$$\frac{(\text{number of sporozoites in four outer large fields} / 4) \times 10^4 \times \text{dilution factor}}{=} \\ \text{number of sporozoites / ml}$$

2.14 Animal experimental methods

Mice were purchased from Charles River Laboratories, Sulzfeld or Janvier, France with an age of typically 18-20 days. A maximum of 4-5 mice were kept in Makrolon cages and cared for in the central animal facility of the University of Heidelberg (Interfakultäre Biomedizinische Forschungseinrichtung, IBF). Within the animal rooms of the facility a constant room temperature of 22°C and a constant humidity of 50-60% were maintained. The light/dark cycle was 12 hours. Mice were fed with standard dry pellet food (SSNIFF).

2.14.1 Anesthesia and blood withdrawal from malaria infected mice

Mice infected with *Plasmodium berghei* were anesthetized and blood was removed finally by heart puncture using a heparinized syringe. Blood was either used for a transfer into a new naïve mouse by intraperitoneal injection or substituted with freezing solution to obtain parasite stabilates.

2.14.2 Application methods

Blood stage parasites were typically injected into the abdominal cavity (intraperitoneal) of naïve mice, while purified sporozoites were usually injected into the tail vein (intravenous) of the mouse. To reproduce a natural transmission, the anesthetized mouse was exposed to infected *Anopheles* mosquitoes on top of the cage. Thus, infectious salivary gland sporozoites were transmitted during the blood meal by the mosquitoes. Recombinant Adeno-associated viral (rAAV) particles were typically injected intravenously.

2.14.3 Isolation of livers from mice

Livers were isolated from naïve mice and mice infected with *Plasmodium berghei* for subsequent isolation of RNA and protein. For this purpose, mice were anesthetized or sacrificed, thorax and abdomen were opened, 3-4 small cuts were placed in the different lobes of the liver and the mouse was perfused by intracardiac application of 10-20 ml 1x PBS. The liver was quickly removed, cut into several small pieces using clean scissors, immediately shock frozen in liquid nitrogen and transferred to pre-cooled 2 ml Eppendorf tubes. Liver pieces were stored at -80°C.

2.14.4 Isolation and purification of primary hepatocytes

Primary hepatocytes were separated from the remaining liver cells of either naïve mice or mice infected with *Plasmodium berghei* liver-stages. Prior to the procedure, buffers were heated to 42°C

for perfusion, tubes and catheters were filled with buffers to avoid occurrence of air bubbles. Buffers were kept at 42°C in a water bath during the whole procedure. Mice were sacrificed and abdomen was opened by cutting through skin and abdominal wall without injuring liver and intestines. Intestines were shifted to expose *vena cava* and portal vein. Vein catheter was carefully inserted into *vena cava inferior* without piercing through it. Pump was switched on (5-8 ml/min) and portal vein was cut to perfuse the liver for 15-20 minutes with 1x EGTA buffer followed by 20 minutes perfusion with 1x collagenase buffer. Afterwards the liver was carefully removed from the abdomen and kept in a petri dish with the remaining 1x collagenase buffer. Connective tissue around the liver was carefully pulled off to release the cells. Suspension was aspirated several times to singularize cells followed by filtering the suspension through a 100 µm cell strainer. Petri dish and cell strainer were subsequently washed with 5-10 ml Williams E medium, combined with the suspension in a 50 ml polypropylene tube and centrifuged for 5 minutes at 28 x g and 4°C. Supernatant was discarded, pellet was resuspended in 19 ml Percoll (9,748 ml Percoll (1.124 g/ml, Biochrom AG), 10.252 ml HBSS) and centrifuged for 10 minutes at 50 x g and 4°C, without brake. Upper cell layer containing remaining liver cells and Kupffer cells was transferred to a new 50 ml polypropylene tube and supernatant without cells was discarded. Cell pellet containing hepatocytes was resuspended in 25 ml Williams E medium and the previously transferred upper cell layer was filled up with Williams E medium. All cells were centrifuged for 5 minutes at 28 x g and 4°C. Supernatants were discarded. Hepatocytes were resuspended in 2 ml QIAzol, transferred to two fresh nuclease-free Eppendorf tubes (1ml per tube), remaining liver cells including Kupffer cells were resuspended in 1 ml QIAzol and transferred to one fresh nuclease-free Eppendorf tube. All resuspended cells were instantly frozen and stored at -80°C.

2.15 Biochemical methods

2.15.1 Protein isolation from hepatic tissue

Proteins were isolated from frozen pieces of mouse liver (section 2.14.3). For this purpose frozen liver pieces were weighed and 10 µl pre-cooled RIPA buffer, supplemented with 1 mM DTT and protease inhibitor, per 10 mg tissue were provided in 5 ml FACS tubes. The frozen liver pieces were transferred in this RIPA buffer and immediately disrupted and simultaneously homogenized for 20-30 seconds on ice using a TissureRuptor (Qiagen). Homogenized samples were incubated on a shaking platform for 2 hours at 4°C and subsequently centrifuged for 20 minutes at 12,000 rpm and 4°C in a table microcentrifuge. Supernatants were carefully aspirated and transferred to fresh 1.5 ml microfuge tubes and kept on ice. For long-term storage samples were frozen at -20°C.

2.15.2 Determination of protein concentration according to Bradford

This method for determining the concentration of proteins is based on the binding of Coomassie brilliant blue G-250 to proteins. After binding of this dye to proteins the absorption peak is shifted from 465 nm prior to protein binding to 595 nm after binding (Bradford, 1976). Concentration of proteins was determined in this work using Roti-Quant (Roth) according to the manufacturer's manual. According to the manual a standard curve was generated and the resulting equation (y = 0.0007 x; with x being the absorption and y representing the protein concentration) was used to determine the protein concentration in respect to the absorption. The typical sample volume was 1 µl.

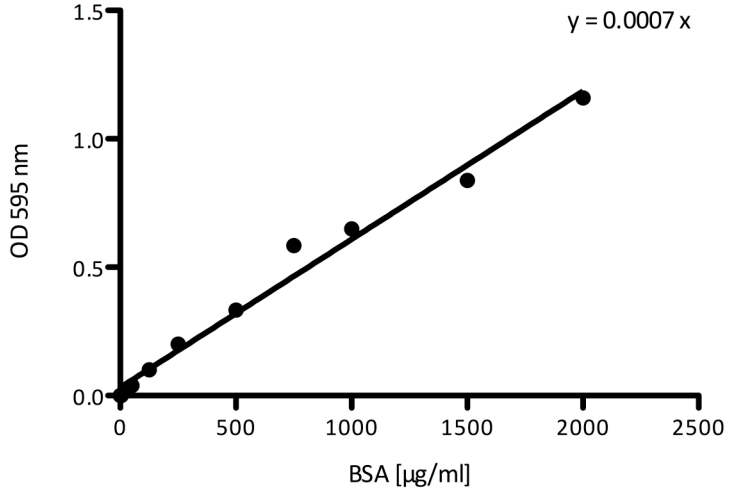

Figure 2.15.1: Standard curve for determination of protein concentration according to Bradford.

2.15.3 SDS polyacrylamide gel electrophoresis (SDS-PAGE)

SDS polyacrylamide gel electrophoresis (SDS-PAGE) according to Laemmli (Laemmli, 1970) was used to separate proteins. The separation takes place because proteins migrate differently through an electrical field due to their different sizes and charges. Small proteins migrate faster than lager ones and less charged slower than more charged ones. In addition, differences in the concentration of acrylamid also have influences on the migration properties of the proteins. The more acrylamid is present in the gel, the smaller are the resulting pores of the gel and the better the separation of small proteins. Another important component is sodium dodecyl sulfate (SDS). It is an anionic detergent, which denatures secondary and non-disulfide-linked tertiary structures and applies a negative charge to each protein in proportion to its mass. In addition to SDS, the 2x SDS loading buffer contained β-mercaptoethanol to reduce the disulfide bonds of the proteins. The volume, containing 5 µg protein sample, was adjusted to 10 µl with RIPA buffer. 10 µl of 2x SDS loading buffer were added, mixed and incubated for 5 minutes at 95°C. Thus, the proteins were denatured and the SDS was facilitated to bind. For SDS-PAGE in this work pre-cast gels with a acrylamid/bisacrylamid gradient from 4-12% were used (NuPAGE, Invitrogen). Samples were loaded into the wells along with a pre-stained protein ladder (Fermentas) allowing afterwards determination of protein sizes. An electrical field was applied across the gel in 1x MOPS buffer (NuPAGE, Invitrogen) for 45-60 minutes at 200 V and room temperature, causing the negatively charged proteins to migrate towards the anode. After appropriate separation, gels were processed to Western blotting.

2.15.4 Western blot analysis

In order to make the proteins accessible for antibody detection and subsequent visualization by a chemiluminescence reaction (Thorpe and Kricka, 1986), they were transferred from the SDS gel onto a PVDF membrane (Millipore) using the wet blot technique. The configuration of the proteins within the gel is maintained during this process. For transfer of the proteins, the PVDF membrane as well as several blotting sponges and Whatman filter papers were soaked in 1x transfer buffer prior to assembly of the blotting chamber. Assembling of the blot was started with placing one blotting sponge (when blotting two gels) or two blotting sponges (when blotting one gel) on the cathode side of the blotting cassette, followed by one piece of Whatman filter paper, the SDS gel, which was vertically inverted, the PVDF membrane, another piece of Whatman filter paper and a second blotting sponge. If only one gel was blotted, the remaining space within the cassette was filled with another two blotting sponges. In case a second gel was blotted on a second membrane at the same time, the whole order starting with Whatman filter paper was repeated. After covering the membrane with Whatman filter paper, air bubbles were carefully removed without moving the membrane. Finally the blotting cassette was closed and inserted into the blotting chamber. The space within the blotting

cassette was filled with 1x transfer buffer while the outside was filled with de-ionized water. Proteins were blotted onto the membrane for 90 minutes at 30 V and room temperature.

After blotting the membranes were blocked for 60 min at room temperature or over night at 4°C with 5% dry milk in TBST to block unspecific binding of the subsequently applied antibodies. Afterwards, membranes were horizontally separated and incubated with primary antibodies either over night at 4°C if previous blocking took place one hour at room temperature or one hour at room temperature if previous blocking was performed over night at 4°C. The upper halves were incubated in 5% dry milk in TBST with either polyclonal rabbit anti-mouse Drosha antibody (1:1000 dilution; Abcam) or polyclonal rabbit anti-mouse Exportin-5 antibody (1:400 dilution; Abcam). The lower halves were incubated under the same conditions with monoclonal mouse anti-mouse β-Actin antibody (1:1000 dilution; Santa Cruz Biotechnology). Afterwards membranes were washed three times in 1x TBST for 10-20 minutes, followed by incubation with either horseradish peroxidase-conjugated goat anti-rabbit immunoglobulin G (IgG) (1:10,000 dilution; Jackson ImmunoResearch Laboratories) or goat anti-mouse IgG (1:10,000 dilution; Sigma) for 1 hour at room temperature. The horseradish peroxidase conjugated to the secondary antibodies catalyses the oxidation of luminol and thus triggers the production of chemiluminescence. The membranes were washed again and both components of the Western Lightning Plus-ECL (Perkin Elmer) kit were mixed in a 1:1 ratio, applied on the membranes and the membranes were transferred to a light protecting film cassette. The light emitted by the chemiluminescence reaction was detected by light sensitive films, which were placed on the membrane for different time periods ranging from 10 seconds to 10 minutes and up to an hour. The light sensitive films were subsequently developed. The size of the proteins was determined according to the pre-stained protein ladder. All incubation and washing steps were performed under constant agitation of the membranes.

2.16 Bioinformatical methods

2.16.1 Statistical analysis of microarray data

Statistical analysis of microarray data was performed by Dr. Bettina Knapp, PhD (AG Kaderali, Bioquant, Heidelberg). Raw data was collected using GenePix Pro 6 software (Axon Instruments/Molecular Devices Corp.) with an optimal setting of Hy3 and Hy5 channels as described in 2.9.2.5. The generated raw data has then been processed using the R language (www.r-project.org) and the "limma" (Linear Models for Microarray) package from the Bioconductor project (http://www.bioconductor.org/). The mean of the pixel distribution for the foreground and background signal was used as estimators of the raw signal values in both channels. By dividing foreground through background intensities, signal-to-noise ratios (SNR) were calculated. Spots which have been automatically flagged during the scanning process with Genepix and which have a SNR smaller than one were weighted with only 10% in the following analyses. Data were normalized by using loess normalization on the normexp-background corrected signal intensities. Thereafter, a quantile normalization was used to normalize all expression values against the naïve control given in the Cy3 channel of each microarray. All methods were used as provided in the limma package. Furthermore, for each spot the log-ratio M of the samples with the different parasites and treatments versus the naïve samples without parasites were computed. Using the M values, differentially expressed miRNAs have been calculated by applying the Welch one-sample *t*-test as implemented in R. In addition, an ANOVA analysis on the M values of all treatments was performed. For the resulting miRNAs with a p-value smaller than 0.05, the Welch two-sample *t*-test was used on pairs of the different treatments to identify those which have significant different expression values.

2.16.2 Translation of dys-regulated miRNAs into affected networks and pathways

For finding cellular networks and pathways within the host liver that might be affected by dys-regulated miRNAs due to an infection with *Plasmodium berghei* liver-stages the results from the two independent microarray analyses (sections 3.2 and 3.3) served as basis. The lists of dys-regulated miRNAs that had been generated were first of all translated into potential target genes using the free web-based prediction tool GeneTrail (http://genetrail.bioinf.uni-sb.de/mirna_geneset_converter.php). The resulting lists with potentially affected genes were entered into another web-based tool called GeneGo (http://www.genego.com/) to search for affected networks and pathways. The last web page was used in tight collaboration with Kathleen Börner (AG Kräusslich, Virology, Heidelberg) since access to this page has to be purchased.

2.16.3 Quantification of relative protein abundance after Western blot analysis

After Western blot analysis (section 2.15.4) the relative abundance of the detected proteins was quantified according to the intensity of the corresponding band visualized on the light sensitive film. For this purpose, the light sensitive films were scanned and saved as uncompressed TIFF files. These files were loaded into the free program Fiji (http://fiji.sc/wiki/index.php/Fiji) and converted into greyscale images. By using the rectangular selection tool each band of interest on the light sensitive film image was selected. It was important that rectangles drawn around corresponding bands had exactly the same size. Afterwards a profile plot for each lane was drawn, which represents the relative density of the content covered by the respective rectangle. The area enclosed by each profile plot is measured and used for the subsequent calculations as they are described in section 3.1.3.

3 Results

3.1 Interplay between the host hepatic RNAi machinery and the liver-stage of *Plasmodium berghei*

There is growing evidence that components of the RNAi machinery themselves may be highly regulated during disease and development, and that miRNAs are at least partly involved in these processes (Asirvatham et al., 2008; Ren et al., 2012; Sekine et al., 2009; Shu et al., 2011; Wiesen and Tomasi, 2009). Therefore, I was curious to find out whether intrahepatic infections with *Plasmodium berghei* NK65 WT, GAP and RAS parasites (Castoldi et al., 2011; Kumar et al., 2009; Mueller et al., 2005a; Mueller et al., 2007; Mueller et al., 2005b; Tarun et al., 2007) induce changes in the expression of components comprising the host liver RNAi machinery. To answer this question I analyzed the hepatic mRNA transcription levels of *Exportin-5* (*Xpo-5*), *Argonaute-2* (*Ago-2*), *Dicer*, *TRBP* (human immunodeficiency virus transactivating response RNA-binding protein) and *Drosha* at 24h and 40h after intravenously infection of mice with *Pb*NK65 WT, GAP and RAS infectious salivary gland sporozoites, respectively. In addition I also determined the protein expression levels of Xpo-5 and Drosha in these samples by Western blotting.

3.1.1 Animal groups

For further experiments inbred C57BL/6 mice were injected intravenously with 50,000 *Plasmodium berghei* NK65 WT, GAP and RAS salivary gland sporozoites, respectively. 24h and 40h after injection, the infected livers were harvested and total RNA (section 2.9.11) as well as protein (section 2.15.1) was isolated from small pieces of these livers. In addition, livers were isolated from naïve mice and processed the same way as just described. They serve as naïve controls for all experiments. For each of the seven groups of interest three animals were infected to obtain biological replicates. Table 3.1.1 summarizes all animal groups used for the subsequent experiments, except for those experiments that are described in section 3.1.4.

Table 3.1.1: Summary of samples used for subsequent experiments, except for experiments in section 3.1.4.

parasite genotype	hours post infection	animal number	sample name
not applicable	not applicable	1	naïve 1
		2	naïve 2
		3	naïve 3
WT	24h	1	WT 24h 1
		2	WT 24h 2
		3	WT 24h 3
GAP	24h	1	GAP 24h 1
		2	GAP 24h 2
		3	GAP 24h 3
RAS	24h	1	RAS 24h 1
		2	RAS 24h 2
		3	RAS 24h 3
WT	40h	1	WT 40h 1
		2	WT 40h 2
		3	WT 40h 3
GAP	40h	1	GAP 40h 1
		2	GAP 40h 2
		3	GAP 40h 3
RAS	40h	1	RAS 40h 1
		2	RAS 40h 2
		3	RAS 40h 3

3.1.2 Transcriptional analysis of components comprising the host hepatic RNAi machinery

The isolated total RNA of the seven groups of interest (table 3.1.1) was subjected to DNase digest prior to cDNA synthesis to exclude possible contaminations with genomic DNA (gDNA).

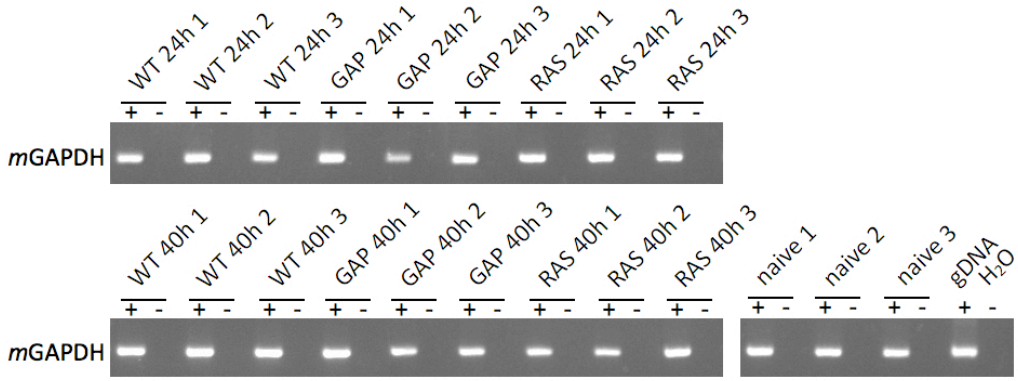

Figure 3.1.1: Verification of gDNA-free cDNA preparations. RNA was isolated from mouse livers 24h and 40h after infection with *Pb*NK65 WT, GAP and RAS, respectively, DNase digested and reverse transcribed. Each sample was conducted to two reverse transcription reactions. One reaction was performed in the presence of reverse transcriptase (+RT) and one reaction was performed without reverse transcriptase (-RT) for tracing contaminations with gDNA. RT-PCR was performed using primers amplifying a *m*GAPDH fragment of 496 bp.

To confirm absence of gDNA from the samples each reverse transcription reaction was set up twice: once with addition of reverse transcriptase (+RT) and once without addition of reverse transcriptase (-RT) as a negative control. For the subsequent control, RT-PCR primers amplifying a 496 bp fragment of

the *Mus musculus* glyceraldehyde-3-phosphate dehydrogenase (GAPDH) coding sequence were used (*m*GAPDH_For; *m*GAPDH_Rev) under standard PCR conditions (section 2.9.1.6). These RT-PCR analysis revealed cDNA preparations without any traces of gDNA as indicated by presence of bands only in the +RT preparations (figure 3.1.1).

After having confirmed purity of the cDNA preparations quantitative real-time PCR (qPCR) was performed to determine relative abundance of *Xpo-5*, *Ago-2*, *Dicer*, *TRBP* and *Drosha* transcripts.

A) B)

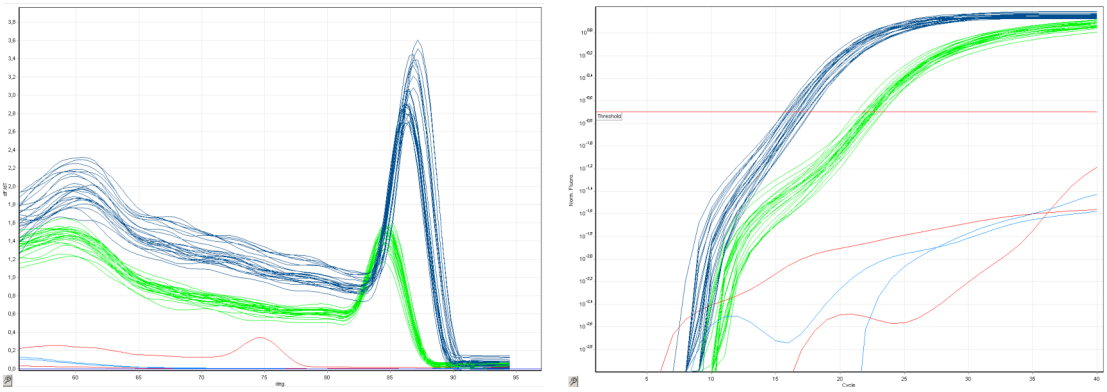

Figure 3.1.2: Exemplary melting and amplification curves. After each qPCR amplification run a melting curve profile was performed (A). qPCR for each primer pair resulted in generating amplification curves (B). In green the melting and amplification curves of the gene of interest specific primer assays are shown and in red the corresponding negative water control, while dark blue depicts the melting and amplification curves amplified with housekeeping primers and light blue represents again the corresponding negative water control.

For amplification of these genes of interest pre-designed primer assays were used while primers for the housekeeping gene *mGAPDH* were self designed (*m*GAPDH_qPCR_For; *m*GAPDH_qPCR_Rev). All samples (table 3.1.1) were pipetted in duplicates for each primer pair by a pipetting robot (Qiagility, Qiagen). To rule out any contaminations of the reaction mix for each primer pair, a negative water control was added, which contained no cDNA. Suitability of the primer assays was tested during each qPCR run by performing a melting curve. Only in case the melting curve showed one single peak as exemplarily depicted in figure 3.1.2A, the respective amplification curve was used for determination of C_T-values. The C_T-value represents the intersection of an amplification curve and the defined threshold and gives the concentration of target cDNA within the PCR reaction. The threshold was set in the linear phase of the amplification plot (figure 3.1.2B). An increase of the C_T-values corresponded to a decreasing amount of target cDNA. The C_T-values were the basis for the further mathematical calculations. Relative transcript abundance of the genes of interest *Xpo-5*, *Ago-2*, *Dicer*, *TRBP* and *Drosha* were determined according to the $2^{-\Delta\Delta CT}$ method. First, the mean expression data of the gene of interest as well as of the housekeeping gene for each duplicate was calculated. Second, the mean expression data of each sample was normalized using the housekeeping gene and finally the gene expression levels of the naïve mice were used as reference values. Thus I obtained the relative

expression of each of the genes of interest in infected mice compared to the expression of the respective gene in naïve mice.

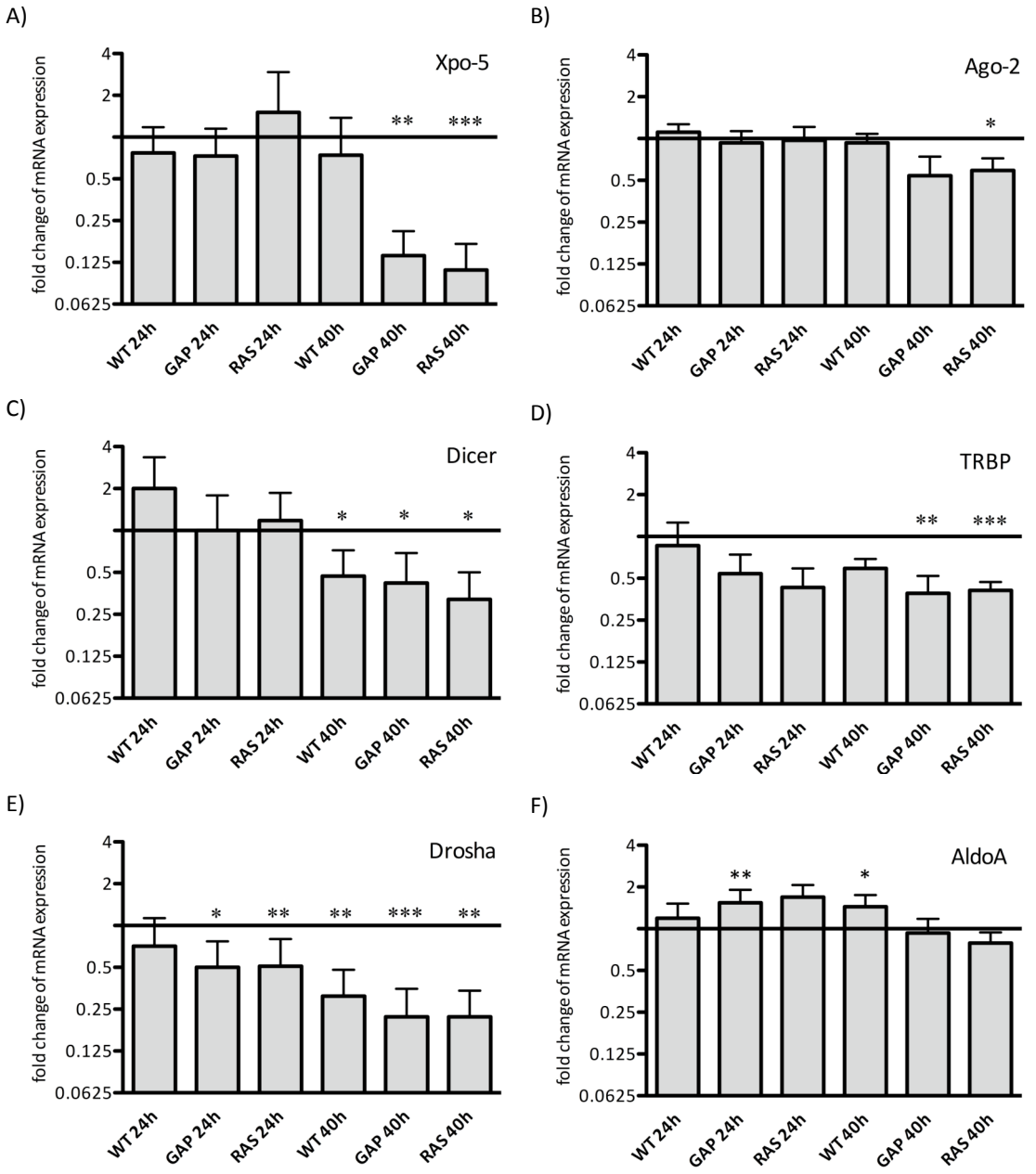

Figure 3.1.3: Transcript levels of components comprising the minimal RNAi machinery throughout malaria liver-stage development of attenuated and WT parasites. qPCR analysis of *Xpo-5* (A), *Ago-2* (B), *Dicer* (C), *TRBP* (D), *Drosha* (E) and *AldolaseA1* (F) transcript levels in mouse livers 24h and 40h after infection with *Pb*NK65 WT, GAP or RAS parasites. Fold change of mRNA expression and SD compared to naïve mice of three animals per group. * $p < 0.05$; ** $p < 0.01$; *** $p < 0.001$, unpaired t-test.

Interestingly, transcription levels for *Xpo-5* were 8-fold down-regulated in livers infected with GAP and RAS 40h post infection while the remaining groups investigated showed *Xpo-5* transcription levels comparable to naïve livers (figure 3.1.3A). A much less significant down-regulation was observed for *Ago-2* transcription 40h post infection with GAP and RAS (figure 3.1.3B) while *Ago-2* transcription was

unchanged in the remaining groups. *Dicer* transcription levels were 2- to 3-fold down-regulated 40h post infection with any of the chosen parasite lines while the levels stayed unchanged or slightly up-regulated at the early time point (figure 3.1.3C). In contrast to these results, *TRBP* transcription already decreased 2- to 3-fold 24h post infection with GAP and RAS while infection with WT parasites at this time point did not induce a change in comparison to naïve livers. 40h post infection *TRBP* transcription levels were down-regulated 2- to 3-fold in all livers investigated (figure 3.1.3D). For *Drosha* transcription a down-regulation at all time points investigated was observed. This down-regulation increased from 2-fold 24h post infection up to 3- to 4-fold 40h post infection and was more pronounced at both time points in livers infected with attenuated parasites compared to WT infected livers (figure 3.1.3E). To rule out any unspecific general down-regulation in the liver after infection with *Plasmodium* parasites I also quantified the transcription of *AldolaseA1*, which was shown previously to be regulated by miR-122 in the liver (Su et al., 2011b). Transcription of this gene was not down-regulated in any of the groups investigated (figure 3.1.3F) which is in good agreement with the observation that miR-122 transcription levels were as well unchanged in the groups investigated (figure 3.3.6B).

3.1.3 Expression levels of hepatic Exportin-5 and Drosha protein

After having identified a down-regulation on transcript level of components comprising the host hepatic RNAi machinery, I aimed at confirming this observation on protein level. For this purpose proteins were isolated from small liver pieces of all seven groups (table 3.1.1), separated according to their molecular weight using polyacrylamid gels under denaturing conditions and blotted onto PVDF membranes (section 2.15). These membranes were subsequently subjected to immunodetection using polyclonal antibodies specifically detecting either Xpo-5 or Drosha protein.

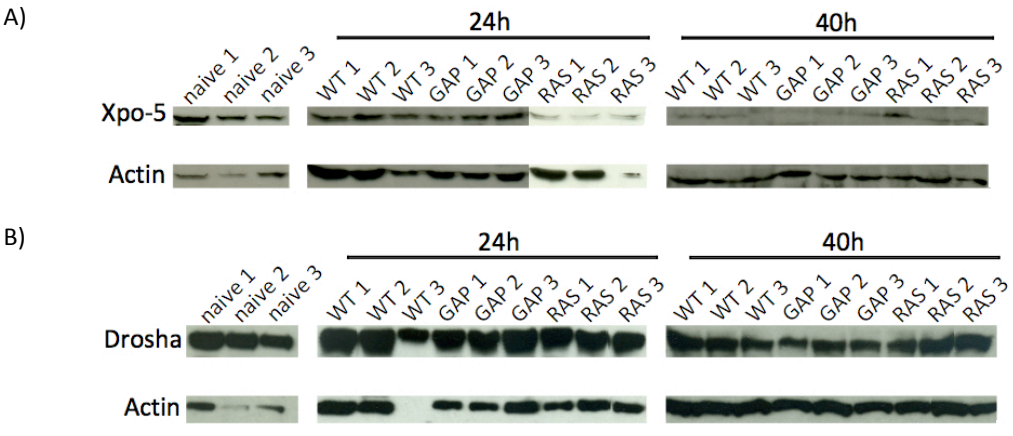

Figure 3.1.4: Western blot analysis of Xpo-5 and Drosha protein expression during malaria liver-stage development. Hepatic protein expression of Xpo-5 and Drosha was investigated among the seven groups of interest. Polyclonal antibodies against Xpo-5 (A) and Drosha (B) detected protein within the samples. Monoclonal anti-β-actin antibody was used to normalize applied protein amounts (A, B).

To normalize the amount of protein loaded onto the gel β-actin was used as internal reference and detection was performed with a monoclonal antibody against β-actin. Secondary antibodies conjugated to horseradish peroxidase were applied and after induction of a chemiluminescence reaction, signals were detected by exposure of the membrane to light sensitive films. Figure 3.1.4 shows the bands specific to Xpo-5 (A), Drosha (B) and β-actin (A,B) in every individual sample. The band intensities already implied a decreased protein expression of Xpo-5 and Drosha within infected livers when compared to naïve livers, which served as controls. For quantification of relative protein expression of Xpo-5 and Drosha, band intensities of each single sample were first normalized to the corresponding β-actin band intensity to rule out varying protein amounts by using Fiji (section 2.16.3). Afterwards, these corrected intensities of infected livers were calculated as percentage of the corrected band intensities of naïve livers.

The Xpo-5 (figure 3.1.5A) protein expression was decreased in all groups to 30-70% of the protein expression observed in naïve livers. The strongest decrease was observed after infection with RAS at both time points, while infection with GAP induced only a slight decrease at both time points. 24h after infection with WT and RAS hepatic Drosha protein expression (figure 3.1.5B) was reduced to 51% and 64%, respectively, while infection with GAP at this time point did not change the protein expression much compared to expression in naïve livers. In contrast to these findings at the early time point, only 20% to 25% of Drosha protein was still expressed 40h after infection with each of the parasite genotypes, reflecting the down-regulation of *Drosha* transcript levels at this time point (figure 3.1.3E).

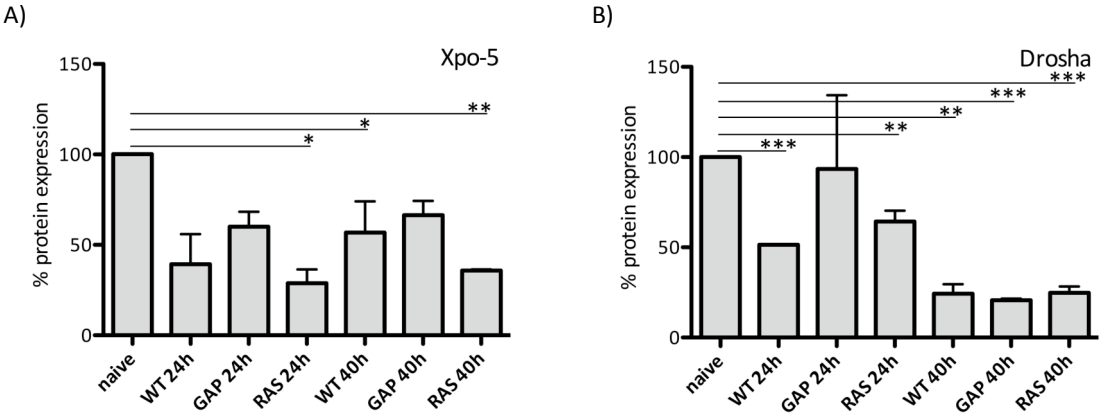

Figure 3.1.5: Quantification of relative expression of Xpo-5 and Drosha protein during malaria liver-stage development. Relative Xpo-5 (A) and Drosha (B) protein expressions were calculated as percentage of protein expression in naïve mouse livers. * $p < 0.05$; ** $p < 0.01$; *** $p < 0.001$ unpaired t-test.

3.1.4 Cellular distribution of affected components comprising the host hepatic RNAi machinery during malaria intrahepatic infecitions

So far the transcriptional and protein expression analysis of components comprising the host hepatic RNAi machinery was performed on samples taken from whole livers. However it would be even more interesting to exactly determine whether the affected cells are the host hepatocytes, which serve as the place for parasite growth and multiplication during the liver-stage development or whether the Kupffer cells may also contribute to this specific decrease in transcriptional levels, which are traversed by the parasite before it establishes it's liver phase. To approach this question, mice were infected intravenously with 50,000 *Pb*NK65 WT, GAP or RAS sporozoites. 24h and 40h post infection livers were perfused with collagenase to disperse cell-cell-connections and by subsequent density centrifugation steps hepatocytes were separated from remaining liver cells including Kupffer cells (section 2.14.4). Unfortunately, perfusion of mice did not work out in all cases, thus the number of samples for the subsequent analyses is reduced (table 3.1.2). Cases in which perfusion failed and thus no material was purified are crossed-out in table 3.1.2.

Table 3.1.2: Summary of samples after separation of hepatocytes and Kupffer cells. Samples for which perfusion of the liver failed and thus no cells were recovered are crossed.

parasite genotype	hours post infection	animal number	sample name
not applicable	not applicable	1	naïve 1
		2	naïve 2
		~~3~~	~~naïve 3~~
WT	24h	~~1~~	~~WT 24h 1~~
		2	WT 24h 2
		3	WT 24h 3
GAP	24h	1	GAP 24h 1
		2	GAP 24h 2
		3	GAP 24h 3
RAS	24h	1	RAS 24h 1
		2	RAS 24h 2
		3	RAS 24h 3
WT	40h	~~1~~	~~WT 40h 1~~
		~~2~~	~~WT 40h 2~~
		3	WT 40h 3
GAP	40h	1	GAP 40h 1
		2	GAP 40h 2
		~~3~~	~~GAP 40h 3~~
RAS	40h	1	RAS 40h 1
		2	RAS 40h 2
		3	RAS 40h 3

RNA was isolated from those isolated hepatocytes and remaining liver cells including Kupffer cells and further processed and validated for quantitative real-time PCR (qPCR) as described in section 3.1.2. Control RT-PCR analysis was performed with GAPDH primers to exclude gDNA contamination (*m*GAPDH_For; *m*GAPDH_Rev; see section 3.1.2). The RT-PCR analysis demonstrated gDNA free cDNA preparations (figure 3.1.6).

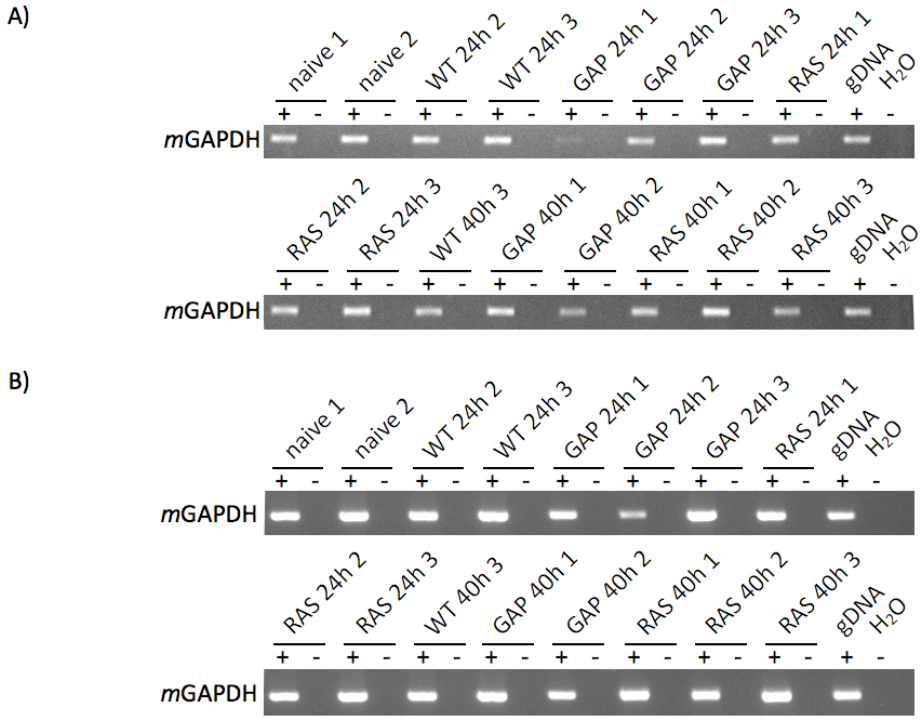

Figure 3.1.6: Verification of gDNA-free cDNA preparations. RNA was isolated from mouse hepatocytes (A) and remaining liver cells including Kupffer cells (B) 24h and 40h after infection with *Pb*NK65 WT, GAP or RAS, DNase digested and reverse transcribed. Each sample was conducted to two reverse transcription reactions. One reaction was performed in the presence of reverse transcriptase (+) and one reaction was performed without reverse transcriptase (-) for tracing contaminations with gDNA. RT-PCR was performed using primers amplifying a *m*GAPDH fragment of 496 bp.

The qPCR analysis was performed and evaluated as described in section 3.1.2 with the same pre-designed primer assays as well as the same self designed housekeeping primers. For these analyses the pipetting robot pipetted all samples in duplicates. When analyzing the transcription levels of *Xpo-5*, *Ago-2*, *Dicer*, *TRBP* and *Drosha* in purified hepatocytes (figure 3.1.7) striking differences were observed in comparison to transcription levels in whole liver samples (figure 3.1.3). In those whole liver samples a down-regulation of transcript levels was found for all genes investigated especially at 40h after infection with the attenuated malarial parasites. But after separation of hepatocytes from all remaining liver cells the transcript levels of *Xpo-5*, *Ago-2*, *Dicer* and *Drosha* were up-regulated in most of the groups investigated (figure 3.1.7A, B, C and E). Only hepatocytes infected with GAP showed *Drosha* transcript levels comparable to naïve hepatocytes (figure 3.1.7E). *TRBP* transcript levels of purified infected hepatocytes were either very similar to levels of naïve purified hepatocytes or had high standard deviations (figure 3.1.7D). As some of the groups investigated lacked biological replicates (table 3.1.2) no statistical analysis was performed. *Xpo-5* transcript levels in GAP infected hepatocytes at 40h could not be determined due to technical problems during the qPCR run (figure 3.1.7A).

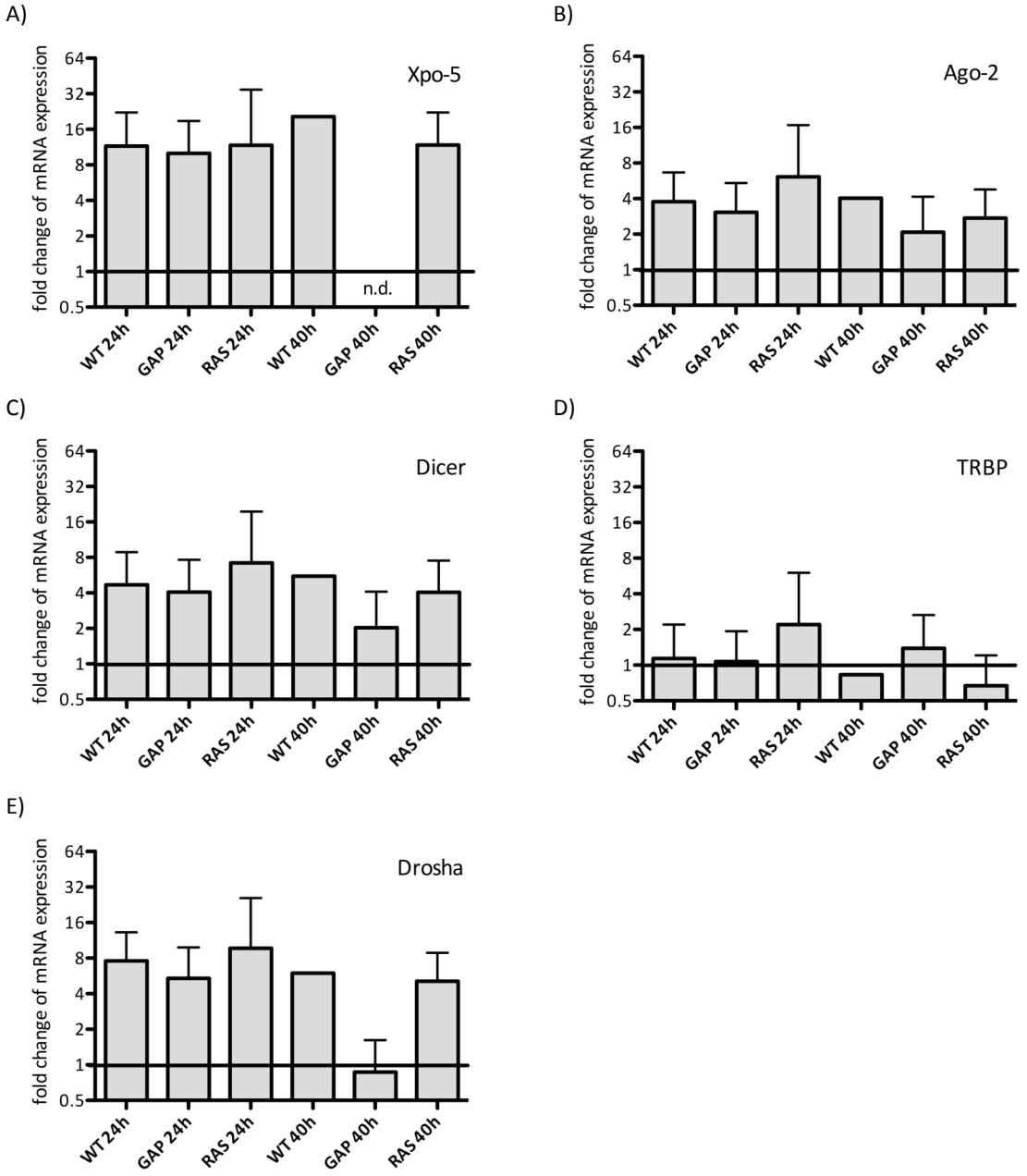

Figure 3.1.7: Relative transcript levels of components comprising the minimal RNAi machinery in purified hepatocytes. qPCR analysis of *Xpo-5* (A), *Ago-2* (B), *Dicer* (C), *TRBP* (D) and *Drosha* (E) transcript levels in purified mouse hepatocytes 24h and 40h after infection with *Pb*NK65 WT, GAP or RAS parasites. Fold change of mRNA expression and SD compared to purified hepatocytes of naïve mice. No statistical analysis was performed as biological replicates are missing in some groups. N.d. = not determined due to technical problems.

As these results were highly contradictory to those results obtained from whole liver preparations the question arose, whether up-regulation is a true effect or whether it is an artifact due to the prolonged procedure, which is necessary to obtain purified hepatocytes. To answer this question transcription levels of the chosen RNAi machinery components were compared in purified hepatocytes and purified remaining liver cells including Kupffer cells from naïve mice to transcript levels in preparations from whole naïve livers (figure 3.1.8).

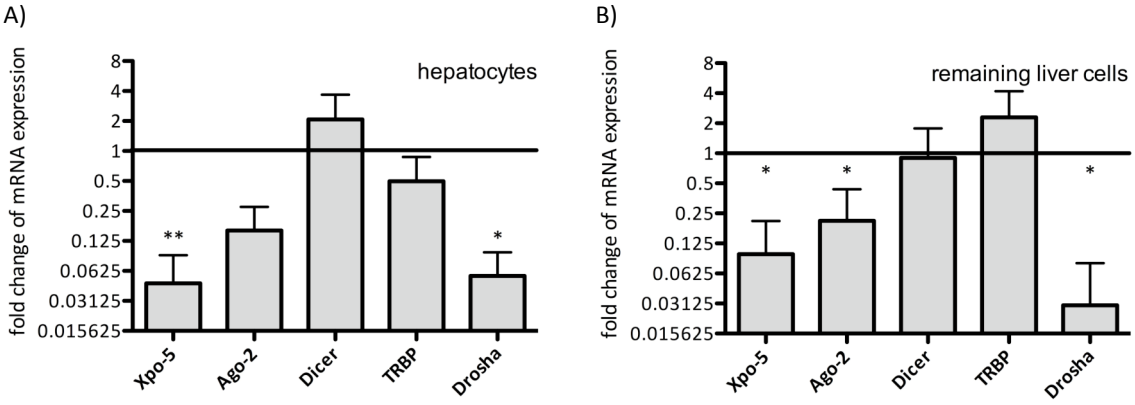

Figure 3.1.8: Transcript levels of components comprising the minimal RNAi machinery in purified hepatocytes and remaining liver cells including Kupffer cells from naïve mice. qPCR analysis of *Xpo-5*, *Ago-2*, *Dicer*, *TRBP* and *Drosha* transcript levels in purified naïve mouse hepatocytes (A) and remaining cells including Kupffer cells (B) in comparison to transcription in whole liver preparations from naïve mice. Fold change of mRNA expression and SD compared to whole liver preparations of naïve mice. * < 0.05; ** < 0.01, unpaired t-test.

Xpo-5, *Ago-2* and *Drosha* transcript levels were down-regulated in purified naïve hepatocytes (figure 3.1.8A) and naïve remaining liver cells (figure 3.1.8B) when compared to naïve whole livers. *Dicer* and *TRBP* transcript levels were either similar to transcript levels in naïve whole liver preparations or slightly up-regulated. These results clearly demonstrate that the time needed for sample preparation may affect mRNA transcript levels. While livers used for the whole liver preparations have been removed and shock frozen in liquid nitrogen within less than two minutes, the isolation of primary hepatocytes takes more than an hour with several steps, which potentially can induce stress responses within the liver. Thus, with the protocols available to date for isolation of primary hepatocytes it is not possible to answer the initial question regarding the cell type that has the major impact on the changes in transcript levels of components comprising the host hepatic RNAi machinery induced by liver infection with different *Plasmodium berghei* strains.

3.1.5 Influence of Dicer on pre-patency

As *Dicer* transcript levels are 2- to 3-fold down-regulated in livers 40h post infection with WT, GAP and RAS parasites I further wanted to assess whether this host RNase may play a role for the parasite development within the liver. Therefore Dicer-ko (d/d) mice and backcrossed WT (+/+) control mice (all mice provided by Philippe Georgel, Strasbourg) were primed by infection with *Pb*NK65 WT salivary gland sporozoites. This infection was performed by intravenous injection (i.e. experimental route of infection) of 10,000 infectious sporozoites into 3 d/d and 3 +/+ mice and by bite infection (i.e. natural route of malaria transmission) of 3 d/d and 3 +/+ mice, respectively. Thin blood smears from all primed mice were monitored starting at day 3 post infection for presence of blood stage parasites (pre-patency). The infection regimen is depicted in figure 3.1.9A.

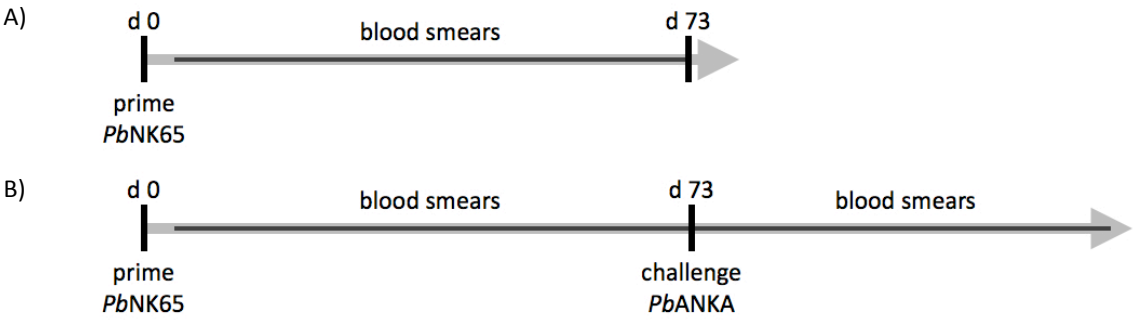

Figure 3.1.9: Prime-challenge-regimen for Dicer-ko and WT mice. Dicer-ko (d/d) and WT control (+/+) mice were primed with 10,000 *Pb*NK65 sporozoites either by intravenous injection or by bite. Presence of blood stage parasites was monitored by daily blood smears (A). On day 73 after this prime all blood stage negative mice were re-challenged by intravenous injection of 10,000 heterologous *Pb*ANKA (severe *P. berghei* strain) sporozoites. Again daily blood smears were taken to determine pre-patency (B).

After priming the d/d and +/+ groups by intravenous injection of 10,000 *Pb*NK65 sporozoites two out of three d/d mice developed parasite blood stages at days 7 and 8 post infection, resulting in an average day 7.5 for blood stage pre-patency. The third mouse in this group remained blood stage negative until day 18 post infection (table 3.1.3). Two out of three intravenously primed +/+ mice resulted in a blood stage infection on days 6 and 8 post infection while the third mouse in this group did not develop blood stage parasites at all (table 3.1.3). When primed by natural transmission (bite) with *Pb*NK65 sporozoites, blood stage parasites were present in one d/d mouse on day 8 post infection and in one +/+ mouse on day 6 post infection. Remaining mice of these groups remained blood stage negative (table 3.1.3). Parasitemia was followed until day 73 post infection.

Table 3.1.3: Pre-patency of Dicer-ko (d/d) and backcrossed WT control (+/+) mice upon prime by intravenous injection of 10,000 *Pb*NK65 sporozoites or by bite.

mouse genotype	administration route prime *Pb*NK65	no. of blood stage positive/ no. of infected (pre-patency)
d/d	10,000 sporozoites iv	2/2 (d 7.5) / 1/1 (d 18)
d/d	by bite	1/3 (d 8)
+/+	10,000 sporozoites iv	2/3 (d 7)
+/+	by bite	1/3 (d 6)

At day 73 post infection two remaining blood-stage negative d/d mice and three remaining blood-stage negative +/+ mice were intravenously re-challenged with 10,000 *Pb*ANKA (more severe form of *P.berghei*, induces experimental cerebral malaria) sporozoites each (figure 3.1.8B). Again daily blood smears were taken for determination of pre-patency. In this case all challenged mice resulted in a fulminant blood-stage patency on day 4 post infection, demonstrating no striking influence of host Dicer for liver-stage development (table 3.1.4).

Table 3.1.4: Pre-patency of Dicer-ko (d/d) and backcrossed WT control (+/+) mice upon heterologous challenge by intravenous injection of 10,000 *Pb*ANKA sporozoites.

mouse genotype	prime *Pb*NK65	challenge *Pb*ANKA	no. of blood stage positive/ no. of infected (pre-patency)
d/d	by bite	10,000 spz. iv	2/2 (d 4)
+/+	10,000 spz. iv	10,000 spz. iv	1/1 (d 4)
+/+	by bite	10,000 spz. iv	2/2 (d 4)

3.2 Influence of a persistent intrahepatic infection with *Plasmodium berghei* WT, GAP and RAS upon the host hepatic miRNA expression profile

The previous section demonstrated that components comprising the mouse liver RNAi machinery like Xpo-5, Ago-2, Dicer, TRBP and Drosha were highly influenced by the presence of *Plasmodium berghei* intrahepatic stages. Especially infection with attenuated parasites such as GAP and RAS induced a down-regulation of mRNA transcription of these genes at 40h post infection, which was reflected by decreased Xpo-5 and Drosha protein expression levels. These findings raised the question whether not only the host liver RNAi machinery is impaired upon infection with arresting parasites but whether also the miRNA expression pattern in general might be affected. To answer this question I performed two independent host miRNA profilings. The first miRNA profiling included only a small number of animals, namely three mice, each intravenously injected with 50,000 *Pb*NK65 WT, GAP and RAS sporozoites, respectively, which were sacrificed for liver removal 40h post infection. One naïve mouse served as control. This first miRNA profiling was conducted by Febit, Heidelberg (now Comprehensive Biomarker Center GmbH, Heidelberg).

3.2.1 RNA integrity

Samples were prepared as briefly described in 3.1.1 and section 2.9.1. For microarray analysis, as performed in this work, it is important to use RNA with a high degree of integrity.

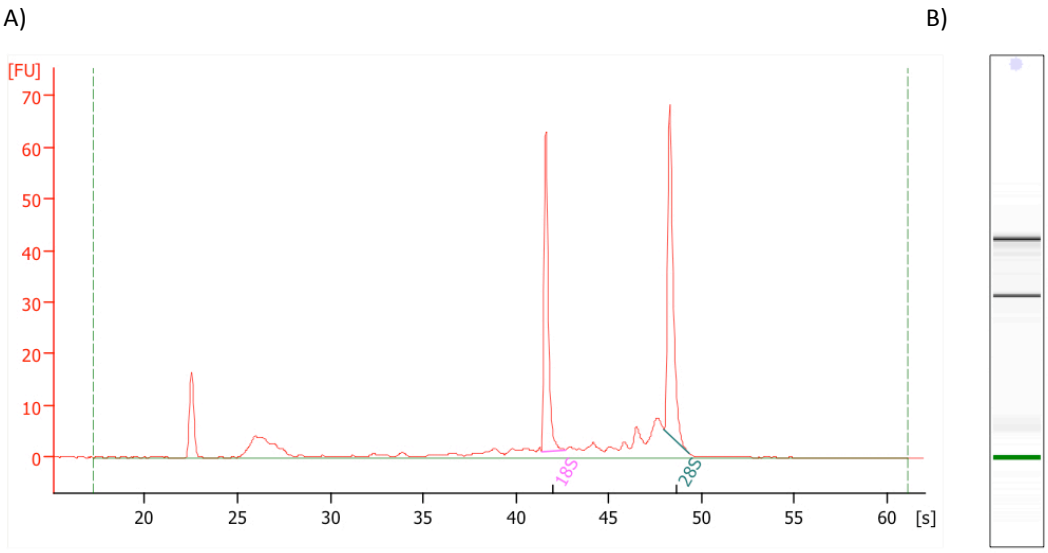

Figure 3.2.1: Exemplary electropherogram and gel-like image. The Agilent software compares unknown samples to ladder fragments added during the chip set-up and thus determines concentration of the unknown sample as well as identifies ribosomal RNA peaks and shows them as electropherograms (A) and gel-like images (B).

To avoid degradation of RNA and thus loss of samples, all RNA isolation steps were performed as quick as possible without unwanted thawing of samples and obtained RNA. Concentration and possible contamination of RNA was measured using a NanoDrop® spectrophotometer. RNA preparations with 260/280 ratios between 1.8 and 2.0 were used for further analysis.

To determine the integrity of the RNA preparations, samples were analyzed with an Agilent 2100 bioanalyzer. After preparation of a polymer matrix, RNA mixed with dye molecules, which intercalate with the RNA strands, is applied. The RNA molecules are then separated according to their size and the intercalating dye molecules are detected. The resulting data is visualized as electropherograms and gel-like images as exemplarily depicted in figure 3.2.1A and 3.2.1B. The RNA integrity number (RIN) is calculated by a software with specific algorithms taking not only the 28S to 18S ratio of rRNA into account but the entire electrophoretic trace of the RNA sample (figure 3.2.2). Thus also the presence of degraded RNA is considered. The higher the amount of degraded RNA within the sample, the lower the RIN. For subsequent microarray analysis only RNA samples with a RIN of 8 and higher were further processed.

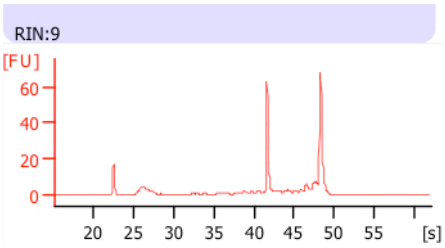

Figure 3.2.2: RNA integrity number. The RNA integrity number (RIN) assesses the integrity of the RNA preparation and is calculated via algorithms taking the entire electrophoretic trace into account.

3.2.2 Dys-regulated miRNAs

This first miRNA microarray profiling was conducted by Febit from provided samples. For this profiling RNA from only four mice was used, one mouse per group of naïve as well as *Pb*NK65 WT, GAP and RAS infected livers, 40h post infection. They are referred to as samples naïve 1, WT 40h 1, GAP 40h 1 and RAS 40h 1, according to table 3.1.1. Resulting data were normalized and ANOVA was performed to differentiate between the groups. MiRNAs with p-values < 0.01 were further considered and dys-regulation of these miRNAs between livers from naïve mice and livers from *Pb*NK65 WT, GAP or RAS infection was assessed. As miRNAs had been fluorescently labeled before being hybridized onto the microarray, calculation was performed on basis of fluorescence intensities. Thus, a higher fluorescence intensity represents a higher amount of a specific miRNA. Whether a miRNA was up- or down-regulated in *Pb*NK65 WT, GAP and RAS infected livers was calculated by subtraction of fluorescence intensity of non-naïve liver RNA from fluorescence intensity of naïve liver RNA. A resultant list of dys-regulated miRNAs is summarized in table 3.2.1. It can be observed that infection with each of the chosen parasite strains induced a distinct pattern of dys-regulated miRNAs when compared to naïve livers. This demonstrates that these parasites behave differently within the host

liver, which most probably is due to their differential developmental properties. But there are some miRNAs that are dys-regulated in two of the groups. MiR-26 for example was up-regulated upon infection with WT liver-stages as well as upon infection with GAP liver-stages. In contrast to this, miR-29b* and miR-30e were up-regulated in WT infected livers while their counterparts miR-29a* and miR-30e* were down-regulated in livers infected with RAS. Members of the let-7-family were more abundant in GAP infected livers when compared to naïve livers but less abundant in livers infected with RAS.

Table 3.2.1: Up- and down-regulated miRNAs according to Febit microarray. Dys-regulation after subtracting value of non-naïve mouse from value of naïve mouse.

naïve - WT		naïve - GAP		naïve - RAS	
up-regulated	down-regulated	up-regulated	down-regulated	up-regulated	down-regulated
miR-24-1*	miR-1	miR-26a	miR-297a	miR-10b*	miR-29a*
miR-26a	miR-105	miR-34b-5p	miR-323-5p	miR-24-1*	miR-30e*
miR-29b*	miR-150	miR-141*	miR-432	miR-124*	miR-135a*
miR-30e	miR-425*	miR-142-3p	miR-449c	miR-141*	miR-141
miR-129-5p	miR-409-5p	miR-143	miR-466i	miR-154*	miR-150
miR-130b*	miR-449c	miR-145	miR-466j	miR-199b*	miR-483
miR-132	miR-464	miR-148a	miR-877	miR-220	miR-1897-5p
miR-141*	miR-467d	miR-365	miR-1188	miR-375	miR-1188
miR-145	miR-470	miR-375	miR-1941-5p	miR-384-3p	miR-1892
miR-151-3p	miR-485*	miR-1964		miR-411*	miR-1894-3p
miR-154*	miR-665	miR-2135		miR-590-5p	miR-1934
miR-181b	miR-674	miR-2142		miR-669k	miR-1936
miR-199b*	miR-680	let-7f		miR-1952	miR-2132
miR-221	miR-743b-3p				miR-2134
miR-302b*	miR-1898				miR-2136
miR-328	miR-1941-5p				miR-2146
miR-346	miR-1954				let-7c-2*
miR-365	miR-2132				let-7f
miR-379	miR-2146				let-7i
miR-451					
miR-599					
miR-874					
miR-877*					
miR-1952					

3.2.3 Cellular networks affected by dys-regulated miRNAs

After proving distinctive influences of the different parasite strains on the host hepatic miRNA expression, I aimed at receiving an impression about possible impacts of the dys-regulated miRNAs on the hepatic system of the host. Thus, I searched for interesting networks that might be affected by these miRNAs. For this analysis web-based prediction tools were used (section 2.16.2). In a first step, the list of dys-regulated miRNAs (table 3.2.1) was converted into putative target genes. These predicted genes were then used for an enrichment analysis that proposes networks containing these affected, putative genes and thus being probably affected by the presence of the different parasite strains within the liver. Table 3.2.2 summarizes networks that may be affected by the dys-regulated miRNAs. Again it is obvious that infection with the different parasite strains has an influence on

different networks within the host. But as just described for the miRNA expression, also on the next level similarities in addition to the differences can be observed. Signal transduction as well as organ development were not only affected by an infection with malarial WT liver-stages but also upon an infection with GAP and RAS liver-stages (the experimental malarial whole-organism vaccine lines). In contrast to this, cellular component movement was only affected upon WT infection, while cell cycle and regulation of metabolic processes were influenced after infection with GAP. RAS infection had influences on cytoskeleton organization as well as cell proliferation.

Table 3.2.2: Networks affected by dys-regulated miRNAs.

Affected network	naive - WT	naive - GAP	naive - RAS
signal transduction	●	●	
cellular component movement	●		
organ development	●		●
cell cycle		●	
cytoskeleton organization			●
cell proliferation			●
regulation of metabolic processes		●	

3.3 Investigations on the interplay between *Plasmodium berghei* WT, GAP and RAS liver-stages and the host hepatic miRNA expression

The Febit miRNA profiling proved an influence of *Plasmodium berghei* liver-stages on the host liver miRNA expression profile. It further demonstrated that the host liver's reaction is dynamic during the parasite development and that attenuation of the parasite elicits specific reactions. But that profile only took one sample per group into account, which has its obvious biological drawbacks as it not necessarily represents the average. Therefore, for the second miRNA profiling the number of animals was increased to three mice per group and an earlier time point, 24h post infection (mid-liver-stage development), was included. An overview of the experimental groups is summarized in table 3.1.1. The second miRNA expression profiling was conducted by me with technical assistance in some more specialized experimental steps including RNA labeling, hybridization of RNA to pre-spotted commercially available microarrays, scanning of the microarrays and analysis of the obtained microarray images. The statistical analysis was performed by a bioinformatic scientist.

3.3.1 MiRNA labeling and hybridization

For this analysis the miRNA expression in 15 non-naïve samples was compared to the miRNA expression in naïve samples. According to table 3.1.1 the sample groups contained all nine samples of the 24h time point and for the 40h time point the samples WT 40h 2, WT 40h 3, GAP 40h 2, GAP 40h 3, RAS 40h 2 and RAS 40h 3. The remaining samples WT 40h 1, GAP 40h 1 and RAS 40h 1 had been already included in the Febit analysis (section 3.2) and therefore had been excluded from this study. To get most reliable data for the miRNA expression in naïve livers, the samples naïve 1, naïve 2 and naïve 3 (table 3.1.1) had been pooled to equal amounts. Sample RNA went through the same quality control as described in section 3.2.1 and only RNA samples with RIN of 8 and higher were further processed and ultimately applied onto the microarrays. Non-naïve samples and the naïve samplepool were labeled as described in section 2.9.2.2, thereby conjugating Hy3 to the naïve samplepool and Hy5 to the respective non-naïve sample. Equal amounts of one labeled non-naïve sample and the labeled naïve samplepool were hybridized over night to one microarray, resulting in a total of 15 microarrays (section 2.9.2.3).

3.3.2 Microarray scan and analysis of microarray images

Directly after hybridizing the sample RNA to the microarray the slides were scanned. Relative intensities of each fluorophore indicate relative abundance of the distinctive miRNAs. Each spot on the microarray represents the sequences of a distinctive miRNA. All sequences are spotted in quadruplicates as indicated by the black square surrounding one quadrant in figure 3.3.1A. As the

chosen microarrays not only contained mouse miRNA sequences but also miRNA sequences of other species a certain amount of spots did not hybridize to the loaded RNA sample. The microarrays were scanned with different excitation wavelengths. Hy3 was exited at 550 nm and detected at 570 nm (figure 3.3.1A) while Hy5 was exited at 650 nm and detected at 670 nm (figure 3.3.1B). To prevent analysis of images that were either over- or underexposed, several scans of the same microarray were performed with different photomultiplier tube settings. Thus, for subsequent analysis, images of the same microarray scanned with the optimal exposure were chosen. These images were merged (figure 3.3.1C) and used for subsequent image analysis.

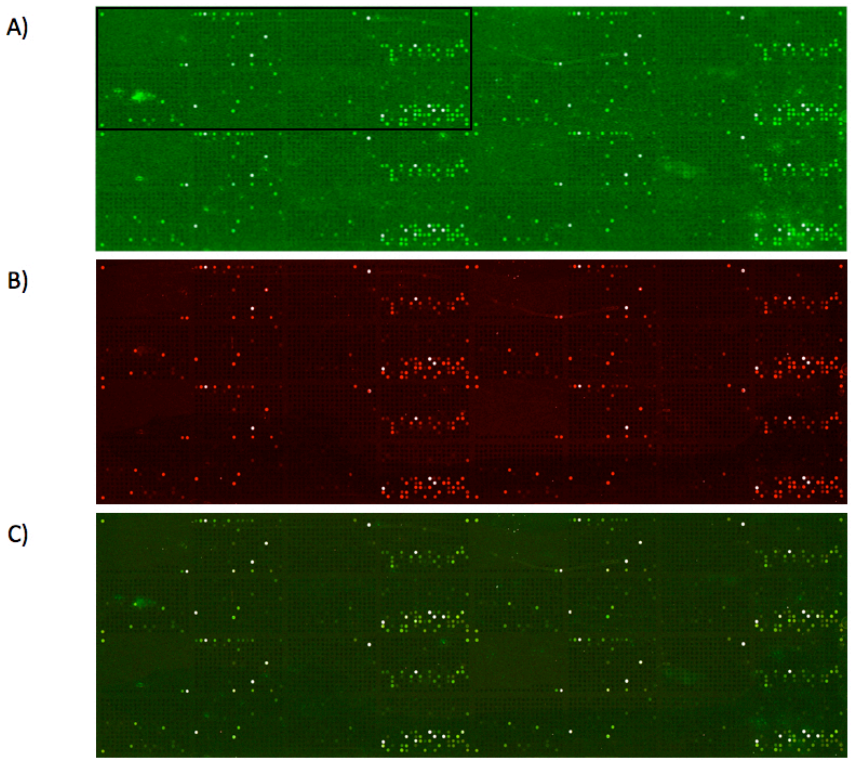

Figure 3.3.1: Exemplary microarray images after scanning. Microarrays hybridized to Hy3 labeled naïve samplepool and Hy5 labeled non-naïve sample. Single scan of Hy3 (A) and Hy5 (B) signal and merged image of both single scans (C). As miRNA sequences are spotted in quadruplicates, square in A frames one of the four quadrants.

Image analysis was performed using the software GenePix®. The optimal merged image was loaded and a presetting recognized all spots by drawing a circle around the respective spots (figure 3.3.2, white circles). As this presetting also recognized unspecific blurs as “true spots” every single spot was manually re-checked to exclude false-positive spots (figure 3.3.2, red circles). In addition the drawn circles had a preset diameter, which did not optimally fit all spots. Therefore also the circle diameter was adjusted to the respective spot diameter in order to reduce background fluorescence as much as possible. Every microarray slide was evaluated in this fashion.

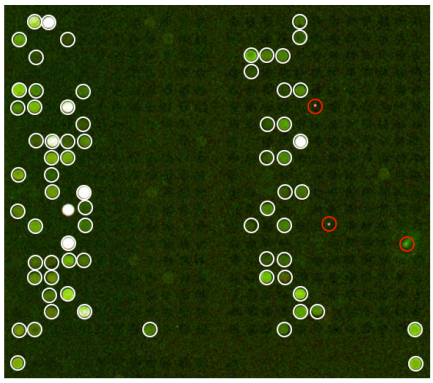

Figure 3.3.2: Recognition of fluorescent spots. The software GenePix® was preset to recognize fluorescent spots of the merged microarray image. The circles in this image are drawn manually as no image showing the automated circles is available to depict the image analysis. White circles represent true positive spots taken into account while red circles mark unspecific blurs which have been excluded from further analysis.

3.3.3 Statistical analysis of miRNA microarray data

After image analysis and determination of true positive spots the data were given to a bioinformatic scientist for statistical analysis. Statistical analysis was performed as described in section 2.16.1.

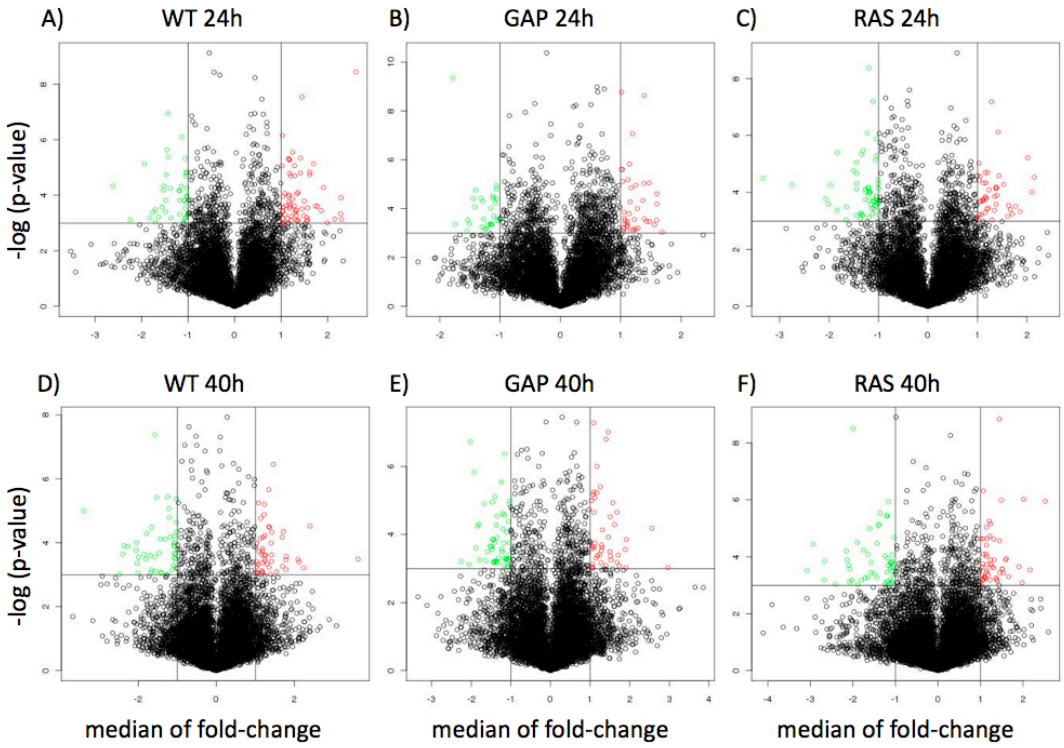

Figure 3.3.3: Volcano plots of miRNAs plotted against the median of their fold-change. MiRNAs with significant different expression values are indicated as green and red circles according to their are up- (red) or down-regulation (green). Each plot depicts the miRNA expression of one group versus expression in naïve livers: WT 24h (A), GAP 24h (B), RAS 24h (C), WT 40h (D), GAP 40h (E) and RAS 40h (F).

In order to get a first impression of the differential miRNA expression within the six groups investigated compared to naïve livers, miRNAs were plotted against the median of fold-change. The volcano plots depict the whole set of miRNAs with those miRNAs having significant different expression values as green and red circles (figure 3.3.3). Distinct miRNA expression patterns can be observed for each of the groups, indicating a defined response of the host liver to the different parasite strains and their developmental behavior during the liver-phase at the time points investigated.

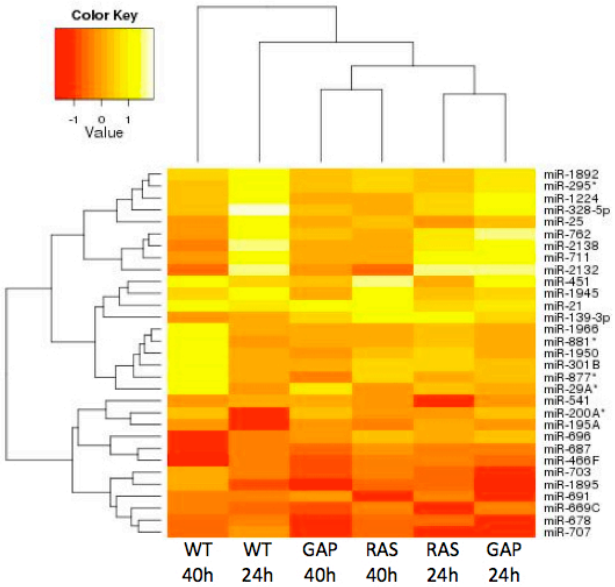

Figure 3.3.4: Hierarchical clustering analysis showed clustering of groups investigated according to their genotype and developmental stage (time point). Dendrogram of hierarchical clustering of differentially expressed miRNAs among mouse livers 24h and 40h after infection with *Pb*NK65 WT, GAP and RAS, respectively, compared with naïve mouse livers. Significance between groups was investigated by performing ANOVA test.

A total of 31 miRNAs were identified that showed a significant dys-regulation at least in one of the groups investigated. These miRNAs were selected to generate a heat map (figure 3.3.4). Hierarchical clustering revealed grouping of the attenuated strains according to the time point hence developmental stage of investigation. These time points were of special interest as GAP were within their arresting phase at 24h post liver infection and had already stopped their intrahepatic development for several hours at the later time point chosen, 40h. As these parasites were genetically identical, they all behaved the same way. This was different in the case of RAS. Due to the irradiation, random point mutations occured in the parasites' genomes, which made them genetically a very heterologous population. And this was also reflected in their arresting behavior. They did not arrest all at the same time point like GAP. Thus, at 24h post infection some of the parasites already arrested while most probably the majority still developed. And also at 40h after liver infection some of the parasites still moved on with their intrahepatic development.

It is striking that among the livers infected with attenuated parasites, the expression profiles of GAP infected livers at both 24h and 40h show the least similarities (figure 3.3.4). This might be due to their specific developmental behavior described above. And although RAS infected livers at 24h show the most similarities to GAP infected livers at the same time point, their miRNA expression pattern did not differ so much from the expression pattern at 40h after RAS infection. In contrast to the GAP infection at these two time points this observation regarding the RAS infection might be explained by the fact that RAS did not stop their development at a defined time point. In fact at both time points some parasites already arrested within their development while others still progressed. The heterogeneity of these attenuated parasites is reflected by the similarities within their miRNA expression profiles. WT infected livers also clustered together and showed similarities within their miRNA expression profiles. But they clearly separated from the expression profiles induced by infection with the attenuated strains.

3.3.4 Dys-regulated hepatic miRNAs upon liver infection with *Plasmodium berghei* NK65 WT, GAP and RAS

In a next step the dys-regulated miRNAs from the global analysis (section 3.3.3) were segregated into those that displayed overlapping expression throughout different groups at each of the chosen developmental stages and those that were exclusively expressed in only one group at these stages (figure 3.3.5). For each group investigated only those miRNAs are shown that were significantly dys-regulated within this group. At 24h post infection nine miRNAs were dys-regulated in all three groups, two miRNAs were only dys-regulated in livers infected with attenuated parasites, two miRNAs were dys-regulated in WT and GAP infected livers and ten miRNAs were uniquely expressed in only one of the groups. WT and RAS without GAP infected livers did not share common dys-regulated miRNAs at this time point (figure 3.3.5A). The rather high number of dys-regulated miRNAs that are expressed in all three groups at this time point may reflect the fact, that WT and most of the RAS still develop while only GAP parasites showed a growth-arrest already at this time point. Their developmental behavior at this early time point was quite similar and this is reflected by their influence on the host hepatic miRNA expression profile. A similar striking observation can be made at 40h post infection. The number of dys-regulated miRNAs in total was smaller with only one miRNA being dys-regulated in all groups, two miRNAs being dys-regulated in GAP and RAS infected livers, three miRNAs being dys-regulated in WT and RAS infected livers and eleven miRNAs being dys-regulated in only one of the groups. WT and GAP without RAS infected livers did not have dys-regulated miRNAs in common (figure 3.3.5B). At this time point only the WT parasites developmentally progress in their liver-stage phase and so also does a small number of RAS. And this correlates with the number of miRNAs being dys-regulated upon these infections. WT infected livers showed at this time point by far the highest number of dys-regulated miRNAs. In addition, there was an overlap between WT and RAS infected livers regarding dys-regulated miRNAs but not between WT and GAP infected livers. Complete

attenuation of the parasite inside the liver elicited hepatic responses that differ from those induced by still developing parasites.

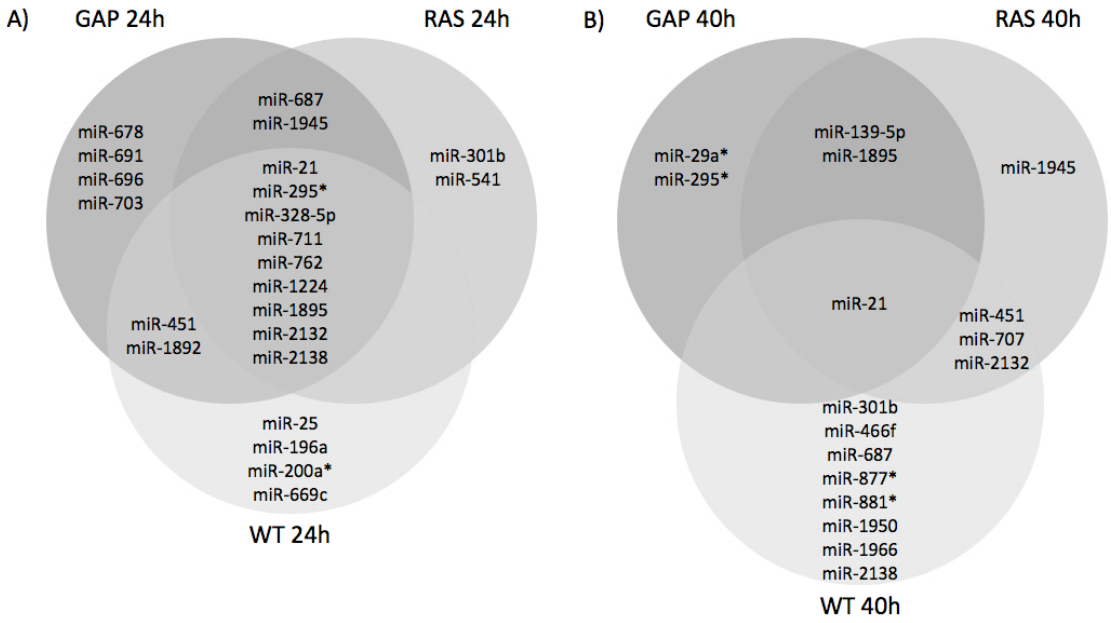

Figure 3.3.5: Overlapping and differential expression of miRNAs between *Pb*NK65 WT, GAP and RAS infected livers at both 24h and 40h post infection. Differentially expressed miRNAs were grouped according to their presence in the different experimental settings investigated independent of whether they are up- or down-regulated. Differentially expressed miRNAs at 24h post injection in *Pb*NK65 WT, GAP and RAS infected livers (A). Differentially expressed miRNAs at 40h post injection in *Pb*NK65 WT, GAP and RAS infected livers (B).

So far, miRNAs were only regarded as dys-regulated, omitting whether they were up- or down-regulated in the groups investigated when compared to naïve livers. In table 3.3.1 these miRNAs are now listed according to their regulation status. The table only contains miRNAs that reached significance ($p < 0.05$) for the corresponding group. The miRNAs might be also dys-regulated within other sample groups investigated but this dys-regulation did not reach significance and therefore they are not listed for other groups. The microarray data revealed in total twenty miRNAs being up-regulated while only twelve miRNAs appeared to be down-regulated. When these data are further deciphered according to the time point of investigation (but not to the parasite strain injected) it is striking to see that nine miRNAs were only up-regulated 24h post infection, five miRNAs were up-regulated at both time points and six miRNAs were only up-regulated at 40h post infection. In the case of down-regulated miRNAs eight miRNAs were observed being unique at the mid-liver-stage development (i.e. 24h post infection), one miRNA being down-regulated both at 24h and 40h post infection and three miRNAs being down-regulated only at the later time point. Two miRNAs, miR-2132 and miR-2138, were up-regulated in livers infected with WT, GAP and RAS at 24h post infection, but were down-regulated in livers infected with WT 40h post infection. And miR-2132 was additionally down-regulated in RAS-infected livers 40h post infection. Only one miRNA, miR-21, was constantly up-regulated at all conditions investigated (figure 3.3.5, table 3.3.1). Taken together the

number of down-regulated miRNAs was much smaller than the number of up-regulated miRNAs throughout both developmental stages (mid and late liver-stage development).

Table 3.3.1: Up- and down-regulated miRNAs in *Pb*NK65 WT, GAP and RAS infected livers 24h and 40h post infection. miRNAs are listed according to whether they were up- or down-regulated in the groups investigated after microarray analysis. Only miRNAs that reached significance ($p < 0.05$) are listed.

	WT 24h	GAP 24h	RAS 24h	WT 40h	GAP 40h	RAS 40h
up-regulated	miR-21	miR-21	miR-21	miR-21	miR-21	miR-21
	miR-25					
					miR-29a*	
					miR-139-3p	miR-139-3p
	miR-295*	miR-295*	miR-295*		miR-295*	
			miR-301b	miR-301b		
	miR-328-5p	miR-328-5p	miR-328-5p			
	miR-451	miR-451		miR-451		miR-451
		miR-696				
	miR-711	miR-711	miR-711			
	miR-762	miR-762	miR-762			
				miR-877*		
				miR-881*		
	miR-1224	miR-1224	miR-1224			
	miR-1892	miR-1892				
		miR-1945	miR-1945			miR-1945
				miR-1950		
				miR-1966		
	miR-2132	miR-2132	miR-2132			
	miR-2138	miR-2138	miR-2138			
down-regulated	miR-196a					
	miR-200a*					
				miR-466f		
			miR-541			
	miR-669c					
		miR-678				
		miR-687	miR-687			
		miR-691				
		miR-703				
						miR-707
	miR-1895	miR-1895	miR-1895		miR-1895	miR-1895
				miR-2132		miR-2132
				miR-2138		

This is somehow surprising as my previous observation regarding the host hepatic RNAi machinery (section 3.1) demonstrated a transcriptional and expressional down-regulation of components comprising this machinery upon intrahepatic malarial infection. According to the down-regulation of the RNAi machinery I would have expected a subsequent pronounced down-regulation of miRNAs, but interestingly this was not the case. Even 40h post infection an up-regulation of miRNAs could still be observed. A possible explanation can be the half-life of the miRNAs, which has been shown to range from some few hours up to more than 14 hours (Grosshans and Chatterjee, 2010) or even several days (van Rooij et al., 2007). Thus, some miRNAs may be stable enough to still be detected as up-regulated within this profiling.

3.3.5 Validation of dys-regulated miRNAs by qPCR

MiRNAs considered as dys-regulated according to the microarray profiling (section 3.3.4, table 3.3.1) were validated by carrying out quantitative real-time PCR (qPCR). For this analysis DNase-treated RNA (section 3.1.2), confirmed for absence of gDNA contamination (figure 3.1.1) was used. Reverse transcription was performed as described in section 2.9.2.6. Prior to the reverse transcription step, miRNAs were polyadenylated by poly(A) polymerase. Thus, during the reverse transcription step miRNAs as well as mRNAs and other small RNAs were converted into cDNA using oligo-dT primers. These oligo-dT primers contained a universal tag sequence at their 5' end, which allowed amplification in the subsequent qPCR reaction. During the qPCR reaction miRNAs were amplified using miRNA-specific primer assays and an universal primer (section 2.9.2.7). The universal primer bound to the universal tag and the primer of the chosen primer assay bound to a specific sequence of the miRNA under study, thus amplifying only the corresponding miRNA and no transcribed mRNAs or other small RNAs. Pre-designed primer assays were available for 27 of the 31 miRNAs that were dys-regulated according to the microarray analysis. For miR-139-3p, miR-328-5p, miR-2132 and miR-2138 these assays were not available and thus these miRNAs have not been further validated. Only qPCR runs showing melting curves as exemplified and depicted in figure 3.1.2 were used for further evaluation. The qPCR validation for the remaining miRNAs was evaluated as described in section 3.1.2. MiRNAs that were excluded from further evaluation according to inadequate melting curves were: miR-196a, miR-200a*, miR-295*, miR-691, miR-707, miR-762, miR-881*, miR-1224, miR-1945 and miR-1950. Thus 17 out of initially 31 miRNAs were validated by qPCR analysis and ten of them showed the same expression properties as in the microarray analysis (table 3.3.2).

Table 3.3.2: Quantitative real-time PCR validation of miRNAs dys-regulated according to microarray analysis. Up- and down-regulated miRNAs in *Pb*NK65 WT, GAP and RAS infected livers 24h and 40h post infection. Quantitative real-time PCR analysis was performed for miRNAs that were dys-regulated according to the miRNA microarray analysis. The table lists those miRNAs whose up- or down-regulation was confirmed by qPCR.

	WT 24h	GAP 24h	RAS 24h	WT 40h	GAP 40h	RAS 40h
up-regulated	miR-21	miR-21	miR-21	miR-21	miR-21	miR-21
				miR-301b		
	miR-451	miR-451		miR-451		miR-451
	miR-711	miR-711	miR-711			
				miR-1966		
down-regulated	miR-669c					
		miR-678				
		miR-687	miR-687			
		miR-696				
					miR-1895	miR-1895

Among these miRNAs miR-21 was confirmed. MiR-21 transcription levels revealed a slight but significant up-regulation in WT and GAP infected livers at both 24h and 40h post infection. In addition, miR-21 transcription was up-regulated in RAS infected livers at both time points but did not reach significance (figure 3.3.6A). As a negative control the transcription level of miR-122 was also

quantified (figure 3.3.6B). This miRNA appears to be the most abundant one in hepatic tissue (Lagos-Quintana et al., 2002) and was shown for example to be down-regulated upon infection with Hepatitis-B virus (Chen et al., 2011). The qPCR analysis was consistent with the microarray data showing no significant change in miR-122 transcription levels.

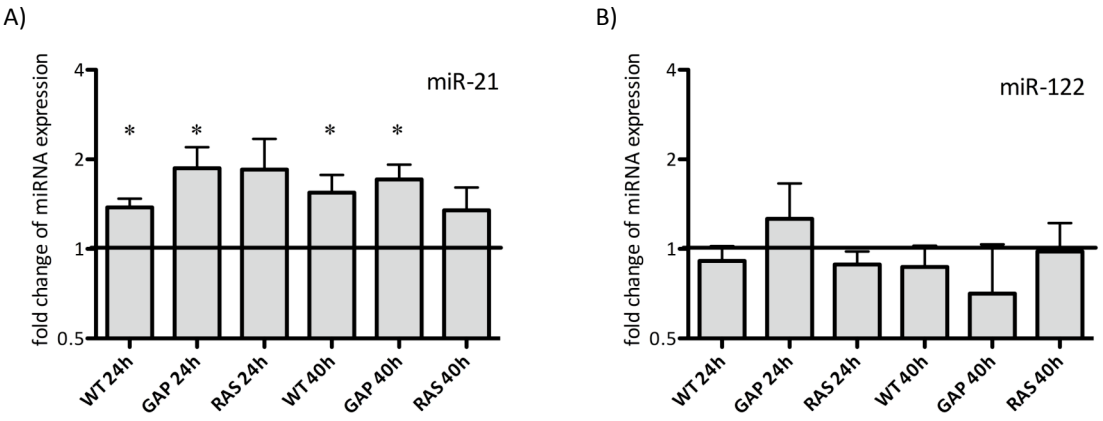

Figure 3.3.6: qPCR validation of intrahepatic miR-21 and miR-122. MiRNA transcription levels were validated by qPCR using sequence specific primers for miR-21 (A) and miR-122 (B). Fold change of miRNA expression and SD compared to naïve mice of three animals per group. * $p < 0.05$, unpaired t-test.

Nevertheless, the number of up- and down-regulated miRNAs after qPCR validation was smaller than according to the miRNA microarray. This might be due to the technical properties of the two different methods of choice. The qPCR analysis might be more sensitive and thus give a more defined picture of the dys-regulated hepatic miRNAs.

3.3.6 Pathways affected by dys-regulated miRNAs

The miRNA expression profile conducted by myself confirmed the observations already made with the initial profiling of miRNAs performed by Febit i.e. each parasite genotype has a distinct influence on the host hepatic miRNA expression profile. It even led to a more comprehensive and extended observation, since I was able to include an earlier time point. It was indeed striking to see, that in addition to the parasite strain injected, also the time point of investigation and thus the time point of parasite development within the host liver, showed a distinct influence on the host hepatic miRNA expression. As this second approach included biological replicates of the groups investigated it also might be more reliable. Due to the additionally included groups the bioinformatic analysis was repeated. The same web based prediction tools were used as described in section 3.2.3. But this time the search did not aim at deciphering affected networks but at unraveling host hepatic pathways that might be influenced by the presence of the different parasite strains at the different developmental time points (table 3.3.3).

Table 3.3.3: Pathways affected by dys-regulated miRNAs.

Affected pathway	WT 24h	GAP 24h	RAS 24h	WT 40h	GAP 40h	RAS 40h
apoptosis and survival		●				
cell adhesion	●		●	●		●
cytoskeleton remodeling	●	●	●	●	●	●
development	●	●	●	●	●	●
DNA damage				●		●
G-protein signaling			●		●	
immune response			●			
regulation of lipid metabolism	●	●	●		●	
signal transduction		●			●	

When comparing the networks affected by the different parasite strains after the Febit analysis (table 3.2.2) with the pathways affected in this screen (table 3.3.3) some overlaps can be observed. In both cases the cytoskeleton organization or remodeling was affected in RAS infected livers 40h post infection and signal transduction was affected in GAP infected livers at the same time point. Organ development or development in general was influenced by the presence of WT and RAS at 40h post infection while GAP infection at 40h had an influence on the regulation of lipid metabolism or metabolic processes in general. But there were also differences when comparing the two screens. According to the Febit analysis cellular component movement, cell cycle and cell proliferation were affected after infection with some of the parasite strains. These networks were not affected according to the results of the second screen. But the results from this second screen demonstrated an influence of GAP infection at 24h on apoptosis and survival. Cell adhesion was affected by infection with WT and RAS, both at 24h and 40h post infection. WT and RAS infection at the later time point also affected pathways associated with DNA damage. RAS infection at 24h as well as GAP infection at 40h had some impact on G-protein signaling. And also immune responses were influenced by the presence of RAS 24h post infection.

3.3.7 Transcriptional analysis of miRNAs involved in immune responses

A particularly interesting aspect of the pathway analysis described in the previous section was the influence on immune responses, although only RAS infection at 24h seemed to have some impact on this pathway. But as demonstrated before, the microarray analysis was not as sensitive as the qPCR analysis (section 3.3.5). Thus, some miRNAs involved in immune responses dys-regulated due to the presence of intrahepatic WT and GAP parasites might have been overseen. It was demonstrated that both sporozoite-neutralizing antibodies as well as cell-mediated immunity contribute to immunity due to RAS infection (Doolan and Martinez-Alier, 2006; Frevert and Nardin, 2008; Nardin and

Nussenzweig, 1993). The principal cytotoxic effector cells involved not only in the response to infection with irradiation attenuated but also in response to genetically attenuated parasites are $CD8^+$ T cells (Mueller et al., 2007). Also dendritic cells play a crucial role in induction of immune responses (Leiriao et al., 2005b). Therefore, I decided to additionally focus on further miRNAs known regulating immune responses (O'Connell et al., 2007; Rodriguez et al., 2007; Taganov et al., 2006; Tili et al., 2007; Turner and Vigorito, 2008).

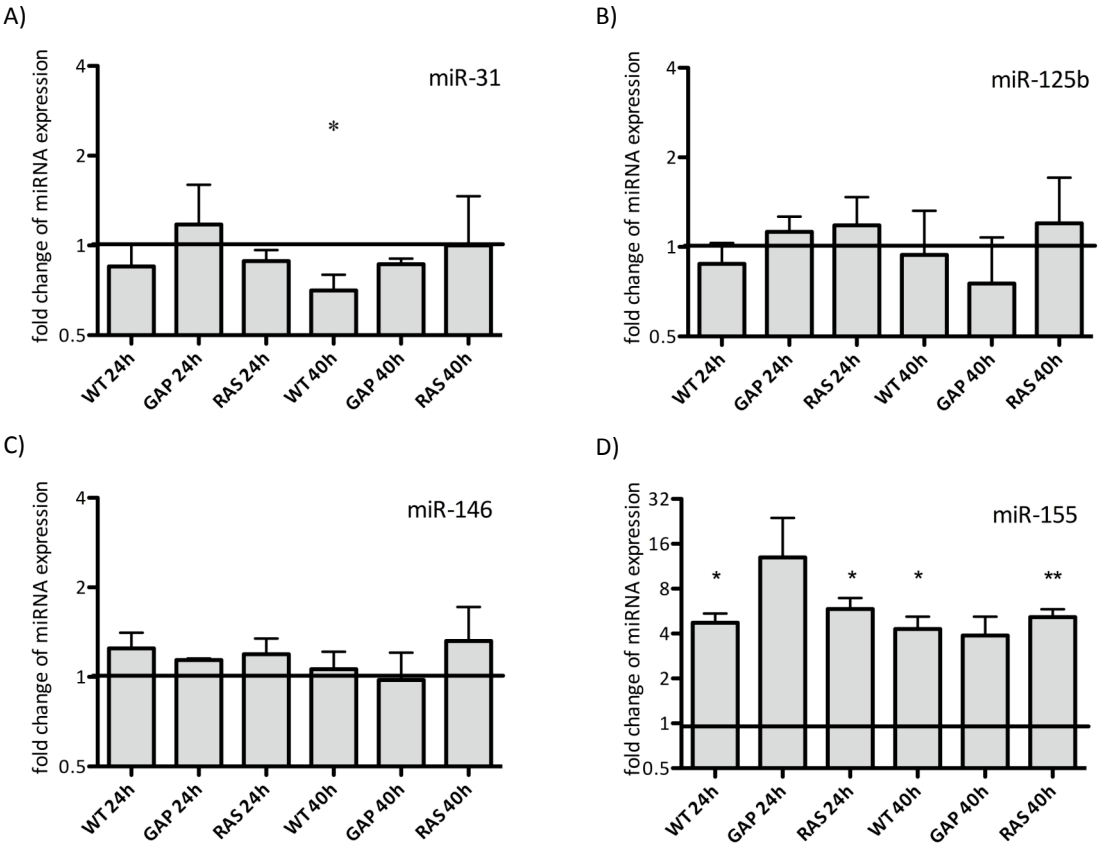

Figure 3.3.7: qPCR validation of miR-31, miR-125b, miR-146 and miR-155. MiRNA transcription levels were validated by qPCR using sequence specific primers for miR-31 (A), miR-125b (B), miR-146 (C) and miR-155 (D). Fold change of miRNA expression and SD compared to naïve mice of three animals per group. * $p < 0.05$; ** $p < 0.01$, unpaired t-test.

Transcription levels of known immune response regulating miRNAs such as miR-31, miR-125b, miR-146 and miR-155 were quantified by qPCR analysis as mentioned in section 3.3.5 (figure 3.3.7). MiR-31 transcript levels were similar to naïve livers, except for WT infection at 40h when the transcription was significantly reduced (figure 3.3.7A). For miR-125b and miR-146 no significant changes of miRNA expression was observed in the groups investigated in comparison to naïve livers (figure 3.3.7B, 3.3.7C). In striking contrast to these results, miR-155 transcription was 4- to 10-fold up-regulated in all groups investigated (figure 3.3.7D). As this miRNA was not detected as significantly dys-regulated in the microarray analysis, these results show once more the different sensitivities of the two different methods.

3.4 Analyses of the biological functions of miR-21 and miR-155

The analyses described in the section before implied an important role for both miR-21 and miR-155 in the interaction between the intrahepatic stages of *Plasmodium berghei* WT, GAP and RAS and the host hepatic tissue. Only these two miRNAs were constantly up-regulated upon infection with the three parasite strains investigated as well as the different developmental stages. Furthermore, both miRNAs were shown to be important for immune responses (O'Connell et al., 2007; Quinn and O'Neill, 2011; Salaun et al., 2011; Turner and Vigorito, 2008) and miR-21 is additionally involved in the control of apoptosis (Chan et al., 2005; Li et al., 2009; Sayed et al., 2010). To further investigate their implication in this tight interaction between liver-stage parasite and host liver several *ex vivo*, *in vitro* and *in vivo* experiments were performed.

3.4.1 Firefly luciferase expression plasmids for *ex vivo* imaging of miR-21 and miR-155 expression

At different malarial intrahepatic developmental stages such as 24h and 40h post infection I was able to demonstrate a significant up-regulation of both miR-21 and miR-155 transcript levels in livers intravenously infected with *Pb*NK65 WT, GAP and RAS infectious sporozoites, respectively. I therefore in a next step aimed at visualizing these expression differences *ex vivo*. For this purpose plasmids containing a firefly luciferase cassette and a binding site for miR-21 (figure 2.8.2A) or miR-155 (figure 2.8.2B) positioned in the 3'UTR of the firefly luciferase cassette were generated. For reference measurements the same plasmid without miRNA binding site was used (figure 2.8.2C). All constructs have been provided by AG Grimm from the Bioquant, Heidelberg.

Due to the introduction of the different binding sites into the 3'UTR of the firefly luciferase cassette binding of the respective miRNAs would induce a translational inhibition of the luciferase, which in turn would lead to a decreased conversion of luciferin, the appropriate substrate of the luciferase. Thus, less luminescence compared to the control construct without any miRNA binding site would be detected and represent the presence of the respective miRNA within the investigated tissue, in my case within the liver.

Before enveloping these plasmids in recombinant Adeno-associated viral (rAAV) particles they were tested *in vitro* for the efficiency of their respective binding sites. For this purpose the Luc2 m21 plasmid and the Luc2 empty plasmid, respectively, were co-transfected with a *Renilla* luciferase control construct into human immortalized hepatocarcinoma (HuH7) cells. No additional construct expressing miR-21 was needed, as HuH7 cells express miR-21 endogenously. After two days a Dual Luciferase assay was performed by adding firefly and *Renilla* luciferase substrate as described in section 2.11.3. The *Renilla* luciferase substrate was converted by the co-transfected control construct while the firely luciferase encoded in the Luc2 plasmid converted the firefly luciferase substrate. But

as the endogenously expressed miR-21 bound to the respective binding site of the Luc2 m21 plasmid the translation of firefly luciferase was inhibited. According to this reduced amount of firefly luciferase less substrate was converted. The luminescent signals from the firefly and the *Renilla* reactions were sequentially detected. Firefly luciferase values were normalized to the corresponding *Renilla* luciferase values. Afterwards the Luc2 m21 values were normalized to Luc2 empty values and expressed as percentage of relative light units (RLU) (figure 3.4.1A). The same assay was performed to analyze the efficiency of the Luc2 m155 plasmid. But in this case the plasmid was not only co-transfected with the *Renilla* luciferase control construct into Hek293T cells. An additional construct expressing miR-155 was co-transfected as well because these cells do not express appropriate amounts of endogenous miR-155 (figure 3.4.1B). Normalization and calculations were performed as just described.

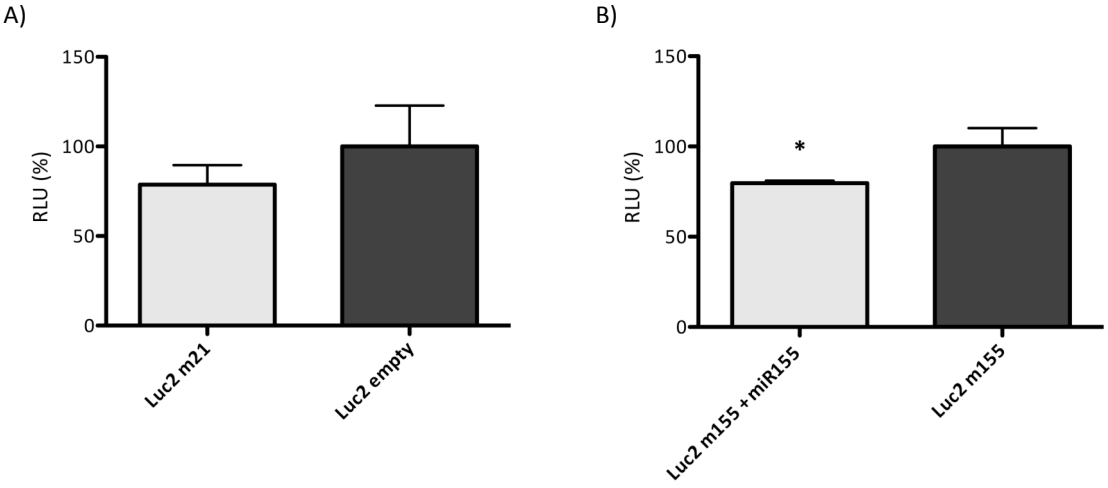

Figure 3.4.1: Dual Luciferase assay for determination of firefly Luc2 plasmid binding site efficiencies. Luc2 m21 and Luc2 empty plasmids were co-transfected with *Renilla* control construct into HuH7 cells and relative light units (RLU) were calculated for estimating m21 binding site efficiency (A). Luc2 m155 plasmid was co-transfected with *Renilla* control construct and with or without miR-155 expression construct into Hek293T cells and relative light units (RLU) were calculated for estimating m155 binding site efficiency (B). Error bars represent the standard deviation. * $p < 0.05$, unpaired t-test.

Both plasmids, Luc2 m21 and Luc2 m155, contained efficient binding sites for the respective miRNAs. Binding of these miRNAs induced a reduction in firefly luciferase activity of around 20% when compared to control conditions (figure 3.4.1). Although the reduction was only significant for the Luc2 m155 plasmid, both constructs were considered suitable for the subsequent *in vivo* application.

3.4.2 *Ex vivo* imaging of miR-21 and miR-155 expression

After validating the Luc2 m21 and Luc2 m155 plasmids *in vitro* as described in section 3.4.1 they were enveloped in recombinant Adeno-associated viral (rAAV) particles of serotype 8 and intravenously injected into naïve C57BL/6 mice. The chosen serotype has been demonstrated to confer specificity to

the host liver (Gao et al., 2004; Gao et al., 2002; Grimm et al., 2006; Malato et al., 2011; Nakai et al., 2005; Thomas et al., 2004). For normalization the same plasmid with a luciferase cassette but without any miRNA binding site (Luc2 empty) was used and applied as described above.

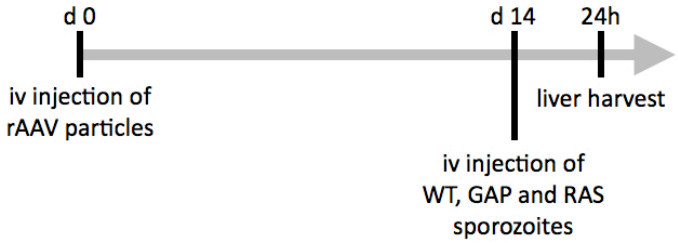

Figure 3.4.2: Injection regimen for *ex vivo* imaging. Naïve C57BL/6 mice were pretreated by intravenous (iv) injection of 2 x 10^{11} viral particles, containing either Luc2 m21, Luc2 m155 or Luc2 empty plasmid. 14 days later mice received intravenously 10,000 *Pb*NK65 WT, GAP and RAS sporozoites, respectively. 24h after parasite injection livers were harvested.

14 days after having administered the rAAV particles, mice were intravenously injected with 10,000 *Pb*NK65 WT, GAP and RAS infectious sporozoites, respectively. 24h later, mice were sacrificed and livers were removed (figure 3.4.2). For *ex vivo* imaging luciferin was added to the isolated livers (figure 3.4.3A) and the luciferase activity was measured using an IVIS instrument (figure 3.4.3B).

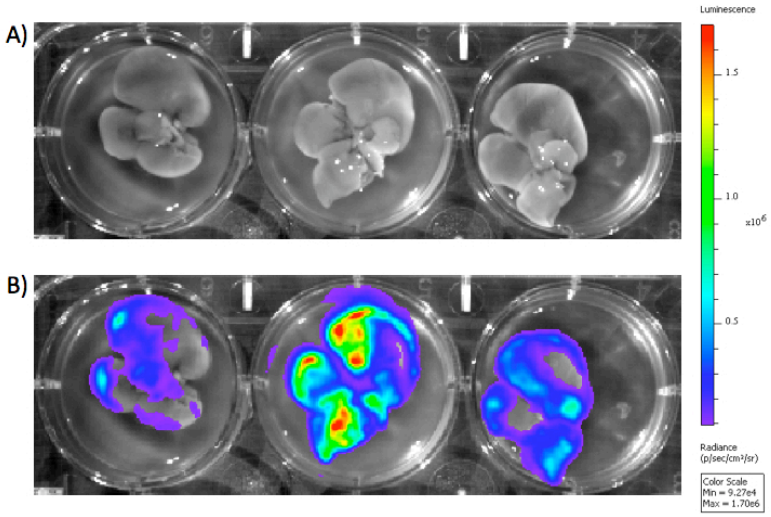

Figure 3.4.3: *Ex vivo* imaging. Exemplary black-and-white image of isolated livers (A). Exemplary image of luciferase activity measured with an IVIS instrument after application of luciferin to the isolated livers (B). Livers depicted in (A) and (B) were removed from three mice, which have received Luc2 empty plasmid, followed by injection of 10,000 *Pb*NK65 WT sporozoites.

Luciferase activity was set to 100% for mice receiving the Luc2 empty plasmid without any miRNA binding site (figure 3.4.4, light grey bars). An up-regulation of miR-21 and miR-155 would induce translational inhibition of the luciferase and thus would lead to a reduction in luciferase activity. This reduction was measurable as decreased luciferin luminescence signal. The luminescence signals of livers pretreated with Luc2 m21 and Luc2 m155, respectively (figure 3.4.4, middle grey and dark grey bars), were expressed as percentage of relative light units (RLU) compared to livers pretreated with

Luc2 empty (figure 3.4.4, light grey bars). For WT and GAP injected mice a luciferase activity decrease of at least 50% was observed associated with both miR-21 and miR-155 expression. The decrease was not as strong for RAS infected livers regarding miR-21. For miR-155 these livers showed a slight increase of luciferase activity indicating a decrease in miR-155 expression, which is contradictory to the qPCR data. A possible reason for this decrease in miR-155 expression in RAS infected livers might be the procedure during sample processing. As described in section 3.1.4 long sample processing times might have an influence on transcription levels. In the case of the *ex vivo* imaging livers were removed from the mice more or less in parallel and stored on ice until application of luciferin and luminescence detection. The first samples measured were livers from WT infected mice, followed by livers from GAP infected mice and finally livers from RAS infected mice were processed. Within these groups livers pretreated with Luc2 empty were handled first, followed by livers pretreated with Luc2 m21 and the last ones were livers that received the Luc2 m155 construct. Taken together RAS infected livers were stored longest on ice, which might already be reflected by a relatively stronger signal of RAS Luc2 m21 samples. As the RAS Luc2 m155 samples have been the very last for detection, the long time period *ex vivo* might have influenced the miR-155 transcription. But this cannot be proven for sure as this experiment was performed only once. Repetition of this experiment with a different sample order might clarify whether this decreased miR-155 transcription is a true effect or an artifact due to the experimental handling time of the samples.

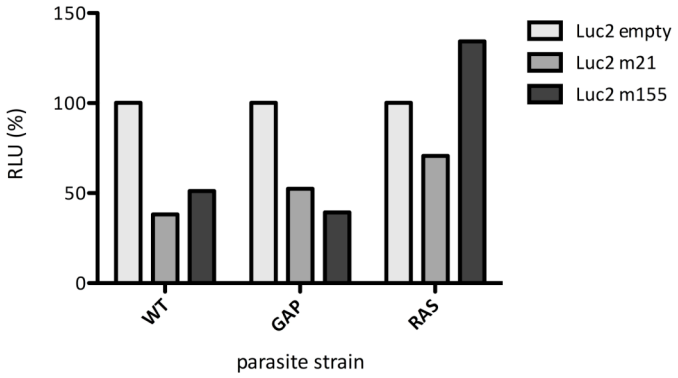

Figure 3.4.4: *Ex vivo* imaging of miR-21 and miR-155 expression. Naïve C57BL/6 mice were pretreated with rAAV particles containing Luc2 empty, Luc2 m21 and Luc2 m155 plasmids, respectively. 14 days later mice received intravenously 10,000 *Pb*NK65 WT, GAP and RAS sporozoites, respectively. After 24h livers were harvested, luciferin was added and the luminescence signal was measured. Binding of miR-21 and miR-155 to the respective binding sites reduced luciferase tanslation and thus luciferin conversion. Decreased luciferin signals are expressed as percentage of relative light units (RLU) compared to Luc2 empty.

Furthermore, these results demonstrated that the experimental design chosen in this study and amount of rAAV particles injected into mice worked well for expression of given plasmids. Thus, plasmids enveloped in rAAV particles were injected into mice for further experiments (section 3.4.5).

3.4.3 *In vitro* down-regulation of miR-21 and miR-122

After having identified miR-21 and miR-155 as interesting candidate miRNAs involved in the parasite-host-interplay *in vitro* experiments were designed to further strengthen their biological role. The *in vitro* experiments focused on miR-21 (sponge provided by AG Grimm, Bioquant, Heidelberg). MiR-122 was selected as a control miRNA because it was not affected by the presence of the parasite within the host liver (sponge provided by AG Grimm, Bioquant, Heidelberg). These sponges used for the down-regulation of both miRNAs belong to a relatively new class of miRNA inhibitors (Ebert et al., 2007), which are encoded in mRNA transcripts carrying multiplexed binding sites for a specific miRNA in their 3' UTR. The expression of these sponges both *in vitro* and *in vivo* results in quantitative sequestration of the respective miRNA.

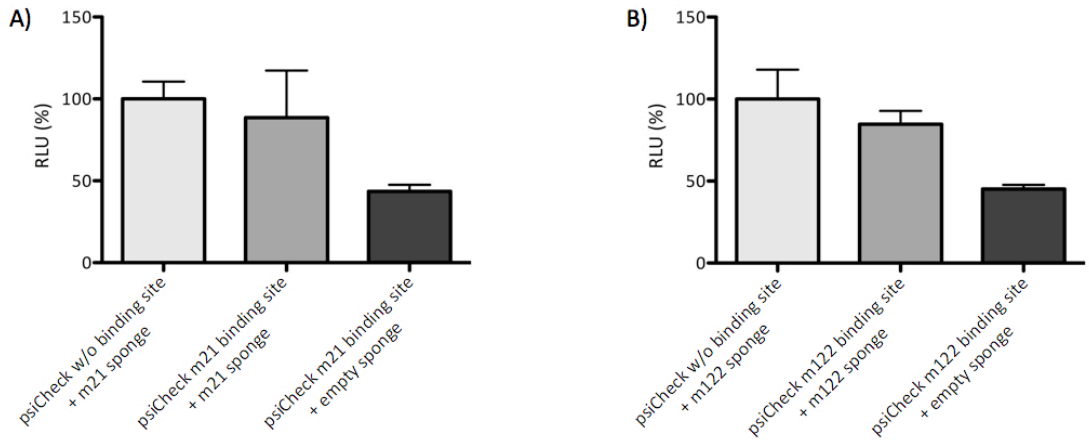

Figure 3.4.5: Dual Luciferase assay for determination of m21 and m122 sponge binding site efficiencies. PsiCheck™-2 plasmids containing no binding site or binding site for miR-21, were co-transfected with m21 sponge or empty sponge into HuH7 cells and relative light units (RLU) were calculated for estimating m21 binding site efficiency (A). PsiCheck™-2 plasmids containing no binding site or binding site for miR-122, were co-transfected with m122 sponge or empty sponge into HuH7 cells and relative light units (RLU) were calculated for estimating m122 binding site efficiency (B). Error bars represent the standard deviation.

Efficiency of the sponges (figure 3.4.5) was tested in HuH7 cells by performing a Dual Luciferase assay similar to section 3.4.1. In this case m21 sponge and m122 sponge plasmids, respectively were co-transfected with re-designed psiCheck™2 plasmids that co-encode both firefly and *Renilla* luciferase. As control psiCheck™2 plasmids without any miRNA binding site were chosen (light grey bars), which would not show a decrease of *Renilla* luciferase signal. In contrast to this control, the re-designed psiCheck™2 plasmids contained an additional binding site for either miR-21 or miR-122 3' to the synthetic *Renilla* luciferase gene. Thus in the presence of endogenously expressed miR-21 or miR-122 and transfected empty sponge (containing no binding site for any known miRNA) the translation of the *Renilla* luciferase gene was inhibited resulting in a decreased *Renilla* luciferase signal (dark grey bars). But in case these re-designed psiCheck™2 plasmid were co-transfected with an efficiently working sponge for the respective miRNA, the miRNA was sequestered by the sponge and translation

of the *Renilla* luciferase gene was no longer inhibited or less inhibited (middle grey bar). An increased *Renilla* luciferase signal could be detected and the efficiency of the sponge could be calculated. Figure 3.4.5 demonstrates efficiency of binding sites for miR-21 and miR-122 in the chosen sponge plasmids.

After verifying the efficiency of m21 and m122 sponges the *in vitro* experiments were performed. First of all HuH7 cells were transfected with m122 sponge and an empty sponge or not transfected at all as control (PBS). 48h after transfection cells were infected with 20,000 *Pb*NK65 WT infectious salivary gland sporozoites. 24h and 60h post invasion the parasite's liver-stage development was experimentally stopped, intrahepatic parasites were stained using an anti-*Pb*Hsp70 antibody (Tsuji et al., 1994) and number of liver-stages as well as sizes of liver-stages (developmental status) were determined.

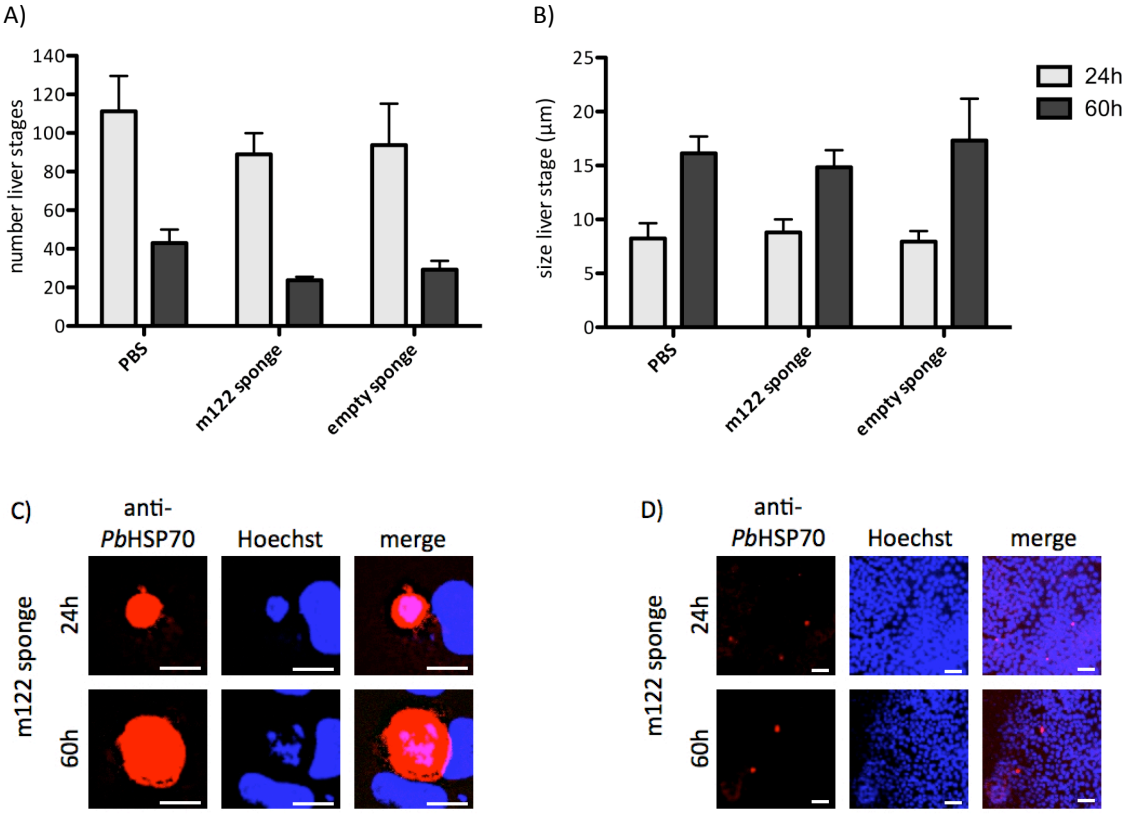

Figure 3.4.6: Number and sizes of liver-stages after down-regulation of hepatic miR-122. 2 x 10^4 HuH7 cells / well were transfected with m122 sponge, empty sponge or no sponge at all (PBS). 48h later cells were infected with 20,000 *Pb*NK65 WT sporozoites. Liver-stages were stained with anti-*Pb*Hsp70 antibody 24h (light bars) and 60 h (dark bars) post invasion. Number of liver-stages (A) and size of liver-stages (B) were determined by confocal microscopy. Representative images of liver-stages after application of m122 sponge: 63x magnification scale bar 10 µm (C), 10x magnification scale bar 50 µm (D). Size of liver-stages was measured using Fiji. Experiment was performed in quadruplicates. Error bars represent the standard deviation.

The number (figure 3.4.6A) and size (figure 3.4.6B) of liver-stages after transfection with m122 sponge was similar to values after transfection with an empty sponge as well as comparable to number and sizes of liver-stages that had not been transfected at all (PBS). These observations are true for liver-

stages 24h and 60h post invasion. Thus, down-regulation of miR-122 had no influence on the development of liver-stages in HuH7 cells *in vitro*. This was expected, as this miRNA was not dys-regulated upon liver infection (figure 3.3.6B). In addition this experiment proved no unspecific influence of the transfection procedure as well as application of miRNA sponges in general on parasite liver-stage development.

A second *in vitro* experiment was carried out in order to investigate the influence of down-regulating miR-21 and thus to determine its *in vitro* impact on liver-stage development in HuH7 cells. MiR-21 was significantly up-regulated in mouse livers 24h and 40h post infected with *Pb*NK65 WT parasites (figure 3.3.6A). As up-regulation of miR-21 is associated in many biological systems with an inhibition of apoptosis (Chan et al., 2005; Li et al., 2009; Sayed et al., 2010) a down-regulation of this miRNA may *vice versa* induce host cell apoptosis or at least no longer inhibit host cell apoptosis and thus may show a negative influence on the parasite's liver-stage development. Before verifying this hypothesis by evaluating number and size of liver-stages, a two-color host cell invasion assay was performed to prove that invasion of HuH7 cells by sporozoites was not impaired at all through down-regulation of miR-21.

Again HuH7 cells were transfected either with m21 sponge, empty sponge or not transfected at all (PBS) and 48h later *Pb*NK65 WT sporozoites were co-incubated with transfected cells. Sporozoites were allowed to invade into HuH7 cells for 90 min. Afterwards non-invaded sporozoites were removed. During a two-step immuno fluorescence assay (IFA) sporozoites attached to but not invaded into HuH7 cells were first stained with anti-*Pb*CSP antibody followed by staining with secondary antibody (Alexa 488, green). In a second step HuH7 cells were permeabilized and invaded sporozoites were also stained with anti-*Pb*CSP antibody, followed by secondary antibody (Alexa 546, red). According to the respective choice of secondary antibodies sporozoites attached to HuH7 cells were stained in green and red, while sporozoites inside HuH7 were only stained in red. Sporozoites that were fixed during their invasion process (invasion blockage) were stained in green and red, while the already invaded part of these sporozoites was only stained in red. Exemplary images of all three possibilities are displayed in figure 3.4.7A. These images were taken from HuH7 cells after transfection with m21 sponge. They demonstrate that down-regulation of miR-21 did not completely inhibit the invasion behavior of the sporozoites. But nevertheless, down-regulation of miR-21 may still impair parasite's invasive capacity. To check this, 50 sporozoites per well were counted after transfection with m21 sponge, empty sponge and no transfection (PBS) and the amount of sporozoites inside the HuH7 cells as well as outside was determined. Also the amount of sporozoites that were stopped during their invasion and thus were partly inside and outside of the cell was considered (figure 3.4.7B). When comparing the distribution of sporozoites after transfection with m21 sponge and empty sponge no significant differences can be observed. In both cases around 30% of sporozoites invaded the cells, 10% displayed an invasion blockage and 60% remained outside the

host cells. The same relative distributions of sporozoites were determined when counting invasion of cells that were not transfected at all. Thus down-regulation of miR-21 has no influence on the invasive capacity of *Pb*NK65 sporozoites at all. The same was proven for the transfection procedure.

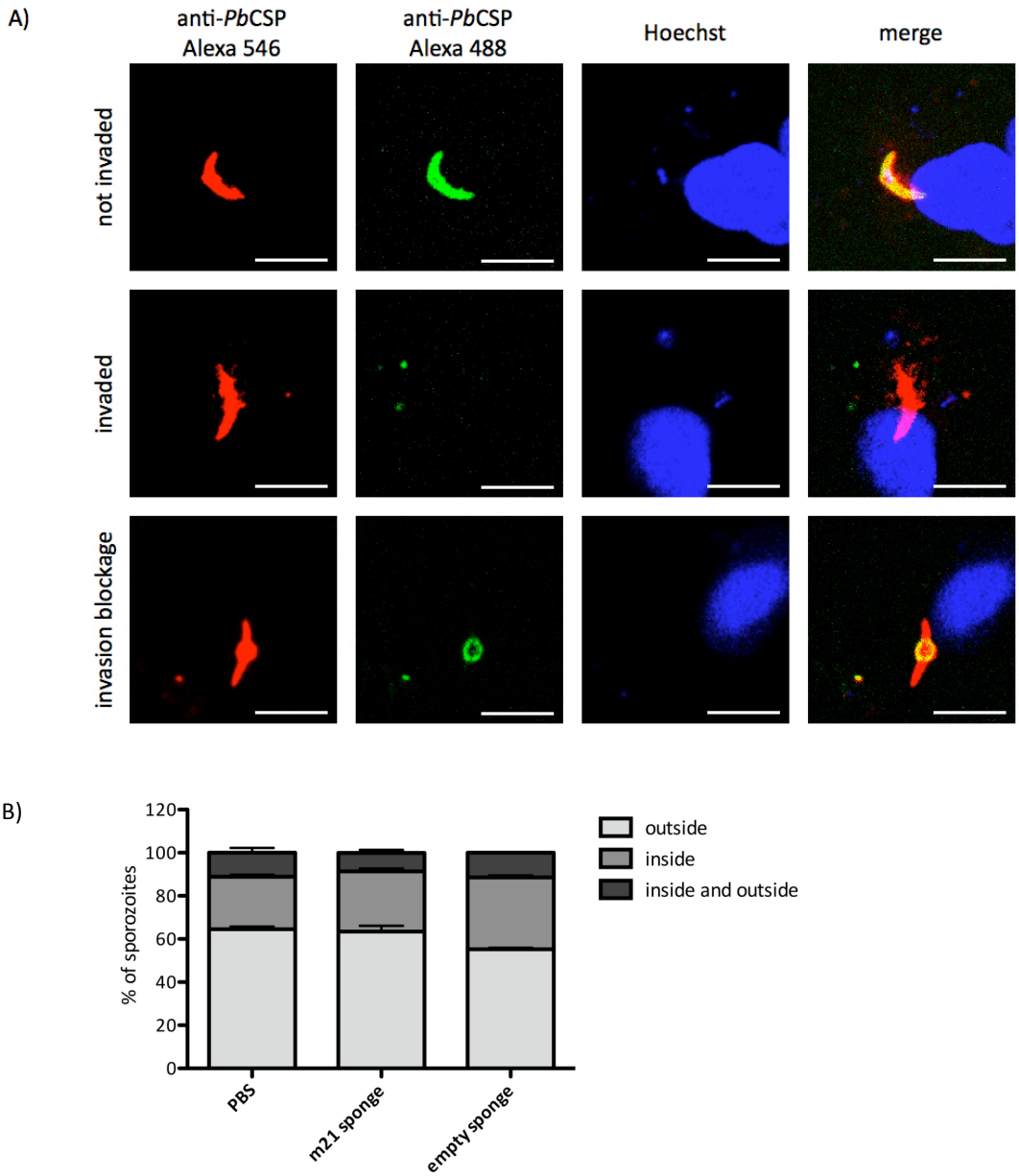

Figure 3.4.7: Invasion of HuH7 cells after down-regulation of hepatic miR-21. Exemplified confocal microscopic images of sporozoites inside and outside of HuH7 cells after 90 min invasion as well as of sporozoites that were fixed during their invasion process (invasion blockage). Sporozoites outside HuH7 cells were stained with anti-*Pb*CSP antibody and Alexa 488 (green). After permeabilization of host cells, invaded sporozoites were stained with anti-*Pb*CSP antibody and Alexa 546 (red). Scale bar 10 µm (A). 50 sporozoites were counted after transfection with m21 sponge, empty sponge and no transfection (PBS) and their distribution was determined (B). Experiment was performed in duplicates. Error bars represent the standard deviation.

After confirming that the invasion of HuH7 cells by the sporozoites was not impaired due to down-regulation of miR-21, the influence of this down-regulation on the liver-stage development was subsequently monitored. Therefore 24h and 40h after sporozoite invasion liver-stage development

was stopped and intracellular liver-stages were stained with anti-*Pb*HSP70. Again the number of liver-stages (figure 3.4.8A) as well as the size of liver-stages (figure 3.4.8B) was determined at the two developmental stages of interest. Down-regulation of host miR-21 did not show any effects on intrahepatic parasite growth. The number of intrahepatic parasites as well as their size at the two time points were indisthingushable when compared to the controls (figure 3.4.8A and B).

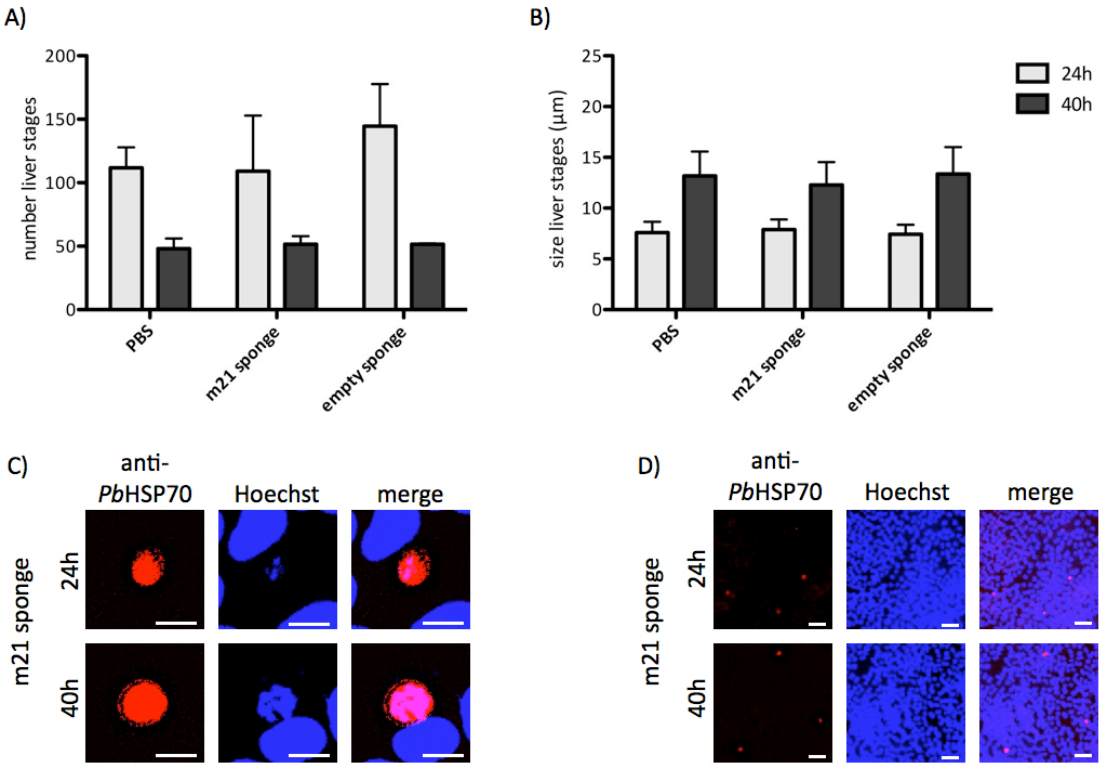

Figure 3.4.8: Number and sizes of liver-stages after down-regulation of hepatic miR-21. 2 x 10^4 HuH7 cells / well were transfected with m21 sponge, empty sponge or no sponge at all (PBS). 48h later cells were infected with *Pb*NK65 WT sporozoites. Liver-stages were visualized with anti-*Pb*HSP70 antibody 24h (light bars) and 40 h (dark bars) post invasion. Number of liver-stages (A) and size of liver-stages (B) were determined by confocal microscopy. Representative images of liver-stages after application of m21 sponge: 63x magnification scale bar 10 µm (C), 10x magnification scale bar 50 µm (D). Size of liver-stages was measured using Fiji. Experiment was performed in duplicates. Error bars represent the standard deviation.

While the experiments described above were carried out by me, Stefan Mockenhaupt (AG Grimm, Bioquant, Heidelberg) designed slightly different miRNA down-regulating constructs. The so-called *tough decoy RNAs* (TuD) possess a different secondary structure which makes them more stable and more efficient in inhibiting corresponding miRNAs (Haraguchi et al., 2009). Thus the above described m21 sponge experiment was repeated with the TuD constructs. Again HuH7 cells were transfected either with m21 TuD, empty TuD (containing no binding site for any known miRNA) or not transfected at all. 48h later sporozoites were allowed to invade the cells and liver-stage development was stopped 10h, 24h and 40h post invasion. In this case only the number of liver-stages was determined. When down-regulating miR-21 using the TuD it could be observed that 10h post invasion the number of liver-stages was higher than in control cells (figure 3.4.9). Normally within the first hours after

invasion the number of liver-stages severely drops (personal communication by F. Frischknecht). Down-regulation of miR-21 seems to have a beneficial effect onto very early liver-stages as more of them were present at 10h post invasion compared to the control conditions. During further liver-stage development this beneficial effect was no longer present as the numbers adjusted from 24h to 40h post invasion. Nevertheless, the observation 10h post invasion is striking as the initial hypothesis supposed a disadvantage for the liver-stage development when miR-21 is down-regulated.

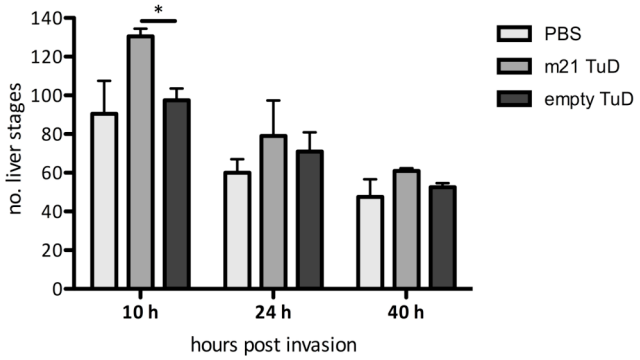

Figure 3.4.9: Number of liver-stages after down-regulation of hepatic miR-21. 2 x 10^4 HuH7 cells / well were transfected with m21 TuD, empty TuD or no TuD at all (PBS). 48h later cells were infected with *Pb*NK65 WT sporozoites. Liver-stages were stained with anti-*Pb*HSP70 antibody 10h, 24h and 40 h post invasion. Number of liver-stages was determined by confocal microscopy. Experiment was performed in duplicates. Error bars represent the standard deviation. * < 0.05, unpaired t-test.

3.4.4 *In vitro* up-regulation of miR-21

After gaining this striking result upon down-regulation of miR-21 using the TuD the question arose whether the exact opposite effect, namely a decrease in liver-stage numbers, can be induced by up-regulating hepatic miR-21. For this purpose, HuH7 cells were transfected with a pre-designed miR-21 *mimic* that increased the quantity of intracellular miR-21. In addition, HuH7 cells were either transfected with a miR-191 *mimic* as negative control or transfected without any DNA (mock) or not transfected at all (PBS). 24h later, *Pb*NK65 WT sporozoites were applied onto the cells, were allowed to invade for 90 min and 10h, 24h and 40h post invasion liver-stage development was stopped and the number of liver-stages was determined. When miR-21 was up-regulated 10h post invasion the number of liver-stages decreased compared to the control conditions (figure 3.4.10). Which is in good agreement with the results after application of the m21 TuD (figure 3.4.9). Again an adjustment of liver-stage numbers hence development was observed for the later time points, similar to the situation after transfection with the m21 TuD. This observation is highly contradictory to the initial miRNA profiling (section 3.3.5) where the presence of the parasite leads to an increase of miR-21 transcription levels. One would assume that such an increase would be beneficial for the parasite as it obviously survives the liver phase.

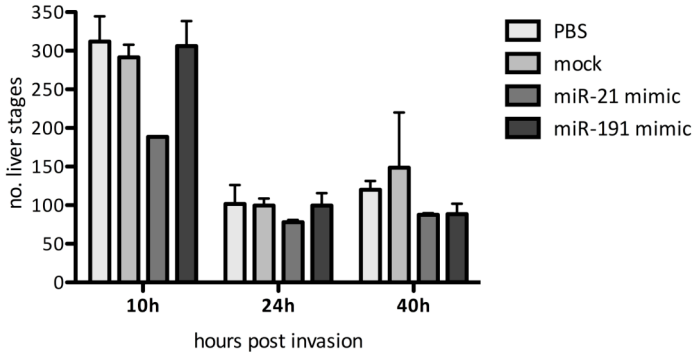

Figure 3.4.10: Number of liver-stages after up-regulation of hepatic miR-21. 2 x 10^4 HuH7 cells / well were transfected with miR-21 *mimic*, miR-191 *mimic*, with no DNA (mock) or not transfected at all (PBS). 24h later cells were infected with *Pb*NK65 WT sporozoites. Liver-stages were stained with anti-*Pb*HSP70 antibody 10h, 24h and 40 h post invasion. Number of liver-stages was determined by confocal microscopy. Experiment was performed in duplicates. Error bars represent the standard deviation. No statistical significance, unpaired t-test.

3.4.5 Influence of *in vivo* down-regulation of miR-21 and miR-155 on pre-patency

After having received those results from the *in vitro* experiments, I aimed at evaluating the effect of down-regulating both miR-21 and miR-155 on the intrahepatic development of the parasite *in vivo*. Although liver-stage development assays *in vitro* are an accepted tool to investigate influences on the parasite during this stage of its life cycle, it however hardly represents the complicated interplay between host and parasite that generally takes place *in vivo*. The initial observations regarding the up-regulation of host hepatic miR-21 and miR-155 upon the presence of *Plasmodium berghei* liver-stages were made *in vivo* and thus may involve more pathways, cellular interactions and cell types than only hepatocytes. Unfortunately it was not possible to narrow down the respective cell type that is responsible for the observed effects induced by the presence of a parasitic liver infection (section 3.1.4) and thus the *in vitro* analyses most probably do not give a complete and comprehensive picture. Therefore the following experiments were performed *in vivo* in order to ensure that the whole complicated interplay between the different organisms and cell types is taken into account.

For the down-regulation of miR-21 and miR-155 plasmids encoding the respective sponges were provided by Nina Schürmann (AG Grimm, Bioquant, Heidelberg) (figure 2.8.4). Binding efficiency of the sponges was tested *in vitro* by performing a Dual Luciferase assay as described in section 3.4.1 and 3.4.3 (figure 3.4.11). Thus it was demonstrated that both sponges were suitable for the subsequent *in vivo* experiments.

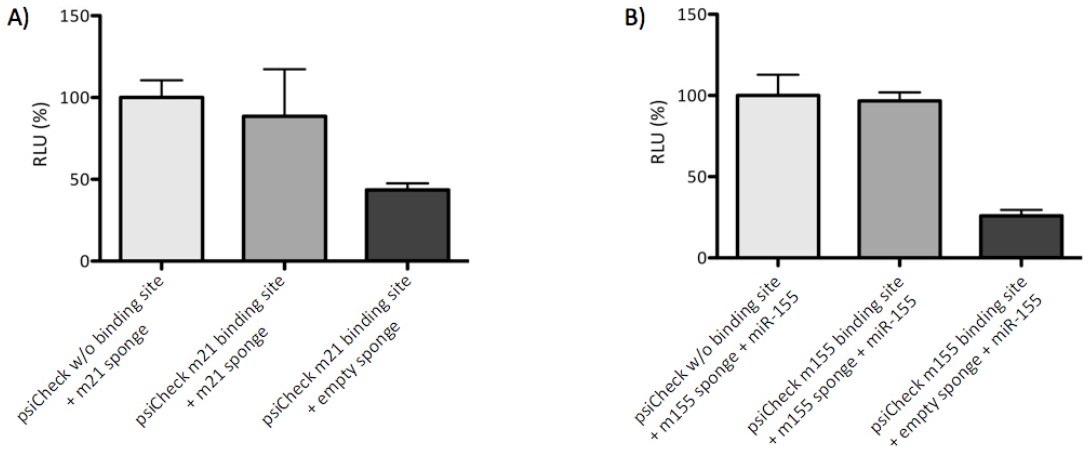

Figure 3.4.11: Dual Luciferase assay for determination of m21 and m155 sponge binding site efficiencies. PsiCheck plasmids containing no binding site or binding site for miR-21, were co-transfected with m21 sponge or empty sponge into HuH7 cells and relative light units (RLU) were calculated for estimating m21 binding site efficiency (A). PsiCheck plasmids containing no binding site or binding site for miR-155, were co-transfected with m155 sponge or empty sponge and miR-155 expression plasmids into Hek294T cells and relative light units (RLU) were calculated for estimating m155 binding site efficiency (B). Error bars represent the standard deviation.

After confirming the efficiency of m21 and m155 sponges, the respective plasmids were enveloped into rAAV-8 particles (section 3.4.2). To rule out any influence of the mere presence of rAAV particles in the liver on the pathological blood-stage pre-patency the empty sponge without binding sites for miRNAs was also enveloped and injected into mice. 14 days after this pretreatment with rAAV particles the animals were primed by intravenous injection of 10,000 *Pb*NK65 WT, GAP and RAS infectious sporozoites, respectively. A control group of mice without rAAV pretreatment was injected with sporozoites as just described. From day 3 post infection onwards, thin blood smears were taken to monitor the presence of parasite blood stages and hence pre-patency was determined (figure 3.4.12).

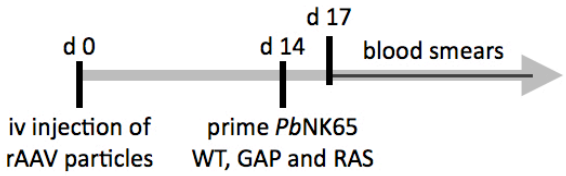

Figure 3.4.12: Injection regimen for *in vivo* down-regulation of hepatic miR-21 and miR-155. Naïve C57BL/6 mice were pretreated by intravenous (iv) injection of 2 x 10^{11} viral particles containing either m21 sponge, m155 sponge or empty sponge. 14 days later mice received intravenously 10,000 *Pb*NK65 WT, GAP and RAS sporozoites, respectively. From day 17 post initial rAAV injection onwards blood smears were taken to monitor pre-patency.

Blood-stage patency was observed in pretreated as well as in control mice injected with infectious WT sporozoites (table 3.4.1). However, animals with down-regulation of miR-21 showed blood stage parasites on day 5.3 post infection while all other WT injected animals displayed first parasites in their blood on day 6 post infection. GAP and RAS primed animals remained blood stage negative for at

least 14 days post infection indicating that down-regulation of neither miR-21 nor miR-155 interferes with GAP and RAS impairment in intrahepatic development (attenuation). This is in contrast to the *in vitro* data of section 3.4.3 and 3.4.4 were a down-regulation of miR-21 had a beneficial effect on the number of WT liver-stages while an up-regulation of miR-21 induced lower numbers of WT liver-stages. But these *in vitro* experiments only reflected the effect of a down-regulated miR-21 in hepatocytes on malarial liver-stage development, as already discussed in the respective sections. The true interaction between host and parasite may involve more liver assembling cell types and thus strong effects of one cell type may be adjusted by counteracting effects of other cell types leading in the end to those results initially seen after performance of the miRNA profiling (section 3.3.4) and during the *ex vivo* imaging (section 3.4.1).

Table 3.4.1: Pre-patency of *Pb*NK65 WT, GAP and RAS infected mice upon down-regulation of miR-21 and miR-155. C57BL/6 mice were pretreated with rAAV delivered sponges against miR-21, miR-155 and empty sponge, respectively. 14 days later mice were intravenously primed with 10,000 *Pb*NK65 WT, GAP and RAS sporozoites, respectively. As control non-pretreated animals were injected with sporozoites as above. Presence of parasites in the blood was monitored by daily blood smears from day 3 post injection onwards.

sponge	prime parasite genotype	no. of blood stage positive/ no. of infected (pre-patency)	starting parasitemia (%)
miR-21	10,000 WT spz. iv	3/3 (d 5.3)	0.04 ± 0.05
	10,000 GAP spz. iv	0/3	
	10,000 RAS spz. iv	0/3	
miR-155	10,000 WT spz. iv	3/3 (d 6)	0.03 ± 0.00
	10,000 GAP spz. iv	0/3	
	10,000 RAS spz. iv	0/3	
empty	10,000 WT spz. iv	3/3 (d 6)	0.02 ± 0.01
	10,000 GAP spz. iv	0/3	
	10,000 RAS spz. iv	0/3	
control	10,000 WT spz. iv	3/3 (d 6)	0.04 ± 0.02
	10,000 GAP spz. iv	0/3	
	10,000 RAS spz. iv	0/3	

3.4.6 Influence of *in vivo* down-regulation of miR-21 and miR-155 on the protective capacity of GAP and RAS

No effect on pre-patency was observed after *in vivo* down-regulation of miR-21 and miR-155 as demonstrated in the previous section. But the protective capacity induced by immunization with GAP and RAS as described earlier may be influenced. In order to shed some light on this important aspect of protection the previously described experiment was extended. Those animals that remained blood-stage negative according to table 3.4.1 were used for the further experiments. 14 days after the prime with *Pb*NK65 GAP and RAS, mice were intravenously challenged with 10,000 *Pb*NK65 WT sporozoites. In order to figure out whether the protective capacity observed in general after priming with attenuated parasites such as GAP and RAS is not affected by the down-regulation of the respective miRNAs the occurrence of erythrocytic parasites was monitored by taking daily thin blood smears (figure 3.4.13).

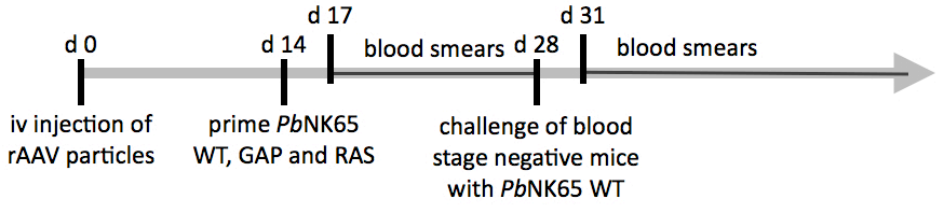

Figure 3.4.13: Injection regimen for *in vivo* down-regulation of hepatic miR-21 and miR-155 with subsequent *Pb*NK65 challenge. Naïve C57BL/6 mice were pretreated by intravenous (iv) injection of 2 x 10^{11} viral particles containing either m21 sponge, m155 sponge or empty sponge. 14 days later mice received intravenously 10,000 *Pb*NK65 WT, GAP and RAS sporozoites, respectively. From day 17 post initial rAAV injection onwards blood smears were taken to monitor pre-patency. Mice that remained blood stage negative on day 28 after initial rAAV injection were intravenously challenged with 10,000 *Pb*NK65 WT sporozoites and from day 31 after the initial rAAV injection onwards daily blood smears were taken to follow pre-patency.

Table 3.4.2 summarizes the results of this experiment. Interestingly, three out of three animals pretreated with miR-21 and miR-155 sponge and primed with GAP showed blood stages on average day 8.7 and 10 pi, respectively. Both control groups primed with GAP showed a delay in pre-patency until day 19 in the case of animals pretreated with empty sponge and day 17.5 for non-pretreated control mice. In the latter case only two out of three animals became blood stage positive.

Table 3.4.2: Pre-patency of *Pb*NK65 GAP and RAS primed and *Pb*NK65 WT challenged mice upon down-regulation of miR-21 and miR-155. C57BL/6 mice were pretreated with rAAV delivered sponges against miR-21, miR-155 and empty sponge, respectively. 14 days later mice were intravenously primed with 10,000 *Pb*NK65 GAP and RAS sporozoites, respectively. As control non-pretreated animals were injected with sporozoites as above. Another 14 days later mice were intravenously challenged with 10,000 *Pb*NK65 WT sporozoites. Presence of parasites in the blood was monitored by daily blood smears from day 3 post injection onwards.

sponge	prime parasite genotype	challenge parasite genotype	no. of blood stage positive/ no. of infected (pre-patency)
miR-21	10,000 GAP spz. iv	10,000 WT spz. iv	3/3 (d 8.7)
	10,000 RAS spz. iv	10,000 WT spz. iv	0/3
miR-155	10,000 GAP spz. iv	10,000 WT spz. iv	3/3 (d 10)
	10,000 RAS spz. iv	10,000 WT spz. iv	0/3
empty	10,000 GAP spz. iv	10,000 WT spz. iv	3/3 (d 19)
	10,000 RAS spz. iv	10,000 WT spz. iv	1/3 (d 28)
control	10,000 GAP spz. iv	10,000 WT spz. iv	2/3 (d 17.5)
	10,000 RAS spz. iv	10,000 WT spz. iv	0/3

Thus a down-regulation of miR-21 as well as miR-155 abolished the GAP induced immunity. It has to be stressed that five out of six GAP primed control animals got blood stage positive, however with a prolonged pre-patency. Hence this experiment demonstrated at the same time that only one prime with 10,000 *Pb*NK65 GAP is not sufficient to induce protective immunity (indicating additional boosts are required for inducing sterile immunity (Mueller et al., 2005a; Mueller et al., 2005b)) as it can be observed after priming with the same number of *Pb*NK65 RAS. In contrast to the effect on GAP induced immunity a down-regulation of miR-21 and miR-155 did not influence RAS induced sterile

protection. The curve in figure 3.4.14 shows in detail the days post infection on which each mouse got blood stage positive.

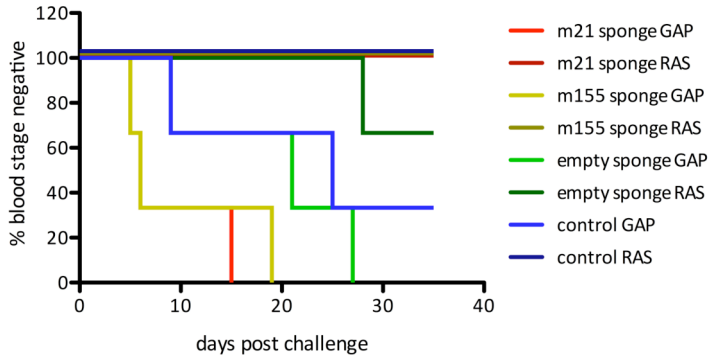

Figure 3.4.14: Development of blood-stages of *Pb*NK65 GAP and RAS primed and subsequently *Pb*NK65 WT challenged mice upon down-regulation of miR-21 and miR-155. After down-regulation of miR-21 and miR-155, respectively, mice were primed with either 10,000 *Pb*NK65 GAP or RAS and subsequently challenged with *Pb*NK65 WT parasites. The curve shows the development of parasites in the blood as decreasing percentage of blood-stage negative mice.

4 Discussion

The initial idea of the present study was to investigate whether the presence of *Plasmodium berghei* liver stages influences the host hepatic RNAi machinery. As the parasite replicates enormously within a short period of time during the clinically silent intraheptic phase of its life cycle, a tight dependency on host-cell factors is highly probable. This is supported by various studies, demonstrating that the parasite may recruit not only lipids but may also take up cholesterol from the host hepatocyte for its rapid intracellular growth (Labaied et al., 2011; Mikolajczak et al., 2007). As *Plasmodium* is unable to synthesize sterols, cholesterol found within the parasitophorous vacuole (PV) must be diverted from host-cell compartments (Bano et al., 2007). Interestingly, observed association of the PV to the host endoplasmatic reticulum (ER) may provide a possibility for the parasite to reach host-cell lipids (Bano et al., 2007; Jayabalasingham et al., 2010). This theory is supported by the observation that many intracellular pathogens like *Toxoplasma gondii*, *Chlamydia trachomatis* or *Salmonella enterica* serovar *Typhimurium* are equipped to gain access to lipids from exogenous and/or endogenous pathways of the host (Carabeo et al., 2003; Catron et al., 2004; Coppens et al., 2000; Kumar et al., 2006). Host-cell transcriptional profiling during the liver-stage infection with *Plasmodium* demonstrated differential expression patterns for a total of 1064 host hepatic genes during this developmental step (Albuquerque et al., 2009). These genes cover biological events, which start with an initial stress response, followed by engagement of host metabolic processes and the maintenance of cell viability throughout the entire liver-stage infection period. But this study lacks a focused glance into the host hepatic RNAi machinery and its reaction upon liver-stage infection, although it is more and more recognized that this machinery is important in intracellular infections (Cai et al., 2005; Sullivan et al., 2005). The RNAi machinery is responsible for correct processing and incorporation of microRNAs (miRNAs) into the miRNA-induced silencing complex (miRISC), followed by post-transcriptional silencing of respective target mRNAs. Although it is speculated that miRNAs of host organisms have evolved as defense mechanisms against viruses (Saumet and Lecellier, 2006), several studies demonstrated that viruses are able to manipulate the host RNAi machinery to ensure their survival. One example for use of the host RNAi machinery for the own benefit is the simian virus 40 (sv40), which accumulates viral miRNAs, processed via the host RNAi machinery, at later stages of infection. These miRNAs target early viral mRNAs for degradation, leading to a down-regulation of viral T-cell specific antigens. This, in turn results in a reduced susceptibility to and an additional reduced cytokine production by cytotoxic T-cells, allowing the virus to escape the host's immune response (Sullivan et al., 2005). Another example is Kaposi's sarcoma-associated herpes virus (KHSV), which expresses distinct miRNAs in latently infected cells. These miRNAs are hypothesized to interact with host mRNAs to support the establishment and/or maintenance of these latent infections (Cai et al., 2005).

So far, no studies investigated the influence *Plasmodium* liver-stages may have on the host hepatic RNAi machinery, although down-regulation of components comprising the hepatic RNAi machinery had been reported previously in other contexts. One study describes a significant down-regulation of

Drosha, *Dicer* and *TRBP* transcription levels during regeneration after partial hepatectomy (Shu et al., 2011). But also the presence of hepatic viruses and malignancies influences the hepatic RNAi machinery. A down-regulation of *Drosha* mRNA and protein expression was observed in cells expressing the hepatitis B virus (HBV) genome (Ren et al., 2012), while *Dicer* transcript levels have been down-regulated in association with hepatocellular carcinoma (HCC) (Wu et al., 2011). All these results demonstrate a tight interaction between the liver as hosting organ and the presence of a pathogen or malignancy, proving a high sensitivity of the hepatic RNAi machinery to changes within the cellular status and rising the question whether an intrahepatic infection with *Plasmodium* parasites influences the host hepatic RNAi machinery in a similar or completely different way.
Thus, in the course of my thesis I have decided to expand my study by including two time-points during *P. berghei* liver-stage development (i.e. 24h and 40h) that will allow me to acquire a more detailed overview of a possible impact of the parasite's exo-erythrocytic stage on the host hepatic RNAi machinery and *vice versa*. Therefore, during mid-liver-stage development at 24h and at a later time point around 40h after intravenous injection of infectious salivary gland sporozoites, infected livers were removed from inbred mice, RNA was isolated, transcribed and transcription levels of *Exportin-5* (*Xpo-5*), *Argonaute-2* (*Ago-2*), *Dicer*, *TRBP* and *Drosha* were analyzed. Furthermore, a possible influence of the protection-inducing experimental vaccines, GAP and RAS, on the host hepatic RNAi machinery was also investigated. Therefore, mice were infected with radiation-attenuated (RAS) and genetically attenuated (GAP) parasites. While the RAS arrest at varying time-points during their liver-stage development, GAP have been shown to arrest at mid-liver-stage development (around 24h after infection). And indeed I observed a down-regulation of transcription levels for all five components comprising the RNAi machinery I investigated (figure 3.1.3), and in the case of *Xpo-5* and *Drosha* this down-regulation was also confirmed on protein expression level (figures 3.1.4 and 3.1.5). This down-regulation was more pronounced in livers infected with the two attenuated parasite strains 40h post infection. It is obvious that the aforementioned conditions as well as an intrahepatic *Plasmodium* infection elicit distinct changes in the expression of RNAi machinery components, mirroring the different, disease-specific impacts a virus infection, a pathogen infection or a malignancy may have on the liver. By investigating the host hepatic RNAi machinery at different time points during *Plasmodium* liver-stage infection and thus during different developmental stages, it was possible to show a dynamic down-regulation of host hepatic RNAi machinery components during development of the parasite as well as upon its arrest. These distinct reactions to the different situations I applied allow us to assume a very well defined hepatic response to different triggers rather than a more general stress response to an exogenous factor.

As I have been able to investigate whole liver preparations it is likely that reactions of single hepatocytes upon infection with the attenuated parasites are transferred to other hepatocytes in a paracrine and/or endocrine manner, resulting in a reaction of the liver as a whole organ. This hypothesis is supported by recent data presented by M. Mota (Lisbon, Portugal), who compares the

cDNA profile of *Plasmodium* infected livers versus non-infected livers (M. Mota, DGP meeting March 2012). M. Mota showed that in these whole-organ preparations differences in cDNA expression could be observed as well, even upon intravenous infection with comparatively low numbers of injected salivary gland sporozoites.

A very interesting point is the more pronounced down-regulation of RNAi machinery components upon infection with attenuated *Plasmodium* liver-stages while wildtype (WT) infected livers resemble more the non-infectious situation. During evolution, host and WT *Plasmodium* parasite co-adapted in a way, which allowed both organisms to survive. A very nice example is the co-localization of malaria and the gene for haemoglobin S (HbS), a structural variant of normal haemoglobin A (HbA) in sub-Saharan Africa (Piel et al., 2010). HbS results from an amino acid substitution at position 6 of the β-globin subunit, leading to the typical sickling of red blood cells under low oxygen tension due to polymerization of HbS (Rees et al., 2010). Homozygotes (HbSS) suffer from a chronic form of haemolytic anaemia, called sickle cell disease, and thus, in contrast to heterozygotes (HbAS), experience negative selection (Herrick, 1910). In the context of malaria it is hypothesized that individuals with HbAS are at lower risk of malaria infection than individuals with HbAA and are additionally at lower risk of progression to severe and fatal disease (Williams and Obaro, 2011). Thus, this situation is advantageous for both, the host as well as the parasite. Because only in case the infected host survives long enough for parasitic gametocytes to develop and being taken up by a female *Anopheles* mosquito during a blood meal, the parasite can be transmitted and thus prevents its own eradication. On the other hand this non-severe development of disease also increases the probability of the host to survive, ensuring its further existence. In contrast to this, HbSS individuals are at even lower risk of malaria infection than HbAS individuals, but if they are infected the mortality rate is even higher than in HbAA individuals, implying a disadvantage for both, the host and the parasite (Williams and Obaro, 2011). But not only the blood-stages of *Plasmodium* found ways of co-existence with the host. Also during the liver-stage development the parasite is able to exist without complete eradication by the host and in turn does not threaten the host. The intrahepatic WT parasite hides from recognition by the host and its immune system by incorporation of both host lipids and cholesterol into the parasitophorous vacuolar membrane (PVM) (Labaied et al., 2011; Mikolajczak et al., 2007). A similar effect of circumventing the host immune response can be observed for released merosomes at the end of liver-stage development. These vesicles, filled with mature liver-stage merozoites, are enveloped into hepatic membrane and thus pretend to be of host origin (Baer et al., 2007a; Sturm et al., 2006). This disguise allows them to reach the host's lung without being recognized by the host immune system. This successful hiding of WT liver-stages from recognition by the host hepatocyte is reflected by the observed low influence on the host hepatic RNAi machinery. In contrast to the well-hidden WT liver-stage parasites, the attenuated parasites lack single genes, which are important for liver-stage development, as they might be generally essential to recruit for instance host-cell factors. And thus, these parasites can no longer hide, are recognized by

the host hepatocytes, and the hepatocytes react with down-regulation of components comprising the RNAi machinery. It was demonstrated that parasitic UIS4 interacts with host Apolipoprotin A1 (ApoA1) (A.-K. Mueller, personal communication; Schulz et al., unpublished data), the major lipoprotein complexed within the high-density lipoprotein (HDL) and the primary acceptor for unesterified cholesterol from the peripheral tissue (von Eckardstein et al., 1993). As the parasite is unable to synthesize cholesterol and cholesterolester *de novo*, it is likely that the parasite recruits cholesterol by recruiting hepatic ApoA1. And indeed, when human hepatocarcinoma cells (HuH7) over-expressing *Rattus norvegicus* ApoA1 were infected with *P. berghei* parasites, these parasites grew and developed faster, supporting the hypothesis that the parasite requires host hepatic factors for its intrahepatic differentiation and development as well as its disguise (Schulz et al., unpublished data). Parasites lacking the upregulated in infectious sporozoites gene *uis4* are unable to complete liver-stage development and due to this growth-arrest induce immune responses in the host (Matuschewski et al., 2002b; Mueller et al., 2005a; Mueller et al., 2005b). A very similar effect is linked to parasitic UIS3. This parasite protein recruits liver fatty-acid-binding protein (L-FABP) to the PVM, a protein involved in trafficking and delivery of lipids within hepatocytes (Mikolajczak et al., 2007). Recruitment of L-FABP to the PVM is another example for exploration of the host hepatocyte by the parasite. Another parallel to UIS4 is the observation that knock-out of *uis3* also leads to developmental arrest of the parasite during mid-liver-stage development and alert the host's immune system resulting in protective capacities to WT challenges. Thus, a lack of host-derived lipids within the PVM no longer provides shelter for the parasite from recognition by the host cell, which in turn induces appropriate reactions, such as e.g. a down-regulation of components comprising the host hepatocytes RNAi machinery. A similar effect was already shown regarding induction of programmed cell-death in infected hepatocytes. Infection with RAS and *p36p* knock-out parasites leads to apoptosis of the affected hepatocyte and activates the host immune system (Leiriao et al., 2005b; van Dijk et al., 2005). In contrast to this, infected hepatocytes are protected from programmed cell-death during infection with WT liver-stage parasites (Leiriao et al., 2005a; Rennenberg et al., 2010; van de Sand et al., 2005). These studies demonstrate recognition of attenuated parasites by the hepatocytes, followed by reactions of the host cells leading to activation of the immune system and induction of host-cell apoptosis. Thus, I hypothesize a similar mode of action in the context of my study. Attenuation of the parasite is recognized by the hepatocytes, which react with down-regulation of key components comprising the RNAi machinery. This down-regulation may play an important role in the aforementioned activation of immune responses and apoptosis. Of course further host-cell reactions that may be taking place in parallel cannot be ruled out. Thus it would be interesting to investigate, whether up-regulation of these affected key components may have additionally opposite effects on the attenuation of the parasites and the resulting induced immune responses.

But not only the host RNAi machinery was shown to specifically react upon infection or disease, thus supporting the tight interaction between hosts and pathogens, which has evolved during evolution.

Further evidence for this specific interplay and the involvement of host miRNAs therein comes from different intracellular pathogens. One example for an intracellular bacterial pathogen is *Salmonella enterica* serovar *Thyphimurium*, which causes lethal typhoid fever in mice and gastroenteritis in human (Cossart and Sansonetti, 2004; Mastroeni et al., 2009). This pathogen on the one hand secretes effector proteins, which directly interact with host proteins, leading to subversion of several host-cell pathways like signal transduction and membrane trafficking (Galan, 2009; McGhie et al., 2009) in some way similar to the *Plasmodium* parasite, which also recruits specific host-cell factors. But on the other hand, a recent study demonstrated miRNA responses of phagocytic and non-phagocytic cells during the course of infection with this pathogen. Bacterial LPS induced long-lasting miRNA programs that lasted during the course of infection (Schulte et al., 2011). Also apicomplexan parasites depend on defined and specific interactions with their host organisms to both establish and successfully complete their complex life cycles (Coppi et al., 2011; Coppi et al., 2007; Labaied et al., 2011; Luder and Gross, 2005; Mikolajczak et al., 2007; Nelson et al., 2008; Persson et al., 2007; Sinnis and Coppi, 2007; van de Sand et al., 2005). Thus, the question arose whether the host's miRNA expression is affected by a persisting infection with the different pathological representatives of this phylum, similar to the observations described above. Investigations of the immune responses of human biliary epithelial cells (cholangiocytes) to infection with *Cryptosporidium parvum*, a coccidian parasite of this phylum, that infects the small intestine as well as the biliary epithelial cells and thus causes biliary tract disease, allowed interesting insights into this interaction. Several studies provide evidence that defense mechanisms against *C. parvum* are fine-tuned by host miRNAs. In infected cholangiocytes the epithelial defense response was activated due to a decrease of host let-7i expression (Chen et al., 2007). Another study demonstrated increase of *C. parvum* burden upon functional inhibition of selected p65-dependent host miRNAs, suggesting a mechanism for the regulation of epithelial anti-microbial defense in general (Zhou et al., 2009). Down-regulation of miR-513 in *C. parvum* infected cholangiocytes was correlated with increase of B7-H1 protein and therewith associated induction of apoptotic cell-death of activated T-cells (Gong et al., 2010). Furthermore, down-regulation of host miR-98 and let-7 during the infection leads to the up-regulation of negative regulators of cytokine signaling (suppressors of cytokine signaling (SOCS) 4, cytokine-inducible Src homology (CIS) 2) thus influencing the regulation of the epithelial anti-microbial response (Hu et al., 2010b; Hu et al., 2009). And finally also controlling and balancing of the inflammatory response at *C. parvum* infection sites is influenced by de-regulation of host miRNAs upon presence of the parasite (Gong et al., 2011; Hu et al., 2010a). While investigations on *C. parvum* revealed already a rather detailed picture of the influence of host miRNAs in the host-parasite-interaction with defined target genes, only initial tentative impressions are gained from other apicomplexan parasites and their influence on the host miRNA expression pattern. Microarray analyses, searching infected host tissue for de-regulated miRNAs were performed in *Eimeria papillata* infected mouse jejunum (Al-Quraishy et al., 2011; Dkhil et al., 2011) and *Toxoplasma gondii* infected human foreskin fibroblasts (HFFs) (Zeiner et al., 2010). While *Eimeria* infections commonly affect the

digestive tract of the host, leading to diarrhea, weight loss, desiccation and ultimately to a fatal outcome of the disease (Gres et al., 2003; Licois et al., 1992; Pakandl, 2005; Ryley and Robinson, 1976), *Toxoplasma gondii* is an ubiquitous pathogen of warm-blooded animals, which is subclinical but persists for the life of the host and only induces serious disease in fetal infections and in primary or recrudescent infection of immuno-compromised individuals (Montoya and Liesenfeld, 2004). In both cases, differentially expressed miRNAs were observed upon infection with the respective apicomplexan parasite. In the context of an *E. papillata* infection no biological roles have been provided by the authors for the de-regulated miRNAs. In contrast to this, the authors, who conducted the microarray of *T. gondii* infected HFFs, speculate whether at least some of the up-regulated miRNAs might be involved in sending alarm signals for guidance of immune mechanisms or are associated with the repair of tissue damage.

These observations and speculations, as well as my previous observation regarding a down-regulation of the host hepatic RNAi machinery upon hepatic infection, give rise to the question whether an intrahepatic *Plasmodium* infection influences the host hepatic miRNA expression as well and if so, whether miRNAs, known to be involved in immunity, are affected. Thus, I further aimed at deciphering possible changes during the course of this exo-erythrocytic malarial infection. Therefore microarray analyses were performed comparing the miRNA expression pattern of livers 24h and 40h after infection with either *P. berghei* WT, GAP or RAS with miRNA expression pattern of naïve livers (sections 3.2 and 3.3). A total number of 31 dys-regulated miRNAs was observed within the different groups investigated (figure 3.3.5). Interestingly, the number of dys-regulated miRNAs correlated nicely with developmental stage and arrest of the parasite. At the early time-point, when most of the RAS and all WT liver-stages progress their development and only the GAP started to arrest, 23 miRNAs were dys-regulated in total and nine of them were dys-regulated jointly in livers infected with WT, GAP and RAS. In contrast to this, at the later time-point, when all GAP parasites are growth-arrested and additionally also a high amount of RAS show the same developmental blockade, the total number of dys-regulated miRNAs was reduced to 17, with only one miRNA being dys-regulated upon infection with all three parasite genotypes and the most miRNAs being dys-regulated in WT infected livers. These very distinct expression patterns for each of the groups investigated prove the specificity of the host response towards the different strains as well as the different developmental situations of the respective parasites.

So far, two studies investigated the influence a *Plasmodium* infection might have on the miRNA expression pattern of the affected host tissue. A first approach concentrated on the host hepatic miRNA expression pattern during a persisting *P. chabaudi* blood-stage infection. They chose the liver because this lymphoid organ is important as effector against blood-stage malaria (Delic et al., 2011). In this study three miRNAs were up-regulated upon infection and 16 miRNAs were down-regulated. But the host hepatic miRNAs identified were either of yet unknown function or associated with apoptosis or induction of cancer. De-regulation of miRNAs involved in innate or adaptive immune responses could not be detected, although it is reported that blood-stage malaria activates Kupffer

cells and thus would imply a dys-regulation of miRNAs involved in immunity, like for example miR-155 (Dockrell et al., 1980; Taverne et al., 1987). When comparing the dys-regulated hepatic miRNAs from my analysis with those discovered upon an ongoing *P. chabaudi* blood-stage infection (Delic et al., 2011), no common miRNAs were detected, although the same host organ was investigated, indicating that the liver reacts in very specific ways depending whether the organ is exposed to a hepatic or erythrocytic *Plasmodium* infection. The second approach aimed at further understanding the differences leading to the two main pathological outcomes of malaria infections: the cerebral and the non-cerebral (anaemic) phenotype. Cerebral malaria is a major complication in infections with *Plasmodium falciparum* and is characterized by coma and neurological impairment, while infection with the other human *Plasmodium* parasites can lead to high parasite densities but normally do not affect the brain (Tuteja, 2007). It is thought that the hallmarks of cerebral malaria, like coma, are caused by sequestration of parasitized red blood cells to cerebral microvascular capillaries as well as release of metabolic factors and inflammatory mediators (Clark and Alleva, 2009). Both pathogenic phenotypes can selectively be modeled in mice, depending on the combination of mouse and parasite strain (Combes et al., 2005). This study compared the expression profile of six pre-selected miRNAs (let-7i, miR-27a, miR-150, miR-210, miR-155, miR-126) which were previously reported to be involved in the regulation of normal immune and inflammatory responses in cerebral versus non-cerebral malaria (El-Assaad et al., 2011). For this purpose CBA mice were infected either with *P. berghei* ANKA parasites, inducing fatal disease with cerebral malaria (Grau et al., 1986) or with *P. berghei* K173 parasites, inducing non-cerebral malaria with hyperparasitemia and anemia (Neill and Hunt, 1992) and expression of the selected miRNAs was investigated in brain as well as heart tissue, which served as control. Let-7i, miR-27a and miR-150 were significantly up-regulated in cerebral malaria whereas the remaining three miRNAs were unchanged. Again no overlap in dys-regulated miRNAs between this study and my investigations can be found. Immunity, elicited at different sides within the infected host, is induced by different miRNAs, strengthening the uniqueness of each host response in the different organs. Further support is given by miR-122, which is the most abundant miRNA in the liver (Lagos-Quintana et al., 2002) and down-regulated upon HBV infection as well as HCC (Chen et al., 2011; Lewis and Jopling, 2010). This miRNA was not differentially expressed in the present study, separating effects induced by HBV infection and HCC from those induced by malaria liver-stages. All these different result even more strengthen the hypothesis that the host liver reacts in very distinct ways to different pathogenic situations.

On a first glance it appears to be contradictory to observe up-regulated miRNAs 40h post infection with either of the parasite strains, as key components of the host hepatic RNAi machinery were down-regulated at this time-point and no further processing of miRNAs should be expected. But when having a more detailed look, the transcriptional analysis of the RNAi machinery components is partly reflected by the miRNA expression profile that I obtained after completion of experimental analysis. 40h post infection the most striking effects on the *Xpo-5*, *Ago-2*, *Dicer*, *TRBP* and *Drosha* mRNA

expression levels were observed upon infection with the two attenuated malarial parasite strains. At the same time the number of dys-regulated miRNAs is lowest in these groups. By far the most dys-regulated miRNAs were detected at this time-point in livers infected with WT parasites and in this case only *Dicer*, *TRBP* and *Drosha* transcription levels were decreased. But nevertheless a certain amount of up-regulated miRNAs was observed in parallel with down-regulated RNAi machinery components. Interestingly, similar observations were also made in the context of hepatitis induced hepatocellular carcinoma. As already mentioned earlier, Wu et al. (2011) observed a down-regulation of *Dicer* mRNA levels in malignant tissue from patients with HCC in comparison to the corresponding non-neoplastic tissues. In contrast to this, several other studies report an up-regulation of different miRNAs in HCC tissue (Jiang et al., 2008; Liu et al., 2011; Marquez et al., 2010). Thus, maybe a down-regulation of components comprising the RNAi machinery not necessarily leads to a complete shut-down of miRNA processing. In addition, the protein levels of Xpo-5 and Drosha had been reduced (figure 3.1.5) but low amounts of both proteins were still detected in Western blot analyses, possibly being enough for processing the up-regulated miRNAs. But it is also possible, that those miRNAs, which are still up-regulated at 40h post infection with the attenuated parasites, are not newly processed. It has been shown, that the half-life of miRNAs can range from only some few hours to more than 14 hours (Grosshans and Chatterjee, 2010) or even several days (van Rooij et al., 2007), giving the possibility, that the detected miRNAs were processed at an early time-point and stable enough for not being degraded until the later time-point of investigation.

Besides several distinct features observed upon infection with the different parasite strains as differentially expressed components of the RNAi machinery as well as dys-regulated miRNAs, infection with the different parasite strains also induce similar host-cell responses. Among these is the consistent up-regulation of miR-21 and miR-155. Both miRNAs were initially described as “oncomiRs” but also proved to be important for induction of immune responses. MiR-21 is associated in many cases with inhibition of apoptosis (Chan et al., 2005; Li et al., 2009; Sayed et al., 2010) but is also reported to be central for Toll-like receptor signaling (Quinn and O'Neill, 2011). MiR-155 is an important regulator of immune responses. It is responsible for the switch to antibody producing plasma B cells as well as induction of T_h1 cells (Turner and Vigorito, 2008). Similar to miR-21, miR-155 is associated with the control of Toll-like receptor signaling (Quinn and O'Neill, 2011). Both miRNAs were found to be up-regulated in antigen-experienced $CD8^+$ T-cell subsets (Salaun et al., 2011). And in addition, miR-155 is induced during the macrophage inflammatory response to viral as well as bacterial triggers (O'Connell et al., 2007).

In vivo down-regulation of neither miR-21 nor miR-155 had any influences on pre-patency after initial prime with *Pb*NK65 WT, GAP or RAS (table 3.4.1). In the case of WT infection, blood-stage parasites were present 5-6 days post injection, as expected. In case of GAP and RAS infection, no presence of blood-stage parasites was expected as these parasites arrest during their liver-stage development and no blood-stage parasites could be observed. When challenging RAS-primed mice, which have not

received any booster injections according to an experimental vaccination scheme (Nussenzweig et al., 1967), ~90% protection was expected (Nussenzweig et al., 1967). I could confirm this almost sterile protective capacity in the RAS-model after down-regulation of both miR-21 and miR-155 as well as in not pretreated control animals (table 3.4.2). Strikingly, for GAP- (e.g. *Pb*NK65 *uis3*$^{-}$) primed mice, it was not investigated so far, whether a single prime without any subsequent booster injections would be sufficient to induce robust and sterile protection, lasting for several month, as it was shown after application of a prime-two-boost-challenge-regimen (Mueller et al., 2005a; Mueller et al., 2005b). Interestingly, the herein described data for the first time show a protection from generation of blood-stage parasites in GAP-primed control mice and GAP-primed mice pretreated with empty sponge for 17.5 - 19 days after infectious sporozoite challenge (table 3.4.2). Thus, protection is not as robust as after prime and two subsequent booster injections with GAP, but nevertheless mice are protected from blood-stage parasites for at least 17.5 days. This time period was reduced to 8.7-10 days in animals pretreated with miR-21 and miR-155 sponge, demonstrating an influence of both miRNAs in induction of protective capacity by administration of *Pb*NK65 *uis3*$^{-}$ GAP (table 3.4.2).

It was reported that GAP induced immunity is mainly associated with induction of strong, interferon-γ-dependent CD8^{+} T-cell responses (Jobe et al., 2007; Mueller et al., 2007; Tarun et al., 2007). Thus, down-regulation of both miRNAs may have a negative influence on these antigen-experienced CD 8^{+} T-cell subsets (Salaun et al., 2011), which in turn reduces the immunity to a subsequent injection with WT sporozoites. The deviating results that I obtained during the course of these immunization studies in both RAS- and GAP-primed mice, which experienced a preceding down-regulation of miR-21 and miR-155, demonstrated different modes of action regarding the induction of immune responses. Although, according to the miRNA profiling, in both cases miR-21 and miR-155 were up-regulated in infected livers, these two miRNAs seem to be more important in GAP-induced immunity, than in RAS-induced immunity. Most probably both miRNAs cannot be considered the only factors being involved in induction of immunity, but in the case of GAP-mediated protection in the host they may play a more pronounced and decisive role than in RAS vaccination, where maybe other factors contribute to vaccination success. This is not surprising, as RAS and GAP (*uis3*$^{-}$, as used in this study) also differ in other characteristics. Intrahepatic infection with RAS induces host-cell death, while exo-erythrocytic infection with GAP does not (personal communication and PhD thesis A.-K. Müller), assuming they may also induce different kinds of immune responses. A potential role for antigen secreting B-cells in RAS-induced immunity but not in GAP-induced immunity may be one of the different factors that lead to the diverse effects of miR-21 and miR-155 down-regulation on induction of immunity by the two strains (Hafalla et al., 2011).

Involvement of miR-155 in the induction of immunity in the context of hepatic diseases is supported by a HBV infection study, although in this case innate immunity was concerned. In human hepatoma cells, up-regulation of miR-155 was demonstrated to serve as positive regulator of JAK/STAT signaling by targeting SOCS1 and thus increasing the expression of IFN-inducible antiviral genes and enhancing innate antiviral immunity, leading to a mild anti-HBV effect (Su et al., 2011a). Furthermore SOCS1 was

shown to inhibit CD 8^+ T-cell maturation (Palmer and Restifo, 2009). And as SOCS1 was proven do be a direct target of miR-155 (di Iasio et al., 2012; Wu et al., 2012; Zhang et al., 2012b), the highly increased up-regulation of miR-155 in GAP and RAS infected livers may inhibit SOCS1 mediated suppression of CD 8^+ T-cell maturation and thus contribute to GAP and RAS induced immunity. Also in WT infected livers a constant up-regulation of miR-155 was observed, but with lower levels than in GAP in RAS infected livers. This implies, that the induction of immunity depends on the amount of hepatic miR-155, although the differences between WT infected livers and GAP and RAS infected livers are not striking but rather subtle. It is possible that a required threshold lies exactly between the observed levels of WT infected and GAP and RAS infected livers. Transcriptional analysis of hepatic SOCS1 could contribute to answering the question of SOCS1 involvement.

Ongoing experiments investigate whether up-regulation of miR-155 in parallel with a GAP prime-challenge-regimen immunization *in vivo* would restore the observed reduced immune phenotype to the phenotype described after application of a typical prime-two-boost-challenge-regimen. And indeed, upon up-regulation of hepatic miR-155 one GAP prime is sufficient to induce prolonged protection against subsequent WT challenge (data not shown). Interestingly, at the time point of finalizing this thesis, animals pre-treated and challenged are still protected after 21 days post challenge and will be further analyzed by tracking blood-stage parasitemias (data not shown). These results may provide first proof-of-principle studies that will now allow to immunize mice with a single dose of GAP combined with up-regulation of hepatic miR-155 and will moreover demonstrate a crucial role for miR-155 in GAP-mediated protection.

A supportive role for miR-21 and/or miR-155 in GAP-induced immunity could also be interesting in the context of clinical application. Although genetically attenuated *P. falciparum* parasites (*Pf*GAP) are not yet administered to humans due to e.g. technical problems, they would provide an alternative to *P. falciparum* RAS, as they consist of a homogenous, defined and safe population of attenuated parasites. Furthermore, RAS have to be given repeatedly to volunteers to elicit protective immunity (Epstein et al., 2007; Hoffman et al., 2002). Thus, a reduction of application to one single dose would be advantageous, especially in rural areas far away from hospitals which are difficult to reach. According to these reasons, application of a single dose of GAP together with an increase in miR-21 and/or miR-155 levels would be more beneficial than those repeated RAS injections. It was successfully shown, that AAV mediated delivery of miR-26a in an animal model of HCC to the affected liver suppressed cancer cell proliferation and activated tumor-specific apoptosis without induction of toxicity (Kota et al., 2009). Furthermore, several studies in primates (Elmen et al., 2008; Lanford et al., 2010) as well as phase IIa trials in humans (Santaris Pharma A/S; http://www.santaris.com) demonstrated the suitability and effectivity of *in vivo* silencing of miR-122 to reduced hepatitis C viral load in the liver. And although miR-122 is highly abundant in hepatic tissue (Lagos-Quintana et al., 2002) the sequestration of this miRNA did not have any long lasting impacts on the study animals'

health. These two examples provide proof-of-concept, that up-regulation as well as down-regulation of hepatic miRNAs can be used for therapy.

Taken together this study further proved the tight interaction between host hepatocyte and *P. berghei* liver-stage during the exo-erythrocytic development of the parasite. For the first time an involvement of both the host-hepatic RNAi machinery and host miRNAs in this interplay was demonstrated. It was shown that different phases of liver-stage development induce very specific reactions in the host organ. Furthermore, two miRNAs, miR-21 and miR-155 were identified as potential factors involved in GAP- and RAS-induced immunity, although their impact on the induction of immunity varies between the two different immunity inducing parasite strains. Especially their pronounced role in GAP-induced immunity may provide a novel tool for therapeutic treatment of pre-erythrocytic stages.

According to these results, a model can be proposed, that implies changes in transcription levels of components comprising the host-hepatic RNAi machinery upon recognition of the parasite by the host hepatocyte. These transcriptional changes are followed by dys-regulation of host hepatic miRNAs and elicitation of host immune responses. These changes are highly specific to ongoing as well as attenuating liver-stage infection and also to the different phases of liver-stage development. Nevertheless, two miRNAs, i.e. miR-21 and miR-155, show similar expression patterns and thus may contribute to induction of $CD8^+$ T-cell mediated immunity, typically induced by GAP and RAS, respectively. In the case of miR-155 the contribution may be directly linked to inhibition of SOCS1 (Su et al., 2011a).

5 References

Al-Quraishy, S., Delic, D., Sies, H., Wunderlich, F., Abdel-Baki, A.A., and Dkhil, M.A. (2011). Differential miRNA expression in the mouse jejunum during garlic treatment of Eimeria papillata infections. Parasitol Res.

Alam, M.M., and O'Neill, L.A. (2011). MicroRNAs and the resolution phase of inflammation in macrophages. Eur J Immunol *41*, 2482-2485.

Albuquerque, S.S., Carret, C., Grosso, A.R., Tarun, A.S., Peng, X., Kappe, S.H., Prudencio, M., and Mota, M.M. (2009). Host cell transcriptional profiling during malaria liver stage infection reveals a coordinated and sequential set of biological events. BMC Genomics *10*, 270.

Amino, R., Thiberge, S., Martin, B., Celli, S., Shorte, S., Frischknecht, F., and Menard, R. (2006). Quantitative imaging of Plasmodium transmission from mosquito to mammal. Nat Med *12*, 220-224.

Arai, M., Billker, O., Morris, H.R., Panico, M., Delcroix, M., Dixon, D., Ley, S.V., and Sinden, R.E. (2001). Both mosquito-derived xanthurenic acid and a host blood-derived factor regulate gametogenesis of Plasmodium in the midgut of the mosquito. Mol Biochem Parasitol *116*, 17-24.

Asirvatham, A.J., Gregorie, C.J., Hu, Z., Magner, W.J., and Tomasi, T.B. (2008). MicroRNA targets in immune genes and the Dicer/Argonaute and ARE machinery components. Mol Immunol *45*, 1995-2006.

Baer, K., Klotz, C., Kappe, S.H., Schnieder, T., and Frevert, U. (2007a). Release of hepatic Plasmodium yoelii merozoites into the pulmonary microvasculature. Plos Pathogens *3*, e171.

Baer, K., Roosevelt, M., Clarkson, A.B., Jr., van Rooijen, N., Schnieder, T., and Frevert, U. (2007b). Kupffer cells are obligatory for Plasmodium yoelii sporozoite infection of the liver. Cell Microbiol *9*, 397-412.

Baltimore, D., Boldin, M.P., O'Connell, R.M., Rao, D.S., and Taganov, K.D. (2008). MicroRNAs: new regulators of immune cell development and function. Nat Immunol *9*, 839-845.

Bano, N., Romano, J.D., Jayabalasingham, B., and Coppens, I. (2007). Cellular interactions of Plasmodium liver stage with its host mammalian cell. Int J Parasitol *37*, 1329-1341.

Bartel, D.P. (2009). MicroRNAs: Target Recognition and Regulatory Functions. Cell *136*, 215-233.

Baum, J., Gilberger, T.W., Frischknecht, F., and Meissner, M. (2008). Host-cell invasion by malaria parasites: insights from Plasmodium and Toxoplasma. Trends Parasitol *24*, 557-563.

Baum, J., Papenfuss, A.T., Mair, G.R., Janse, C.J., Vlachou, D., Waters, A.P., Cowman, A.F., Crabb, B.S., and de Koning-Ward, T.F. (2009). Molecular genetics and comparative genomics reveal RNAi is not functional in malaria parasites. Nucleic Acids Res *37*, 3788-3798.

Beaudoin, R.L., Strome, C.P., Mitchell, F., and Tubergen, T.A. (1977). Plasmodium berghei: immunization of mice against the ANKA strain using the unaltered sporozoite as an antigen. Exp Parasitol *42*, 1-5.

Belnoue, E., Costa, F.T., Frankenberg, T., Vigario, A.M., Voza, T., Leroy, N., Rodrigues, M.M., Landau, I., Snounou, G., and Renia, L. (2004). Protective T cell immunity against malaria liver stage after vaccination with live sporozoites under chloroquine treatment. J Immunol *172*, 2487-2495.

Berns, K.I., and Linden, R.M. (1995). The cryptic life style of adeno-associated virus. Bioessays *17*, 237-245.

Bhanot, P., Schauer, K., Coppens, I., and Nussenzweig, V. (2005). A surface phospholipase is involved in the migration of plasmodium sporozoites through cells. J Biol Chem *280*, 6752-6760.

Bi, Y.J., Liu, G.W., and Yang, R.F. (2009). MicroRNAs: Novel Regulators During the Immune Response. J Cell Physiol *218*, 467-472.

Bihrer, V., Waidmann, O., Friedrich-Rust, M., Forestier, N., Susser, S., Haupenthal, J., Welker, M., Shi, Y., Peveling-Oberhag, J., Polta, A.*, et al.* (2011). Serum MicroRNA-21 as Marker for Necroinflammation in Hepatitis C Patients with and without Hepatocellular Carcinoma. PLoS One *6*, e26971.

Billker, O., Miller, A.J., and Sinden, R.E. (2000). Determination of mosquito bloodmeal pH in situ by ion-selective microelectrode measurement: implications for the regulation of malarial gametogenesis. Parasitology *120 (Pt 6)*, 547-551.

Bradford, M.M. (1976). A rapid and sensitive method for the quantitation of microgram quantities of protein utilizing the principle of protein-dye binding. Anal Biochem *72*, 248-254.

Brownawell, A.M., and Macara, I.G. (2002). Exportin-5, a novel karyopherin, mediates nuclear export of double-stranded RNA binding proteins. J Cell Biol *156*, 53-64.

Bushati, N., and Cohen, S.M. (2007). MicroRNA functions. Annu Rev Cell Dev Bi *23*, 175-205.

Cai, X.Z., Lu, S.H., Zhang, Z.H., Gonzalez, C.M., Damania, B., and Cullen, B.R. (2005). Kaposi's sarcoma-associated herpesvirus expresses an array of viral microRNAs in latently infected cells. P Natl Acad Sci USA *102*, 5570-5575.

Calame, K. (2007). MicroRNA-155 function in B Cells. Immunity *27*, 825-827.

Carabeo, R.A., Mead, D.J., and Hackstadt, T. (2003). Golgi-dependent transport of cholesterol to the Chlamydia trachomatis inclusion. Proc Natl Acad Sci U S A *100*, 6771-6776.

Cardoso, A.L., Guedes, J.R., Pereira de Almeida, L., and Pedroso de Lima, M.C. (2012). miR-155 modulates microglia-mediated immune response by down-regulating SOCS-1 and promoting cytokine and nitric oxide production. Immunology *135*, 73-88.

Carter, B.J. (2005). Adeno-associated virus vectors in clinical trials. Hum Gene Ther *16*, 541-550.

Carter, R., and Mendis, K.N. (2002). Evolutionary and historical aspects of the burden of malaria. Clin Microbiol Rev *15*, 564-594.

Carthew, R.W., and Sontheimer, E.J. (2009). Origins and Mechanisms of miRNAs and siRNAs. Cell *136*, 642-655.

Castoldi, M., Spasic, M.V., Altamura, S., Elmen, J., Lindow, M., Kiss, J., Stolte, J., Sparla, R., D'Alessandro, L.A., and Klingmuller, U. (2011). The liver-specific microRNA miR-122 controls systemic iron homeostasis in mice. J Clin Invest *121*, 1386-1396.

Catron, D.M., Lange, Y., Borensztajn, J., Sylvester, M.D., Jones, B.D., and Haldar, K. (2004). Salmonella enterica serovar Typhimurium requires nonsterol precursors of the cholesterol biosynthetic pathway for intracellular proliferation. Infect Immun *72*, 1036-1042.

Chan, J.A., Krichevsky, A.M., and Kosik, K.S. (2005). MicroRNA-21 is an antiapoptotic factor in human glioblastoma cells. Cancer Res *65*, 6029-6033.

Cheloufi, S., Dos Santos, C.O., Chong, M.M., and Hannon, G.J. (2010). A dicer-independent miRNA biogenesis pathway that requires Ago catalysis. Nature *465*, 584-589.

Chen, X.M., Splinter, P.L., O'Hara, S.P., and LaRusso, N.F. (2007). A cellular micro-RNA, let-7i, regulates Toll-like receptor 4 expression and contributes to cholangiocyte immune responses against Cryptosporidium parvum infection. J Biol Chem *282*, 28929-28938.

Chen, Y., Shen, A., Rider, P.J., Yu, Y., Wu, K., Mu, Y., Hao, Q., Liu, Y., Gong, H., Zhu, Y., *et al.* (2011). A liver-specific microRNA binds to a highly conserved RNA sequence of hepatitis B virus and negatively regulates viral gene expression and replication. FASEB J *25*, 4511-4521.

Cifuentes, D., Xue, H., Taylor, D.W., Patnode, H., Mishima, Y., Cheloufi, S., Ma, E., Mane, S., Hannon, G.J., Lawson, N.D*., et al.* (2010). A novel miRNA processing pathway independent of Dicer requires Argonaute2 catalytic activity. Science *328*, 1694-1698.

Clark, I.A., and Alleva, L.M. (2009). Is human malarial coma caused, or merely deepened, by sequestration? Trends Parasitol *25*, 314-318.

Collins, W.E. (2012). Plasmodium knowlesi: a malaria parasite of monkeys and humans. Annu Rev Entomol *57*, 107-121.

Combes, V., De Souza, J.B., Rénia, L., Hunt, N.H., and Grau, G.E. (2005). Cerebral malaria: Which parasite? Which model? Drug Discov Today Dis Models *2*, 141-147.

Connolly, E., Melegari, M., Landgraf, P., Tchaikovskaya, T., Tennant, B.C., Slagle, B.L., Rogler, L.E., Zavolan, M., Tuschl, T., and Rogler, C.E. (2008). Elevated expression of the miR-17-92 polycistron and miR-21 in hepadnavirus-associated hepatocellular carcinoma contributes to the malignant phenotype. Am J Pathol *173*, 856-864.

Coppens, I., Sinai, A.P., and Joiner, K.A. (2000). Toxoplasma gondii exploits host low-density lipoprotein receptor-mediated endocytosis for cholesterol acquisition. J Cell Biol *149*, 167-180.

Coppi, A., Natarajan, R., Pradel, G., Bennett, B.L., James, E.R., Roggero, M.A., Corradin, G., Persson, C., Tewari, R., and Sinnis, P. (2011). The malaria circumsporozoite protein has two functional domains, each with distinct roles as sporozoites journey from mosquito to mammalian host. J Exp Med *208*, 341-356.

Coppi, A., Tewari, R., Bishop, J.R., Bennett, B.L., Lawrence, R., Esko, J.D., Billker, O., and Sinnis, P. (2007). Heparan sulfate proteoglycans provide a signal to Plasmodium sporozoites to stop migrating and productively invade host cells. Cell Host Microbe *2*, 316-327.

Cossart, P., and Sansonetti, P.J. (2004). Bacterial invasion: the paradigms of enteroinvasive pathogens. Science *304*, 242-248.

Cox, F.E. (2010). History of the discovery of the malaria parasites and their vectors. Parasit Vectors *3*, 5.

Deharo, E., Coquelin, F., Chabaud, A.G., and Landau, I. (1996). The erythrocytic schizogony of two synchronized strains of plasmodium berghei, NK65 and ANKA, in normocytes and reticulocytes. Parasitol Res *82*, 178-182.

Delic, D., Dkhil, M., Al-Quraishy, S., and Wunderlich, F. (2011). Hepatic miRNA expression reprogrammed by Plasmodium chabaudi malaria. Parasitol Res *108*, 1111-1121.

di Iasio, M.G., Norcio, A., Melloni, E., and Zauli, G. (2012). SOCS1 is significantly up-regulated in Nutlin-3-treated p53(wild-type) B chronic lymphocytic leukemia (B-CLL) samples and shows an inverse correlation with miR-155. Invest New Drugs.

Dkhil, M., Abdel-Baki, A.A., Delic, D., Wunderlich, F., Sies, H., and Al-Quraishy, S. (2011). Eimeria papillata: upregulation of specific miRNA-species in the mouse jejunum. Exp Parasitol *127*, 581-586.

Dockrell, H.M., de Souza, J.B., and Playfair, J.H. (1980). The role of the liver in immunity to blood-stage murine malaria. Immunology *41*, 421-430.

Doolan, D.L., and Martinez-Alier, N. (2006). Immune response to pre-erythrocytic stages of malaria parasites. Curr Mol Med *6*, 169-185.

Ebert, M.S., Neilson, J.R., and Sharp, P.A. (2007). MicroRNA sponges: competitive inhibitors of small RNAs in mammalian cells. Nat Methods *4*, 721-726.

Eis, P.S., Tam, W., Sun, L., Chadburn, A., Li, Z., Gomez, M.F., Lund, E., and Dahlberg, J.E. (2005). Accumulation of miR-155 and BIC RNA in human B cell lymphomas. Proc Natl Acad Sci U S A *102*, 3627-3632.

El-Assaad, F., Hempel, C., Combes, V., Mitchell, A.J., Ball, H.J., Kurtzhals, J.A., Hunt, N.H., Mathys, J.M., and Grau, G.E. (2011). Differential MicroRNA Expression in Experimental Cerebral and Noncerebral Malaria. Infect Immun *79*, 2379-2384.

Elmen, J., Lindow, M., Schutz, S., Lawrence, M., Petri, A., Obad, S., Lindholm, M., Hedtjarn, M., Hansen, H.F., Berger, U.*, et al.* (2008). LNA-mediated microRNA silencing in non-human primates. Nature *452*, 896-899.

Enayati, A., and Hemingway, J. (2010). Malaria management: past, present, and future. Annu Rev Entomol *55*, 569-591.

Epstein, J.E., Rao, S., Williams, F., Freilich, D., Luke, T., Sedegah, M., de la Vega, P., Sacci, J., Richie, T.L., and Hoffman, S.L. (2007). Safety and clinical outcome of experimental challenge of human volunteers with Plasmodium falciparum-infected mosquitoes: an update. J Infect Dis *196*, 145-154.

Eulalio, A., Huntzinger, E., and Izaurralde, E. (2008). Getting to the root of miRNA-mediated gene silencing. Cell *132*, 9-14.

Fabian, M.R., Sonenberg, N., and Filipowicz, W. (2010). Regulation of mRNA translation and stability by microRNAs. Annu Rev Biochem *79*, 351-379.

Filipowicz, W., Bhattacharyya, S.N., and Sonenberg, N. (2008). Mechanisms of post-transcriptional regulation by microRNAs: are the answers in sight? Nat Rev Genet *9*, 102-114.

Frevert, U. (2004). Sneaking in through the back entrance: the biology of malaria liver stages. Trends Parasitol *20*, 417-424.

Frevert, U., and Nardin, E. (2008). Cellular effector mechanisms against Plasmodium liver stages. Cell Microbiol *10*, 1956-1967.

Frevert, U., Usynin, I., Baer, K., and Klotz, C. (2006). Nomadic or sessile: can Kupffer cells function as portals for malaria sporozoites to the liver? Cell Microbiol *8*, 1537-1546.

Friedman, R.C., Farh, K.K., Burge, C.B., and Bartel, D.P. (2009). Most mammalian mRNAs are conserved targets of microRNAs. Genome Res *19*, 92-105.

Friesen, J., Silvie, O., Putrianti, E.D., Hafalla, J.C., Matuschewski, K., and Borrmann, S. (2010). Natural immunization against malaria: causal prophylaxis with antibiotics. Sci Transl Med *2*, 40ra49.

Frischknecht, F., Baldacci, P., Martin, B., Zimmer, C., Thiberge, S., Olivo-Marin, J.C., Shorte, S.L., and Menard, R. (2004). Imaging movement of malaria parasites during transmission by Anopheles mosquitoes. Cell Microbiol *6*, 687-694.

Galan, J.E. (2009). Common themes in the design and function of bacterial effectors. Cell Host Microbe *5*, 571-579.

Gao, G., Vandenberghe, L.H., Alvira, M.R., Lu, Y., Calcedo, R., Zhou, X., and Wilson, J.M. (2004). Clades of Adeno-associated viruses are widely disseminated in human tissues. J Virol *78*, 6381-6388.

Gao, G.P., Alvira, M.R., Wang, L., Calcedo, R., Johnston, J., and Wilson, J.M. (2002). Novel adeno-associated viruses from rhesus monkeys as vectors for human gene therapy. Proc Natl Acad Sci U S A *99*, 11854-11859.

Gardner, M.J., Hall, N., Fung, E., White, O., Berriman, M., Hyman, R.W., Carlton, J.M., Pain, A., Nelson, K.E., Bowman, S.*, et al.* (2002). Genome sequence of the human malaria parasite Plasmodium falciparum. Nature *419*, 498-511.

Gatignol, A., Buckler-White, A., Berkhout, B., and Jeang, K.T. (1991). Characterization of a human TAR RNA-binding protein that activates the HIV-1 LTR. Science *251*, 1597-1600.

Girard, A.E., Girard, D., English, A.R., Gootz, T.D., Cimochowski, C.R., Faiella, J.A., Haskell, S.L., and Retsema, J.A. (1987). Pharmacokinetic and in vivo studies with azithromycin (CP-62,993), a new

macrolide with an extended half-life and excellent tissue distribution. Antimicrob Agents Chemother *31*, 1948-1954.

Goel, V.K., Li, X., Chen, H., Liu, S.C., Chishti, A.H., and Oh, S.S. (2003). Band 3 is a host receptor binding merozoite surface protein 1 during the Plasmodium falciparum invasion of erythrocytes. Proc Natl Acad Sci U S A *100*, 5164-5169.

Gong, A.Y., Hu, G., Zhou, R., Liu, J., Feng, Y., Soukup, G.A., and Chen, X.M. (2011). MicroRNA-221 controls expression of intercellular adhesion molecule-1 in epithelial cells in response to Cryptosporidium parvum infection. Int J Parasitol *41*, 397-403.

Gong, A.Y., Zhou, R., Hu, G., Liu, J., Sosnowska, D., Drescher, K.M., Dong, H., and Chen, X.M. (2010). Cryptosporidium parvum induces B7-H1 expression in cholangiocytes by down-regulating microRNA-513. J Infect Dis *201*, 160-169.

Graewe, S., Stanway, R.R., Rennenberg, A., and Heussler, V.T. (2012). Chronicle of a death foretold: Plasmodium liver stage parasites decide on the fate of the host cell. FEMS Microbiol Rev *36*, 111-130.

Grau, G.E., Piguet, P.F., Engers, H.D., Louis, J.A., Vassalli, P., and Lambert, P.H. (1986). L3T4+ T lymphocytes play a major role in the pathogenesis of murine cerebral malaria. J Immunol *137*, 2348-2354.

Greenwood, B.M., Bojang, K., Whitty, C.J., and Targett, G.A. (2005). Malaria. Lancet *365*, 1487-1498.

Gres, V., Voza, T., Chabaud, A., and Landau, I. (2003). Coccidiosis of the wild rabbit (Oryctolagus cuniculus) in France. Parasite *10*, 51-57.

Grieger, J.C., Choi, V.W., and Samulski, R.J. (2006). Production and characterization of adeno-associated viral vectors. Nat Protoc *1*, 1412-1428.

Grieger, J.C., and Samulski, R.J. (2005). Adeno-associated virus as a gene therapy vector: vector development, production and clinical applications. Adv Biochem Eng Biotechnol *99*, 119-145.

Grimm, D., and Kleinschmidt, J.A. (1999). Progress in adeno-associated virus type 2 vector production: promises and prospects for clinical use. Hum Gene Ther *10*, 2445-2450.

Grimm, D., Pandey, K., Nakai, H., Storm, T.A., and Kay, M.A. (2006). Liver transduction with recombinant adeno-associated virus is primarily restricted by capsid serotype not vector genotype. J Virol *80*, 426-439.

Grosshans, H., and Chatterjee, S. (2010). MicroRNases and the Regulated Degradation of Mature Animal miRNAs. Adv Exp Med Biol *700*, 140-155.

Guillemin, J. (2001). Miasma, malaria, and method. Mol Interv *1*, 246-249.

Hafalla, J.C., Silvie, O., and Matuschewski, K. (2011). Cell biology and immunology of malaria. Immunol Rev *240*, 297-316.

Hakansson, S., Charron, A.J., and Sibley, L.D. (2001). Toxoplasma evacuoles: a two-step process of secretion and fusion forms the parasitophorous vacuole. EMBO J *20*, 3132-3144.

Haraguchi, T., Ozaki, Y., and Iba, H. (2009). Vectors expressing efficient RNA decoys achieve the long-term suppression of specific microRNA activity in mammalian cells. Nucleic Acids Res *37*, e43.

Hashimi, S.T., Fulcher, J.A., Chang, M.H., Gov, L., Wang, S., and Lee, B. (2009). MicroRNA profiling identifies miR-34a and miR-21 and their target genes JAG1 and WNT1 in the coordinate regulation of dendritic cell differentiation. Blood *114*, 404-414.

Herrick, J.B. (1910). Peculiar elongated and sickle-shaped red blood copuscles in a case of severe anaemia. Arch Intern Med *6*, 517-521.

Heussler, V., Rennenberg, A., and Stanway, R. (2010). Host cell death induced by the egress of intracellular Plasmodium parasites. Apoptosis *15*, 376-385.

Hoffman, S.L., Goh, L.M., Luke, T.C., Schneider, I., Le, T.P., Doolan, D.L., Sacci, J., de la Vega, P., Dowler, M., Paul, C*., et al.* (2002). Protection of humans against malaria by immunization with radiation-attenuated Plasmodium falciparum sporozoites. J Infect Dis *185*, 1155-1164.

Holder, A.A. (1994). Proteins on the surface of the malaria parasite and cell invasion. Parasitology *108 Suppl*, S5-18.

Hu, G., Gong, A.Y., Liu, J., Zhou, R., Deng, C., and Chen, X.M. (2010a). miR-221 suppresses ICAM-1 translation and regulates interferon-gamma-induced ICAM-1 expression in human cholangiocytes. Am J Physiol Gastrointest Liver Physiol *298*, G542-550.

Hu, G., Zhou, R., Liu, J., Gong, A.Y., and Chen, X.M. (2010b). MicroRNA-98 and let-7 regulate expression of suppressor of cytokine signaling 4 in biliary epithelial cells in response to Cryptosporidium parvum infection. J Infect Dis *202*, 125-135.

Hu, G., Zhou, R., Liu, J., Gong, A.Y., Eischeid, A.N., Dittman, J.W., and Chen, X.M. (2009). MicroRNA-98 and let-7 confer cholangiocyte expression of cytokine-inducible Src homology 2-containing protein in response to microbial challenge. J Immunol *183*, 1617-1624.

Huntzinger, E., and Izaurralde, E. (2011). Gene silencing by microRNAs: contributions of translational repression and mRNA decay. Nat Rev Genet *12*, 99-110.

Hutvagner, G., McLachlan, J., Pasquinelli, A.E., Balint, E., Tuschl, T., and Zamore, P.D. (2001). A cellular function for the RNA-interference enzyme Dicer in the maturation of the let-7 small temporal RNA. Science *293*, 834-838.

Iorio, M.V., Piovan, C., and Croce, C.M. (2010). Interplay between microRNAs and the epigenetic machinery: an intricate network. Biochim Biophys Acta *1799*, 694-701.

Ishino, T., Chinzei, Y., and Yuda, M. (2005a). A Plasmodium sporozoite protein with a membrane attack complex domain is required for breaching the liver sinusoidal cell layer prior to hepatocyte infection. Cell Microbiol *7*, 199-208.

Ishino, T., Chinzei, Y., and Yuda, M. (2005b). Two proteins with 6-cys motifs are required for malarial parasites to commit to infection of the hepatocyte. Mol Microbiol *58*, 1264-1275.

Ishino, T., Yano, K., Chinzei, Y., and Yuda, M. (2004). Cell-passage activity is required for the malarial parasite to cross the liver sinusoidal cell layer. PLoS Biol *2*, E4.

Jayabalasingham, B., Bano, N., and Coppens, I. (2010). Metamorphosis of the malaria parasite in the liver is associated with organelle clearance. Cell Res *20*, 1043-1059.

Jethwaney, D., Lepore, T., Hassan, S., Mello, K., Rangarajan, R., Jahnen-Dechent, W., Wirth, D., and Sultan, A.A. (2005). Fetuin-A, a hepatocyte-specific protein that binds Plasmodium berghei thrombospondin-related adhesive protein: a potential role in infectivity. Infect Immun *73*, 5883-5891.

Jiang, J., Gusev, Y., Aderca, I., Mettler, T.A., Nagorney, D.M., Brackett, D.J., Roberts, L.R., and Schmittgen, T.D. (2008). Association of MicroRNA expression in hepatocellular carcinomas with hepatitis infection, cirrhosis, and patient survival. Clin Cancer Res *14*, 419-427.

Jiang, S., Zhang, H.W., Lu, M.H., He, X.H., Li, Y., Gu, H., Liu, M.F., and Wang, E.D. (2010). MicroRNA-155 functions as an OncomiR in breast cancer by targeting the suppressor of cytokine signaling 1 gene. Cancer Res *70*, 3119-3127.

Jobe, O., Lumsden, J., Mueller, A.K., Williams, J., Silva-Rivera, H., Kappe, S.H., Schwenk, R.J., Matuschewski, K., and Krzych, U. (2007). Genetically attenuated Plasmodium berghei liver stages induce sterile protracted protection that is mediated by major histocompatibility complex Class I-dependent interferon-gamma-producing CD8+ T cells. J Infect Dis *196*, 599-607.

Jopling, C.L., Schutz, S., and Sarnow, P. (2008). Position-dependent function for a tandem microRNA miR-122-binding site located in the hepatitis C virus RNA genome. Cell Host Microbe *4*, 77-85.

Jopling, C.L., Yi, M., Lancaster, A.M., Lemon, S.M., and Sarnow, P. (2005). Modulation of hepatitis C virus RNA abundance by a liver-specific MicroRNA. Science *309*, 1577-1581.

Kalanon, M., and McFadden, G.I. (2010). Malaria, Plasmodium falciparum and its apicoplast. Biochem Soc Trans *38*, 775-782.

Kappe, S.H., Buscaglia, C.A., and Nussenzweig, V. (2004). Plasmodium sporozoite molecular cell biology. Annu Rev Cell Dev Biol *20*, 29-59.

Karakatsanis, A., Papaconstantinou, I., Gazouli, M., Lyberopoulou, A., Polymeneas, G., and Voros, D. (2011). Expression of microRNAs, miR-21, miR-31, miR-122, miR-145, miR-146a, miR-200c, miR-221, miR-222, and miR-223 in patients with hepatocellular carcinoma or intrahepatic cholangiocarcinoma and its prognostic significance. Mol Carcinog.

Kariu, T., Ishino, T., Yano, K., Chinzei, Y., and Yuda, M. (2006). CelTOS, a novel malarial protein that mediates transmission to mosquito and vertebrate hosts. Mol Microbiol *59*, 1369-1379.

Killick-Kendrick, R. (1978). Recent advances and outstanding problems in the biology of plebotomine sandflies. A review. Acta Trop *35*, 297-313.

Kota, J., Chivukula, R.R., O'Donnell, K.A., Wentzel, E.A., Montgomery, C.L., Hwang, H.W., Chang, T.C., Vivekanandan, P., Torbenson, M., Clark, K.R*., et al.* (2009). Therapeutic microRNA delivery suppresses tumorigenesis in a murine liver cancer model. Cell *137*, 1005-1017.

Krol, J., Loedige, I., and Filipowicz, W. (2010). The widespread regulation of microRNA biogenesis, function and decay. Nat Rev Genet *11*, 597-610.

Kumar, K.A., Baxter, P., Tarun, A.S., Kappe, S.H., and Nussenzweig, V. (2009). Conserved protective mechanisms in radiation and genetically attenuated uis3(-) and uis4(-) Plasmodium sporozoites. PLoS One *4*, e4480.

Kumar, Y., Cocchiaro, J., and Valdivia, R.H. (2006). The obligate intracellular pathogen Chlamydia trachomatis targets host lipid droplets. Curr Biol *16*, 1646-1651.

Kwon, I., and Schaffer, D.V. (2008). Designer gene delivery vectors: molecular engineering and evolution of adeno-associated viral vectors for enhanced gene transfer. Pharm Res *25*, 489-499.

Labaied, M., Harupa, A., Dumpit, R.F., Coppens, I., Mikolajczak, S.A., and Kappe, S.H. (2007). Plasmodium yoelii sporozoites with simultaneous deletion of P52 and P36 are completely attenuated and confer sterile immunity against infection. Infect Immun *75*, 3758-3768.

Labaied, M., Jayabalasingham, B., Bano, N., Cha, S.J., Sandoval, J., Guan, G., and Coppens, I. (2011). Plasmodium salvages cholesterol internalized by LDL and synthesized de novo in the liver. Cell Microbiol *13*, 569-586.

Laemmli, U.K. (1970). Cleavage of structural proteins during the assembly of the head of bacteriophage T4. Nature *227*, 680-685.

Lagos-Quintana, M., Rauhut, R., Yalcin, A., Meyer, J., Lendeckel, W., and Tuschl, T. (2002). Identification of tissue-specific microRNAs from mouse. Curr Biol *12*, 735-739.

Landau, I., and Chabaud, A. (1994). Plasmodium species infecting Thamnomys rutilans: a zoological study. Adv Parasitol *33*, 49-90.

Landthaler, M., Yalcin, A., and Tuschl, T. (2004). The human DiGeorge syndrome critical region gene 8 and Its D. melanogaster homolog are required for miRNA biogenesis. Curr Biol *14*, 2162-2167.

Lanford, R.E., Hildebrandt-Eriksen, E.S., Petri, A., Persson, R., Lindow, M., Munk, M.E., Kauppinen, S., and Orum, H. (2010). Therapeutic silencing of microRNA-122 in primates with chronic hepatitis C virus infection. Science *327*, 198-201.

Lee, R.C., Feinbaum, R.L., and Ambros, V. (1993). The C. elegans heterochronic gene lin-4 encodes small RNAs with antisense complementarity to lin-14. Cell *75*, 843-854.

Lee, Y., Ahn, C., Han, J., Choi, H., Kim, J., Yim, J., Lee, J., Provost, P., Radmark, O., Kim, S*., et al.* (2003). The nuclear RNase III Drosha initiates microRNA processing. Nature *425*, 415-419.

Leiriao, P., Albuquerque, S.S., Corso, S., van Gemert, G.J., Sauerwein, R.W., Rodriguez, A., Giordano, S., and Mota, M.M. (2005a). HGF/MET signalling protects Plasmodium-infected host cells from apoptosis. Cell Microbiol *7*, 603-609.

Leiriao, P., Mota, M.M., and Rodriguez, A. (2005b). Apoptotic Plasmodium-infected hepatocytes provide antigens to liver dendritic cells. J Infect Dis *191*, 1576-1581.

Lell, B., Faucher, J.F., Missinou, M.A., Borrmann, S., Dangelmaier, O., Horton, J., and Kremsner, P.G. (2000). Malaria chemoprophylaxis with tafenoquine: a randomised study. Lancet *355*, 2041-2045.

Lewis, A.P., and Jopling, C.L. (2010). Regulation and biological function of the liver-specific miR-122. Biochem Soc Trans *38*, 1553-1557.

Li, J., Huang, H., Sun, L., Yang, M., Pan, C., Chen, W., Wu, D., Lin, Z., Zeng, C., Yao, Y*., et al.* (2009). MiR-21 indicates poor prognosis in tongue squamous cell carcinomas as an apoptosis inhibitor. Clin Cancer Res *15*, 3998-4008.

Licois, D., Coudert, P., Bahagia, S., and Rossi, G.L. (1992). Endogenous development of Eimeria intestinalis in rabbits (Oryctolagus cuniculus). J Parasitol *78*, 1041-1048.

Lin, J.T., Juliano, J.J., and Wongsrichanalai, C. (2010). Drug-Resistant Malaria: The Era of ACT. Curr Infect Dis Rep *12*, 165-173.

Lingelbach, K., and Joiner, K.A. (1998). The parasitophorous vacuole membrane surrounding Plasmodium and Toxoplasma: an unusual compartment in infected cells. J Cell Sci *111 (Pt 11)*, 1467-1475.

Liu, J., Carmell, M.A., Rivas, F.V., Marsden, C.G., Thomson, J.M., Song, J.J., Hammond, S.M., Joshua-Tor, L., and Hannon, G.J. (2004). Argonaute2 is the catalytic engine of mammalian RNAi. Science *305*, 1437-1441.

Liu, W.H., Yeh, S.H., and Chen, P.J. (2011). Role of microRNAs in hepatitis B virus replication and pathogenesis. Biochim Biophys Acta.

Lou, Y., Yang, X., Wang, F., Cui, Z., and Huang, Y. (2010). MicroRNA-21 promotes the cell proliferation, invasion and migration abilities in ovarian epithelial carcinomas through inhibiting the expression of PTEN protein. Int J Mol Med *26*, 819-827.

Lu, L.F., and Liston, A. (2009). MicroRNA in the immune system, microRNA as an immune system. Immunology *127*, 291-298.

Luder, C.G., and Gross, U. (2005). Apoptosis and its modulation during infection with Toxoplasma gondii: molecular mechanisms and role in pathogenesis. Curr Top Microbiol Immunol *289*, 219-237.

Malato, Y., Naqvi, S., Schurmann, N., Ng, R., Wang, B., Zape, J., Kay, M.A., Grimm, D., and Willenbring, H. (2011). Fate tracing of mature hepatocytes in mouse liver homeostasis and regeneration. J Clin Invest *121*, 4850-4860.

Malhotra, P., Dasaradhi, P.V., Kumar, A., Mohmmed, A., Agrawal, N., Bhatnagar, R.K., and Chauhan, V.S. (2002). Double-stranded RNA-mediated gene silencing of cysteine proteases (falcipain-1 and -2) of Plasmodium falciparum. Mol Microbiol *45*, 1245-1254.

Marquez, R.T., Bandyopadhyay, S., Wendlandt, E.B., Keck, K., Hoffer, B.A., Icardi, M.S., Christensen, R.N., Schmidt, W.N., and McCaffrey, A.P. (2010). Correlation between microRNA expression levels and clinical parameters associated with chronic hepatitis C viral infection in humans. Lab Invest *90*, 1727-1736.

Mastroeni, P., Grant, A., Restif, O., and Maskell, D. (2009). A dynamic view of the spread and intracellular distribution of Salmonella enterica. Nat Rev Microbiol *7*, 73-80.

Matsushita, T., Elliger, S., Elliger, C., Podsakoff, G., Villarreal, L., Kurtzman, G.J., Iwaki, Y., and Colosi, P. (1998). Adeno-associated virus vectors can be efficiently produced without helper virus. Gene Ther *5*, 938-945.

Matuschewski, K. (2006). Getting infectious: formation and maturation of Plasmodium sporozoites in the Anopheles vector. Cell Microbiol *8*, 1547-1556.

Matuschewski, K., Hafalla, J.C., Borrmann, S., and Friesen, J. (2011). Arrested Plasmodium liver stages as experimental anti-malaria vaccines. Hum Vaccin *7 Suppl*, 16-21.

Matuschewski, K., Nunes, A.C., Nussenzweig, V., and Menard, R. (2002a). Plasmodium sporozoite invasion into insect and mammalian cells is directed by the same dual binding system. EMBO J *21*, 1597-1606.

Matuschewski, K., Ross, J., Brown, S.M., Kaiser, K., Nussenzweig, V., and Kappe, S.H. (2002b). Infectivity-associated changes in the transcriptional repertoire of the malaria parasite sporozoite stage. J Biol Chem *277*, 41948-41953.

McGhie, E.J., Brawn, L.C., Hume, P.J., Humphreys, D., and Koronakis, V. (2009). Salmonella takes control: effector-driven manipulation of the host. Curr Opin Microbiol *12*, 117-124.

McRobert, L., and McConkey, G.A. (2002). RNA interference (RNAi) inhibits growth of Plasmodium falciparum. Mol Biochem Parasitol *119*, 273-278.

Meister, G., Landthaler, M., Patkaniowska, A., Dorsett, Y., Teng, G., and Tuschl, T. (2004). Human Argonaute2 mediates RNA cleavage targeted by miRNAs and siRNAs. Mol Cell *15*, 185-197.

Mendis, K., Rietveld, A., Warsame, M., Bosman, A., Greenwood, B., and Wernsdorfer, W.H. (2009). From malaria control to eradication: The WHO perspective. Trop Med Int Health *14*, 802-809.

Meng, F., Henson, R., Wehbe-Janek, H., Ghoshal, K., Jacob, S.T., and Patel, T. (2007). MicroRNA-21 regulates expression of the PTEN tumor suppressor gene in human hepatocellular cancer. Gastroenterology *133*, 647-658.

Mikolajczak, S.A., Jacobs-Lorena, V., MacKellar, D.C., Camargo, N., and Kappe, S.H. (2007). L-FABP is a critical host factor for successful malaria liver stage development. Int J Parasitol *37*, 483-489.

Mitchell, G.H., Thomas, A.W., Margos, G., Dluzewski, A.R., and Bannister, L.H. (2004). Apical membrane antigen 1, a major malaria vaccine candidate, mediates the close attachment of invasive merozoites to host red blood cells. Infect Immun *72*, 154-158.

Mohmmed, A., Dasaradhi, P.V., Bhatnagar, R.K., Chauhan, V.S., and Malhotra, P. (2003). In vivo gene silencing in Plasmodium berghei--a mouse malaria model. Biochem Biophys Res Commun *309*, 506-511.

Montoya, J.G., and Liesenfeld, O. (2004). Toxoplasmosis. Lancet *363*, 1965-1976.

Mota, M.M., Pradel, G., Vanderberg, J.P., Hafalla, J.C., Frevert, U., Nussenzweig, R.S., Nussenzweig, V., and Rodriguez, A. (2001). Migration of Plasmodium sporozoites through cells before infection. Science *291*, 141-144.

Mueller, A.K., Camargo, N., Kaiser, K., Andorfer, C., Frevert, U., Matuschewski, K., and Kappe, S.H. (2005a). Plasmodium liver stage developmental arrest by depletion of a protein at the parasite-host interface. Proc Natl Acad Sci U S A *102*, 3022-3027.

Mueller, A.K., Deckert, M., Heiss, K., Goetz, K., Matuschewski, K., and Schluter, D. (2007). Genetically attenuated Plasmodium berghei liver stages persist and elicit sterile protection primarily via CD8 T cells. Am J Pathol *171*, 107-115.

Mueller, A.K., Kohlhepp, F., Hammerschmidt, C., and Michel, K. (2010). Invasion of mosquito salivary glands by malaria parasites: prerequisites and defense strategies. Int J Parasitol *40*, 1229-1235.

Mueller, A.K., Labaied, M., Kappe, S.H., and Matuschewski, K. (2005b). Genetically modified Plasmodium parasites as a protective experimental malaria vaccine. Nature *433*, 164-167.

Mulligan, H.W., Russell, P.F., and Mohan, B.N. (1941). Active immunization of fowls against *Plasmodium gallinaceum* by injections of killed homologous sporozoites. Journal of the Malaria Institute of India *4*, 25-34.

Murray, C.J., Rosenfeld, L.C., Lim, S.S., Andrews, K.G., Foreman, K.J., Haring, D., Fullman, N., Naghavi, M., Lozano, R., and Lopez, A.D. (2012). Global malaria mortality between 1980 and 2010: a systematic analysis. Lancet *379*, 413-431.

Nakai, H., Fuess, S., Storm, T.A., Muramatsu, S., Nara, Y., and Kay, M.A. (2005). Unrestricted hepatocyte transduction with adeno-associated virus serotype 8 vectors in mice. J Virol *79*, 214-224.

Nardin, E.H., and Nussenzweig, R.S. (1993). T cell responses to pre-erythrocytic stages of malaria: role in protection and vaccine development against pre-erythrocytic stages. Annu Rev Immunol *11*, 687-727.

Neill, A.L., and Hunt, N.H. (1992). Pathology of fatal and resolving Plasmodium berghei cerebral malaria in mice. Parasitology *105 (Pt 2)*, 165-175.

Nelson, M.M., Jones, A.R., Carmen, J.C., Sinai, A.P., Burchmore, R., and Wastling, J.M. (2008). Modulation of the host cell proteome by the intracellular apicomplexan parasite Toxoplasma gondii. Infect Immun *76*, 828-844.

Nussenzweig, R.S., and Nussenzweig, V. (1989). Antisporozoite vaccine for malaria: experimental basis and current status. Rev Infect Dis *11 Suppl 3*, S579-585.

Nussenzweig, R.S., Vanderberg, J., Most, H., and Orton, C. (1967). Protective immunity produced by the injection of x-irradiated sporozoites of plasmodium berghei. Nature *216*, 160-162.

O'Connell, R.M., Kahn, D., Gibson, W.S., Round, J.L., Scholz, R.L., Chaudhuri, A.A., Kahn, M.E., Rao, D.S., and Baltimore, D. (2010). MicroRNA-155 promotes autoimmune inflammation by enhancing inflammatory T cell development. Immunity *33*, 607-619.

O'Connell, R.M., Taganov, K.D., Boldin, M.P., Cheng, G., and Baltimore, D. (2007). MicroRNA-155 is induced during the macrophage inflammatory response. Proc Natl Acad Sci U S A *104*, 1604-1609.

Pakandl, M. (2005). Selection of a precocious line of the rabbit coccidium Eimeria flavescens Marotel and Guilhon (1941) and characterisation of its endogenous cycle. Parasitol Res *97*, 150-155.

Palmer, D.C., and Restifo, N.P. (2009). Suppressors of cytokine signaling (SOCS) in T cell differentiation, maturation, and function. Trends Immunol *30*, 592-602.

Papagiannakopoulos, T., Shapiro, A., and Kosik, K.S. (2008). MicroRNA-21 targets a network of key tumor-suppressive pathways in glioblastoma cells. Cancer Res *68*, 8164-8172.

Pedersen, I., and David, M. (2008). MicroRNAs in the immune response. Cytokine *43*, 391-394.

Persson, E.K., Agnarson, A.M., Lambert, H., Hitziger, N., Yagita, H., Chambers, B.J., Barragan, A., and Grandien, A. (2007). Death receptor ligation or exposure to perforin trigger rapid egress of the intracellular parasite Toxoplasma gondii. J Immunol *179*, 8357-8365.

Piel, F.B., Patil, A.P., Howes, R.E., Nyangiri, O.A., Gething, P.W., Williams, T.N., Weatherall, D.J., and Hay, S.I. (2010). Global distribution of the sickle cell gene and geographical confirmation of the malaria hypothesis. Nat Commun *1*, 104.

Pinzon-Ortiz, C., Friedman, J., Esko, J., and Sinnis, P. (2001). The binding of the circumsporozoite protein to cell surface heparan sulfate proteoglycans is required for plasmodium sporozoite attachment to target cells. J Biol Chem *276*, 26784-26791.

Portugal, S., Drakesmith, H., and Mota, M.M. (2011). Superinfection in malaria: Plasmodium shows its iron will. EMBO Rep *12*, 1233-1242.

Prudencio, M., Rodriguez, A., and Mota, M.M. (2006). The silent path to thousands of merozoites: the Plasmodium liver stage. Nat Rev Microbiol *4*, 849-856.

Putrianti, E.D., Silvie, O., Kordes, M., Borrmann, S., and Matuschewski, K. (2009). Vaccine-like immunity against malaria by repeated causal-prophylactic treatment of liver-stage Plasmodium parasites. J Infect Dis *199*, 899-903.

Quinn, S.R., and O'Neill, L.A. (2011). A trio of microRNAs that control Toll-like receptor signalling. Int Immunol *23*, 421-425.

Ralph, S.A., van Dooren, G.G., Waller, R.F., Crawford, M.J., Fraunholz, M.J., Foth, B.J., Tonkin, C.J., Roos, D.S., and McFadden, G.I. (2004). Tropical infectious diseases: metabolic maps and functions of the Plasmodium falciparum apicoplast. Nat Rev Microbiol *2*, 203-216.

Rana, T.M. (2007). Illuminating the silence: understanding the structure and function of small RNAs. Nat Rev Mol Cell Biol *8*, 23-36.

Rathjen, T., Nicol, C., McConkey, G., and Dalmay, T. (2006). Analysis of short RNAs in the malaria parasite and its red blood cell host. FEBS Lett *580*, 5185-5188.

Rees, D.C., Williams, T.N., and Gladwin, M.T. (2010). Sickle-cell disease. Lancet *376*, 2018-2031.

Ren, M., Qin, D., Li, K., Qu, J., Wang, L., Wang, Z., Huang, A., and Tang, H. (2012). Correlation between hepatitis B virus protein and microRNA processor Drosha in cells expressing HBV. Antiviral Res.

Renia, L., Maranon, C., Hosmalin, A., Gruner, A.C., Silvie, O., and Snounou, G. (2006). Do apoptotic Plasmodium-infected hepatocytes initiate protective immune responses? J Infect Dis *193*, 163-164; author reply 164-165.

Rennenberg, A., Lehmann, C., Heitmann, A., Witt, T., Hansen, G., Nagarajan, K., Deschermeier, C., Turk, V., Hilgenfeld, R., and Heussler, V.T. (2010). Exoerythrocytic Plasmodium parasites secrete a cysteine protease inhibitor involved in sporozoite invasion and capable of blocking cell death of host hepatocytes. Plos Pathogens *6*, e1000825.

Rodriguez, A., Griffiths-Jones, S., Ashurst, J.L., and Bradley, A. (2004). Identification of mammalian microRNA host genes and transcription units. Genome Res *14*, 1902-1910.

Rodriguez, A., Vigorito, E., Clare, S., Warren, M.V., Couttet, P., Soond, D.R., van Dongen, S., Grocock, R.J., Das, P.P., Miska, E.A*., et al.* (2007). Requirement of bic/microRNA-155 for normal immune function. Science *316*, 608-611.

Ross, R. (1897a). Observations on a Condition Necessary to the Transformation of the Malaria Crescent. Br Med J *1*, 251-255.

Ross, R. (1897b). On some Peculiar Pigmented Cells Found in Two Mosquitos Fed on Malarial Blood. Br Med J *2*, 1786-1788.

Ryley, J.F., and Robinson, T.E. (1976). Life cycle studies with Eimeria magna Perard, 1925. Z Parasitenkd *50*, 257-275.

Saiki, R.K., Scharf, S., Faloona, F., Mullis, K.B., Horn, G.T., Erlich, H.A., and Arnheim, N. (1985). Enzymatic amplification of beta-globin genomic sequences and restriction site analysis for diagnosis of sickle cell anemia. Science *230*, 1350-1354.

Salaun, B., Yamamoto, T., Badran, B., Tsunetsugu-Yokota, Y., Roux, A., Baitsch, L., Rouas, R., Fayyad-Kazan, H., Baumgaertner, P., Devevre, E.*, et al.* (2011). Differentiation associated regulation of microRNA expression in vivo in human CD8+ T cell subsets. J Transl Med *9*, 44.

Saumet, A., and Lecellier, C.H. (2006). Anti-viral RNA silencing: do we look like plants? Retrovirology *3*, 3.

Sayed, D., He, M., Hong, C., Gao, S., Rane, S., Yang, Z., and Abdellatif, M. (2010). MicroRNA-21 is a downstream effector of AKT that mediates its antiapoptotic effects via suppression of Fas ligand. J Biol Chem *285*, 20281-20290.

Scheller, L.F., Wirtz, R.A., and Azad, A.F. (1994). Susceptibility of different strains of mice to hepatic infection with Plasmodium berghei. Infect Immun *62*, 4844-4847.

Schulte, L.N., Eulalio, A., Mollenkopf, H.J., Reinhardt, R., and Vogel, J. (2011). Analysis of the host microRNA response to Salmonella uncovers the control of major cytokines by the let-7 family. EMBO J *30*, 1977-1989.

Schwentke, A., Krepstakies, M., Muller, A.K., Hammerschmidt, C., Motaal, B., Bernhard, T., Hauber, J., and Kaiser, A. (2012). In vitro and in vivo silencing of plasmodial dhs and eIF-5A genes in a putative, non-canonical RNAi-related pathway. BMC Microbiol *12*, 107.

Sekine, S., Ogawa, R., McManus, M.T., Kanai, Y., and Hebrok, M. (2009). Dicer is required for proper liver zonation. J Pathol *219*, 365-372.

Shibuya, H., Iinuma, H., Shimada, R., Horiuchi, A., and Watanabe, T. (2010). Clinicopathological and prognostic value of microRNA-21 and microRNA-155 in colorectal cancer. Oncology *79*, 313-320.

Shu, J., Kren, B.T., Xia, Z., Wong, P.Y., Li, L., Hanse, E.A., Min, M.X., Li, B., Albrecht, J.H., Zeng, Y*., et al.* (2011). Genome-wide microRNA downregulation as a negative feedback mechanism in the early phases of liver regeneration. Hepatology.

Si, M.L., Zhu, S., Wu, H., Lu, Z., Wu, F., and Mo, Y.Y. (2007). miR-21-mediated tumor growth. Oncogene *26*, 2799-2803.

Silvie, O., Franetich, J.F., Charrin, S., Mueller, M.S., Siau, A., Bodescot, M., Rubinstein, E., Hannoun, L., Charoenvit, Y., Kocken, C.H*., et al.* (2004). A role for apical membrane antigen 1 during invasion of hepatocytes by Plasmodium falciparum sporozoites. J Biol Chem *279*, 9490-9496.

Sinden, R.E. (1996). Infection of mousquitoes with rodent malaria. In: Molecular Biology of Insect Disease Vectors: A methods manual. P. 67-91.

Sinden, R.E., and Billingsley, P.F. (2001). Plasmodium invasion of mosquito cells: hawk or dove? Trends Parasitol *17*, 209-212.

Sinden, R.E., and Croll, N.A. (1975). Cytology and kinetics of microgametogenesis and fertilization in Plasmodium yoelii nigeriensis. Parasitology *70*, 53-65.

Sinnis, P., and Coppi, A. (2007). A long and winding road: the Plasmodium sporozoite's journey in the mammalian host. Parasitol Int *56*, 171-178.

Sonntag, F., Kother, K., Schmidt, K., Weghofer, M., Raupp, C., Nieto, K., Kuck, A., Gerlach, B., Bottcher, B., Muller, O.J*., et al.* (2011). The assembly-activating protein promotes capsid assembly of different adeno-associated virus serotypes. J Virol *85*, 12686-12697.

Sonntag, F., Schmidt, K., and Kleinschmidt, J.A. (2010). A viral assembly factor promotes AAV2 capsid formation in the nucleolus. Proc Natl Acad Sci U S A *107*, 10220-10225.

Sturm, A., Amino, R., van de Sand, C., Regen, T., Retzlaff, S., Rennenberg, A., Krueger, A., Pollok, J.M., Menard, R., and Heussler, V.T. (2006). Manipulation of host hepatocytes by the malaria parasite for delivery into liver sinusoids. Science *313*, 1287-1290.

Sturm, A., Graewe, S., Franke-Fayard, B., Retzlaff, S., Bolte, S., Roppenser, B., Aepfelbacher, M., Janse, C., and Heussler, V. (2009). Alteration of the parasite plasma membrane and the parasitophorous vacuole membrane during exo-erythrocytic development of malaria parasites. Protist *160*, 51-63.

Su, C., Hou, Z., Zhang, C., Tian, Z., and Zhang, J. (2011a). Ectopic expression of microRNA-155 enhances innate antiviral immunity against HBV infection in human hepatoma cells. Virol J *8*, 354.

Su, J., Baigude, H., McCarroll, J., and Rana, T.M. (2011b). Silencing microRNA by interfering nanoparticles in mice. Nucleic Acids Res *39*, e38.

Sullivan, C.S., Grundhoff, A.T., Tevethia, S., Pipas, J.M., and Ganem, D. (2005). SV40-encoded microRNAs regulate viral gene expression and reduce susceptibility to cytotoxic T cells. Nature *435*, 682-686.

Taganov, K.D., Boldin, M.P., Chang, K.J., and Baltimore, D. (2006). NF-kappaB-dependent induction of microRNA miR-146, an inhibitor targeted to signaling proteins of innate immune responses. Proc Natl Acad Sci U S A *103*, 12481-12486.

Tam, W. (2001). Identification and characterization of human BIC, a gene on chromosome 21 that encodes a noncoding RNA. Gene *274*, 157-167.

Tam, W., Ben-Yehuda, D., and Hayward, W.S. (1997). bic, a novel gene activated by proviral insertions in avian leukosis virus-induced lymphomas, is likely to function through its noncoding RNA. Mol Cell Biol *17*, 1490-1502.

Tarun, A.S., Baer, K., Dumpit, R.F., Gray, S., Lejarcegui, N., Frevert, U., and Kappe, S.H. (2006). Quantitative isolation and in vivo imaging of malaria parasite liver stages. Int J Parasitol *36*, 1283-1293.

Tarun, A.S., Dumpit, R.F., Camargo, N., Labaied, M., Liu, P., Takagi, A., Wang, R., and Kappe, S.H. (2007). Protracted sterile protection with Plasmodium yoelii pre-erythrocytic genetically attenuated parasite malaria vaccines is independent of significant liver-stage persistence and is mediated by CD8+ T cells. J Infect Dis *196*, 608-616.

Taverne, J., Rahman, D., Dockrell, H.M., Alavi, A., Leveton, C., and Playfair, J.H. (1987). Activation of liver macrophages in murine malaria is enhanced by vaccination. Clin Exp Immunol *70*, 508-514.

Teng, G., Hakimpour, P., Landgraf, P., Rice, A., Tuschl, T., Casellas, R., and Papavasiliou, F.N. (2008). MicroRNA-155 is a negative regulator of activation-induced cytidine deaminase. Immunity *28*, 621-629.

Thomas, C.E., Storm, T.A., Huang, Z., and Kay, M.A. (2004). Rapid uncoating of vector genomes is the key to efficient liver transduction with pseudotyped adeno-associated virus vectors. J Virol *78*, 3110-3122.

Thorpe, G.H., and Kricka, L.J. (1986). Enhanced chemiluminescent reactions catalyzed by horseradish peroxidase. Methods Enzymol *133*, 331-353.

Tili, E., Michaille, J.J., Cimino, A., Costinean, S., Dumitru, C.D., Adair, B., Fabbri, M., Alder, H., Liu, C.G., Calin, G.A., *et al.* (2007). Modulation of miR-155 and miR-125b levels following lipopolysaccharide/TNF-alpha stimulation and their possible roles in regulating the response to endotoxin shock. J Immunol *179*, 5082-5089.

Tsuji, M., Mattei, D., Nussenzweig, R.S., Eichinger, D., and Zavala, F. (1994). Demonstration of heat-shock protein 70 in the sporozoite stage of malaria parasites. Parasitol Res *80*, 16-21.

Turner, M., and Vigorito, E. (2008). Regulation of B- and T-cell differentiation by a single microRNA. Biochem Soc Trans *36*, 531-533.

Turner, M.L., Schnorfeil, F.M., and Brocker, T. (2011). MicroRNAs regulate dendritic cell differentiation and function. J Immunol *187*, 3911-3917.

Tuteja, R. (2007). Malaria - the global disease. FEBS J *274*, 4669.

Vaishnava, S., and Striepen, B. (2006). The cell biology of secondary endosymbiosis--how parasites build, divide and segregate the apicoplast. Mol Microbiol *61*, 1380-1387.

van de Sand, C., Horstmann, S., Schmidt, A., Sturm, A., Bolte, S., Krueger, A., Lutgehetmann, M., Pollok, J.M., Libert, C., and Heussler, V.T. (2005). The liver stage of Plasmodium berghei inhibits host cell apoptosis. Mol Microbiol *58*, 731-742.

van Dijk, M.R., Douradinha, B., Franke-Fayard, B., Heussler, V., van Dooren, M.W., van Schaijk, B., van Gemert, G.J., Sauerwein, R.W., Mota, M.M., Waters, A.P., *et al.* (2005). Genetically attenuated, P36p-deficient malarial sporozoites induce protective immunity and apoptosis of infected liver cells. Proc Natl Acad Sci U S A *102*, 12194-12199.

van Rooij, E., Sutherland, L.B., Qi, X., Richardson, J.A., Hill, J., and Olson, E.N. (2007). Control of stress-dependent cardiac growth and gene expression by a microRNA. Science *316*, 575-579.

Vanderberg, J.P., and Frevert, U. (2004). Intravital microscopy demonstrating antibody-mediated immobilisation of Plasmodium berghei sporozoites injected into skin by mosquitoes. Int J Parasitol *34*, 991-996.

Vaughan, A.M., Aly, A.S., and Kappe, S.H. (2008). Malaria parasite pre-erythrocytic stage infection: gliding and hiding. Cell Host Microbe *4*, 209-218.

Vigorito, E., Perks, K.L., Abreu-Goodger, C., Bunting, S., Xiang, Z., Kohlhaas, S., Das, P.P., Miska, E.A., Rodriguez, A., Bradley, A., *et al.* (2007). microRNA-155 regulates the generation of immunoglobulin class-switched plasma cells. Immunity *27*, 847-859.

von Eckardstein, A., Castro, G., Wybranska, I., Theret, N., Duchateau, P., Duverger, N., Fruchart, J.C., Ailhaud, G., and Assmann, G. (1993). Interaction of reconstituted high density lipoprotein discs containing human apolipoprotein A-I (ApoA-I) variants with murine adipocytes and macrophages. Evidence for reduced cholesterol efflux promotion by apoA-I(Pro165-->Arg). J Biol Chem *268*, 2616-2622.

Waller, R.F., and McFadden, G.I. (2005). The apicoplast: a review of the derived plastid of apicomplexan parasites. Curr Issues Mol Biol *7*, 57-79.

Wang, P., Hou, J., Lin, L., Wang, C., Liu, X., Li, D., Ma, F., Wang, Z., and Cao, X. (2010). Inducible microRNA-155 feedback promotes type I IFN signaling in antiviral innate immunity by targeting suppressor of cytokine signaling 1. J Immunol *185*, 6226-6233.

White, N.J. (2008). Plasmodium knowlesi: the fifth human malaria parasite. Clin Infect Dis *46*, 172-173.

Wiesen, J.L., and Tomasi, T.B. (2009). Dicer is regulated by cellular stresses and interferons. Mol Immunol *46*, 1222-1228.

Wightman, B., Ha, I., and Ruvkun, G. (1993). Posttranscriptional regulation of the heterochronic gene lin-14 by lin-4 mediates temporal pattern formation in C. elegans. Cell *75*, 855-862.

Williams, T.N., and Obaro, S.K. (2011). Sickle cell disease and malaria morbidity: a tale with two tails. Trends Parasitol *27*, 315-320.

Winter, F., Edaye, S., Huttenhofer, A., and Brunel, C. (2007). Anopheles gambiae miRNAs as actors of defence reaction against Plasmodium invasion. Nucleic Acids Res *35*, 6953-6962.

Wu, J.F., Shen, W., Liu, N.Z., Zeng, G.L., Yang, M., Zuo, G.Q., Gan, X.N., Ren, H., and Tang, K.F. (2011). Down-regulation of Dicer in hepatocellular carcinoma. Med Oncol *28*, 804-809.

Wu, L., and Belasco, J.G. (2008). Let me count the ways: mechanisms of gene regulation by miRNAs and siRNAs. Mol Cell *29*, 1-7.

Wu, T., Xie, M., Wang, X., Jiang, X., Li, J., and Huang, H. (2012). miR-155 modulates TNF-alpha-inhibited osteogenic differentiation by targeting SOCS1 expression. Bone.

Wu, Z., Asokan, A., and Samulski, R.J. (2006). Adeno-associated virus serotypes: vector toolkit for human gene therapy. Mol Ther *14*, 316-327.

Xu, J., Wu, C., Che, X., Wang, L., Yu, D., Zhang, T., Huang, L., Li, H., Tan, W., Wang, C., *et al.* (2011). Circulating microRNAs, miR-21, miR-122, and miR-223, in patients with hepatocellular carcinoma or chronic hepatitis. Mol Carcinog *50*, 136-142.

Xue, X., Zhang, Q., Huang, Y., Feng, L., and Pan, W. (2008). No miRNA were found in Plasmodium and the ones identified in erythrocytes could not be correlated with infection. Malar J *7*, 47.

Yang, J.S., Maurin, T., Robine, N., Rasmussen, K.D., Jeffrey, K.L., Chandwani, R., Papapetrou, E.P., Sadelain, M., O'Carroll, D., and Lai, E.C. (2010). Conserved vertebrate mir-451 provides a platform for Dicer-independent, Ago2-mediated microRNA biogenesis. Proc Natl Acad Sci U S A *107*, 15163-15168.

Yi, R., Qin, Y., Macara, I.G., and Cullen, B.R. (2003). Exportin-5 mediates the nuclear export of pre-microRNAs and short hairpin RNAs. Genes Dev *17*, 3011-3016.

Yoeli, M., and Most, H. (1965). Studies on sporozoite-induced infections of rodent malaria. I. The pre-erythrocytic tissue stage of Plasmodium berghei. Am J Trop Med Hyg *14*, 700-714.

Yoeli, M., Vanderberg, J., Nawrot, R., and Most, H. (1965). Studies on sporozoite-induced infections of rodent malaria. II. Anopheles stephensi as an experimental vector of Plasmodium berghei. Am J Trop Med Hyg *14*, 927-930.

Zeiner, G.M., Norman, K.L., Thomson, J.M., Hammond, S.M., and Boothroyd, J.C. (2010). Toxoplasma gondii infection specifically increases the levels of key host microRNAs. PLoS One *5*, e8742.

Zhang, B.G., Li, J.F., Yu, B.Q., Zhu, Z.G., Liu, B.Y., and Yan, M. (2012a). microRNA-21 promotes tumor proliferation and invasion in gastric cancer by targeting PTEN. Oncol Rep *27*, 1019-1026.

Zhang, J., Zhao, H., Chen, J., Xia, B., Jin, Y., Wei, W., Shen, J., and Huang, Y. (2012b). Interferon-beta-induced miR-155 inhibits osteoclast differentiation by targeting SOCS1 and MITF. FEBS Lett.

Zhang, J.G., Wang, J.J., Zhao, F., Liu, Q., Jiang, K., and Yang, G.H. (2010). MicroRNA-21 (miR-21) represses tumor suppressor PTEN and promotes growth and invasion in non-small cell lung cancer (NSCLC). Clin Chim Acta *411*, 846-852.

Zhang, M., Zhang, Q., Liu, F., Yin, L., Yu, B., and Wu, J. (2011). MicroRNA-155 may affect allograft survival by regulating the expression of suppressor of cytokine signaling 1. Med Hypotheses *77*, 682-684.

Zhou, R., Hu, G., Liu, J., Gong, A.Y., Drescher, K.M., and Chen, X.M. (2009). NF-kappaB p65-dependent transactivation of miRNA genes following Cryptosporidium parvum infection stimulates epithelial cell immune responses. Plos Pathogens *5*, e1000681.

Zhu, S., Si, M.L., Wu, H., and Mo, Y.Y. (2007). MicroRNA-21 targets the tumor suppressor gene tropomyosin 1 (TPM1). J Biol Chem *282*, 14328-14336.

Zhu, S., Wu, H., Wu, F., Nie, D., Sheng, S., and Mo, Y.Y. (2008). MicroRNA-21 targets tumor suppressor genes in invasion and metastasis. Cell Res *18*, 350-359.

Ziyan, W., Shuhua, Y., Xiufang, W., and Xiaoyun, L. (2011). MicroRNA-21 is involved in osteosarcoma cell invasion and migration. Med Oncol *28*, 1469-1474.

6 Danksagung

Zu guter Letzt gibt es eine Menge Menschen, die maßgeblich dazu beigetragen haben, dass diese Arbeit entstanden und auch zu Ende geführt worden ist. Und diesen Menschen möchte ich an dieser Stelle danken!

Die Person, die am maßgeblichsten dazu beigetragen hat, ist natürlich **Ann-Kristin**. Es fällt mir sehr schwer all meinen Dank in Worte zu fassen. Denn sie hat mir die nötige zweite Chance gegeben und ohne sie wäre diese Arbeit gar nicht erst entstanden. Ich danke ihr von ganzem Herzen, dass sie mir diese Chance gegeben und das nötige Vertrauen geschenkt hat, unter ihrer Anleitung diese Arbeit anzufertigen. Aufgrund der Diskussionen mit ihr und ihrer niemals versiegenden Quelle an Ideen hat sie mich meine schlechten Erfahrungen vergessen lassen. Mit ihrem unerschütterlichen Optimismus und ihrer scheinbar grenzenlosen Zuversicht, hat sie mich auch in schwierigen Phasen immer wieder motivieren können. Sie war immer für mich da und hatte ein offenes Ohr für meinen Frust, aber auch für meine Freude. Liebe Ann-Kristin, ich danke dir für alles!

Bei Herrn **Prof. Dr. Lanzer** möchte ich mich für die Aufnahme in seine Abteilung bedanken und darüber hinaus für die Bereitschaft, das Erstgutachten meiner Arbeit zu übernehmen.

Ein weiterer großer Dank gebührt **Dirk**. Ohne seine Ideen und die entsprechenden technischen Möglichkeiten, die er mir zur Verfügung gestellt hat, hätte diese Arbeit niemals ihre jetzige Form annehmen können. Auch wenn er zuweilen meinen Freudentaumel nicht ebenso enthusiastisch teilen konnte, fühlte ich mich von ihm doch immer sehr unterstützt. Auch bin ich ihm sehr dankbar, dass er aufgrund einiger wundersamer Umgruppierungen an meiner Prüfung wird teilnehmen können.

Bei **Barbara** möchte ich mich bedanken, dass sie sich ohne zu zögern bereit erklärt hat, an meinen TAC-Meetings und auch an meiner Prüfung teilzunehmen und dafür zuletzt extra aus Erlangen angereist ist. Außerdem danke ich ihr sehr für die lieben und aufbauenden Worte nach meinem ersten TAC-Meeting.

Ein ganz besonders großes Dankeschön gilt **Julia** für ihre fortwährende Hilfe und Unterstützung. Vor allem in den letzten Monaten im Labor wäre ich ohne sie verzweifelt! Ihre ruhige Art und in aller Regel SOFORTIGE Bereitschaft mir unter die Arme zu greifen haben mir einiges an unnötiger Arbeit erspart. Auch ihr offenes Ohr und ihre aufbauenden Worte haben immer sehr, sehr gut getan. Vielen, vielen lieben Dank!

Aber auch **Britta** bin ich nicht weniger dankbar! Auch sie hat mir immer geholfen, besonders bei meinem kleinen Ausflug in die Hefe-Welt und jetzt am Ende während des Schreibens, wo sie sehr

aufmerksam war und jeden Ansatz von Meister-Yoda-Ausdrucksweise im Keim erstickt hat. Es war sehr schön neben ihr und mit ihr zu arbeiten.

I want to thank **Matt**, **Priyanka**, **Yvonne** and **Aina**, especially for taking blood smears over the weekends without complain. You saved me a lot of time sitting in trains between Würzburg and Heidelberg.

Auch **Kirsten**, **Jenny**, **Roland** und **Flo** danke ich für eine wunderbare Zeit im Labor. Jede und jeder von euch hat seinen Teil durch seine Hilfe und Unterstützung zu dieser Arbeit beigetragen.

Eva, meiner Pendelfreundin, danke ich nicht nur für die gemeinsamen Bahnfahrten, die trotz ihrer Häufigkeit nie langweilig waren, sondern ganz besonders auch für die ersten Monate im Labor, in denen sie so viele meiner Fragen beantworten musste und nie müde wurde, mir all die neuen Methoden zu erklären. Sie hat – mit all den anderen – dazu beigetragen, dass die Zeit im Labor für mich unvergesslich sein wird!

Bei **Kathleen** möchte ich mich für die technische und moralische Unterstützung bedanken, ohne die ich schier verzweifelt wäre. Auch sie gehört zu den Menschen, die immer bereit sind zu helfen und einem das Gefühl vermitteln, dass sie es auch gern tun. Ohne sie hätte ich manches Mal sehr ratlos vor diversen Geräten gestanden und mich gewundert, was man wie damit machen kann. Ich danke ihr für die vielen Diskussionen und auch für die Arbeitsbesprechungen, die mir immer sehr gut getan und mich regelmäßig neu motiviert haben.

Den **Grimms** danke ich für das freundliche Asyl, das sie mir während der letzten Jahre gewährt haben. Darüber hinaus möchte ich ganz besonders **Nina** und **Stefan** danken für ihre Unterstützung sowohl in technischer Hinsicht im Labor, als auch während meiner Schreibphase bei der Beantwortung all meiner Fragen (und es waren viele Fragen...)! Ihr habt mir das Leben im Bioquant sehr erleichtert.

Ein weiteres großes Dankeschön gebührt allen Mitgliedern unserer Abteilung. Nachdem sie mich herzlich aufgenommen haben, gaben sie mir während der gesamten Zeit das Gefühl dazu zu gehören. Jeder hat bereitwillig meine Fragen beantwortet und vor allem von **Stefan** und **Marina** kam nie ein „nein“ als Antwort auf verschiedene Anfragen. Sie alle haben dazu beigetragen, dass ich eine sehr schöne Zeit in Heidelberg verbringen durfte!

Miriam möchte ich ganz herzlich für ihre unerschütterliche Hilfsbereitschaft danken. Ohne sie hätte ich mich sicher manches Mal im Verwaltungsdschungel verirrt.

All jenen, die bei den „happy meals“ dabei waren, danke ich von ganzem Herzen für die schönen Abende, die wir gemeinsam verbracht haben – und das leckere Essen!!! Dank euch hatte ich nicht zu viele einsame Abende und werde die Heidelberger Zeit in guter Erinnerung behalten!

Auch möchte ich all denjenigen Freunden außerhalb des Labors danken, die immer noch an meiner Seite sind, obwohl ich sie in letzter Zeit doch sehr vernachlässigt habe. Das zeigt mir, dass ich mich jederzeit auf euch verlassen kann und das macht für mich unsere Freundschaft aus!

Ein ganz besonderer Dank gebührt den vier wichtigsten Menschen in meinem Leben: meinen Eltern, Netti und Daniel. Denn sie alle haben mich immer bedingungslos unterstützt und mir das Gefühl gegeben, dass ich keine falschen Entscheidungen treffen kann, was mir den nötigen Rückhalt gegeben hat, auch schwierige Phasen zu überstehen. Ohne euch hätte ich vieles in meinem Leben nicht geschafft, und wäre nicht der Mensch, der ich nun bin. Ich bin so froh und unendlich dankbar, dass es euch gibt!